Chiral magnetic crystals

Markus Garst

TECHNISCHE UNIVERSITÄT DRESDEN

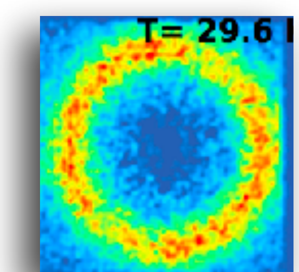

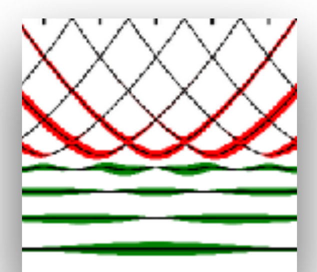

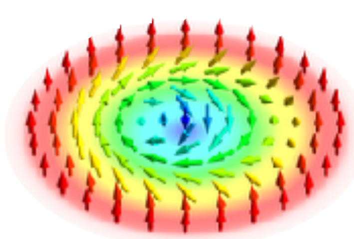

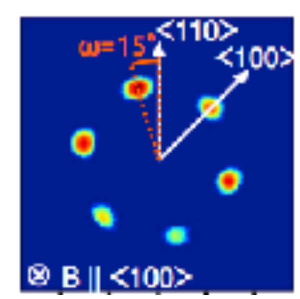

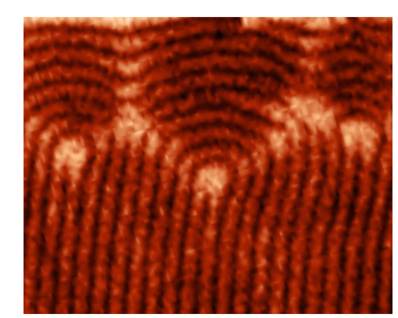

Outline

- introduction to chiral magnetic crystals
- crystallization process
- helimagnon band structure
- skyrmion topology & magnon-driven skyrmion motion
- spinwaves in skyrmion crystals
- orientation of skyrmion crystals
- topological defects and domain walls in helimagnets

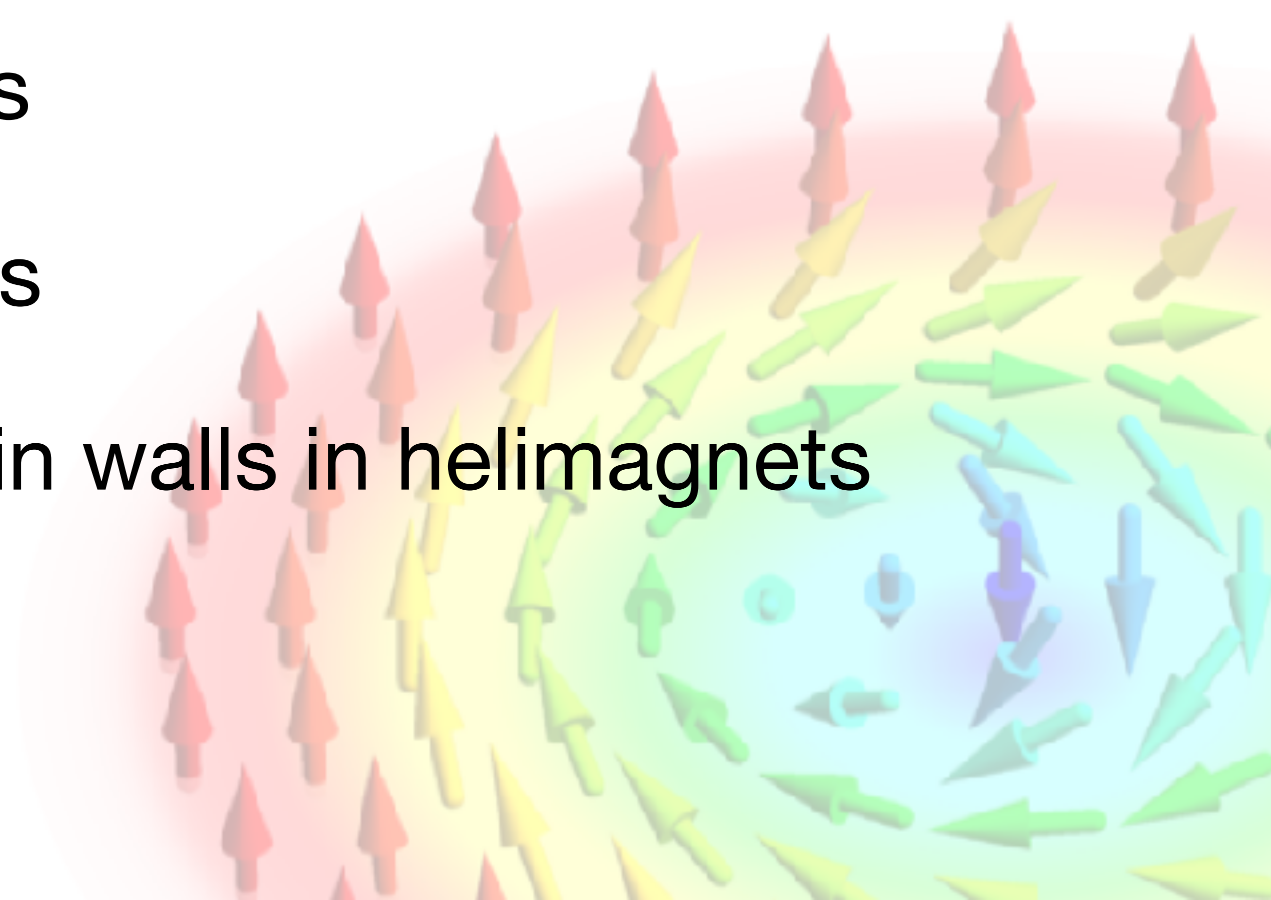

Introduction to chiral magnetic crystals

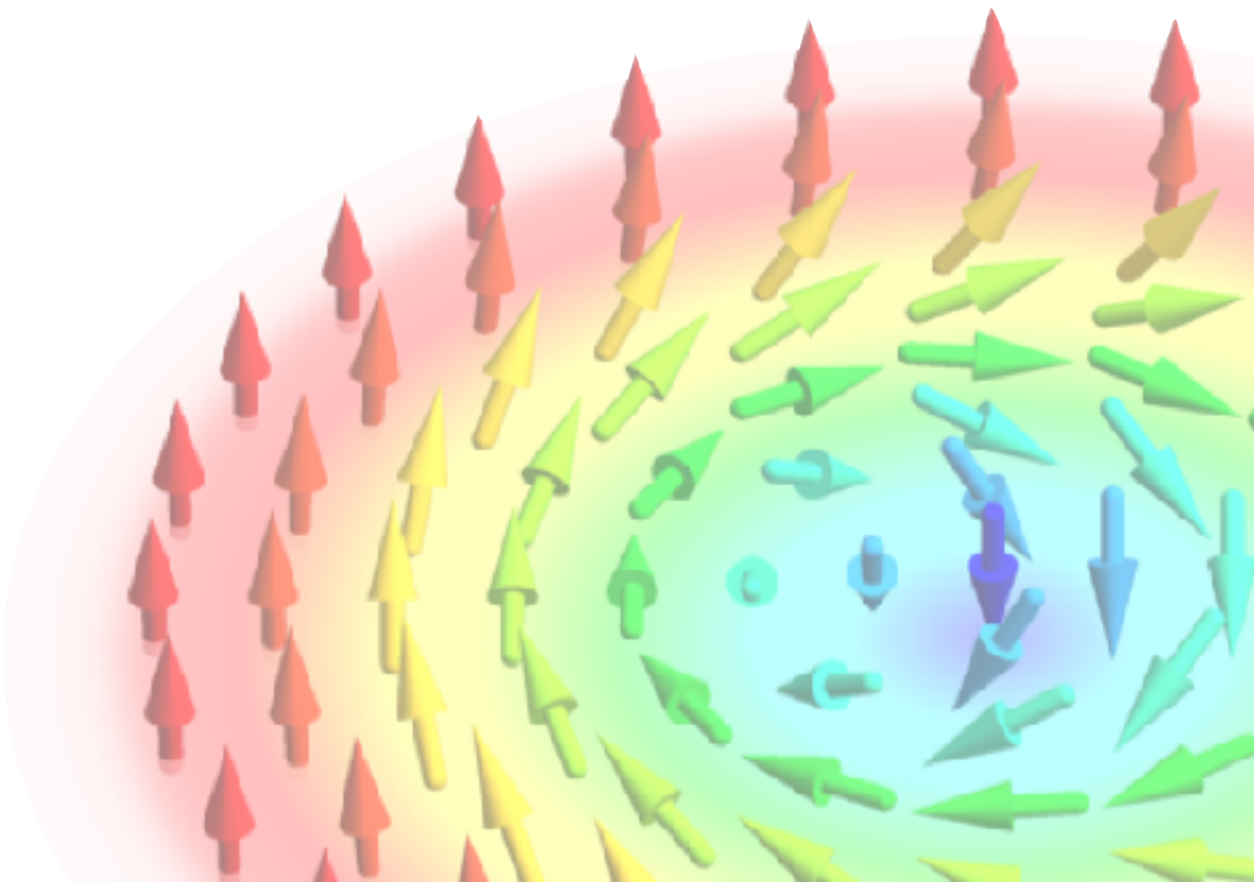

Chiral magnets

magnets with a non-centrosymmetric chiral atomic crystal lattice

- hexagonal $Cr_{1/3}NbS_2$ with strong crystal anisotropies

⇨ monoaxial chiral magnet

Togawa et al PRL (2012)

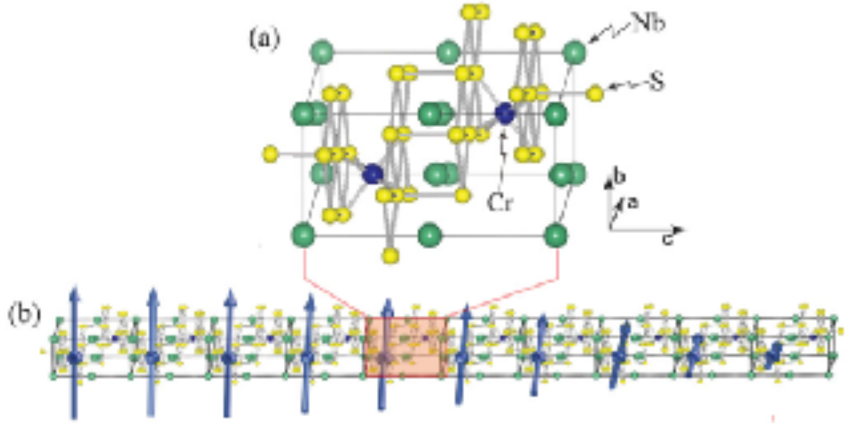

- cubic B20 compounds: MnSi, FeGe, $Fe_xCo_{1-x}Si$, Cu_2OSeO_3, …

Bravais lattice: simple cubic
space group: $P2_13$ (B20)

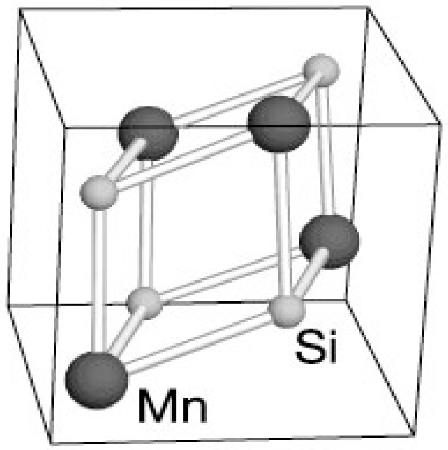

chiral atomic crystal lattice

⇨ cubic chiral magnets

Ginzburg-Landau theory for cubic chiral magnets

Landau-Lifshitz Vol. 8 (2nd edition), §52 helicoidal magnetic structures:

in the limit of small spin-orbit coupling $\lambda_{\rm SOC}$: clear separation of energy/length scales

⇨ universal theory at low energies

Bak & Jensen (1980), Nakanishi et al. (1980)

$$\mathcal{L} = \underbrace{\frac{J}{2}\kappa_0^2\,\vec{M}^2 + \frac{J}{2}(\nabla\vec{M})^2 + \frac{u}{4!}(\vec{M}^2)^2}_{\text{ferromagnetic exchange}} + \underbrace{D\vec{M}(\nabla\times\vec{M})}_{\text{Dzyaloshinskii-Moriya interaction}} + \underbrace{\ldots}_{\text{cubic anisotropies}}$$

linear in $\lambda_{\rm SOC}$

higher-order in $\lambda_{\rm SOC}$

+ dipolar interactions

competition between exchange and DMI ⇨ chiral magnetic crystals

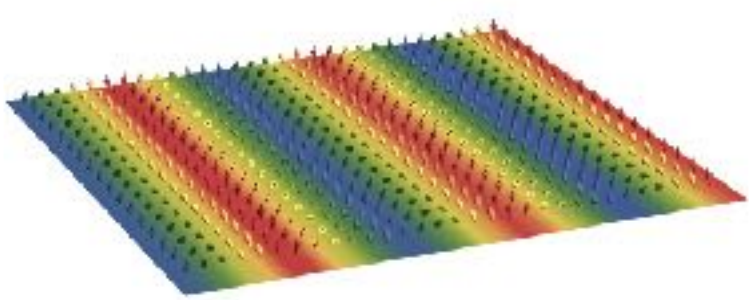

1d helix

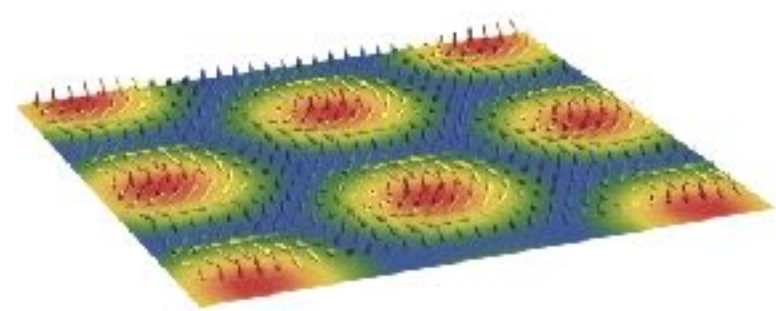

2d skyrmion crystal

MnSi in a magnetic field

Ishikawa *et al.* PRB (1977)
Thessieu *et al.* J. Phys.: Condens. Matter (1997)

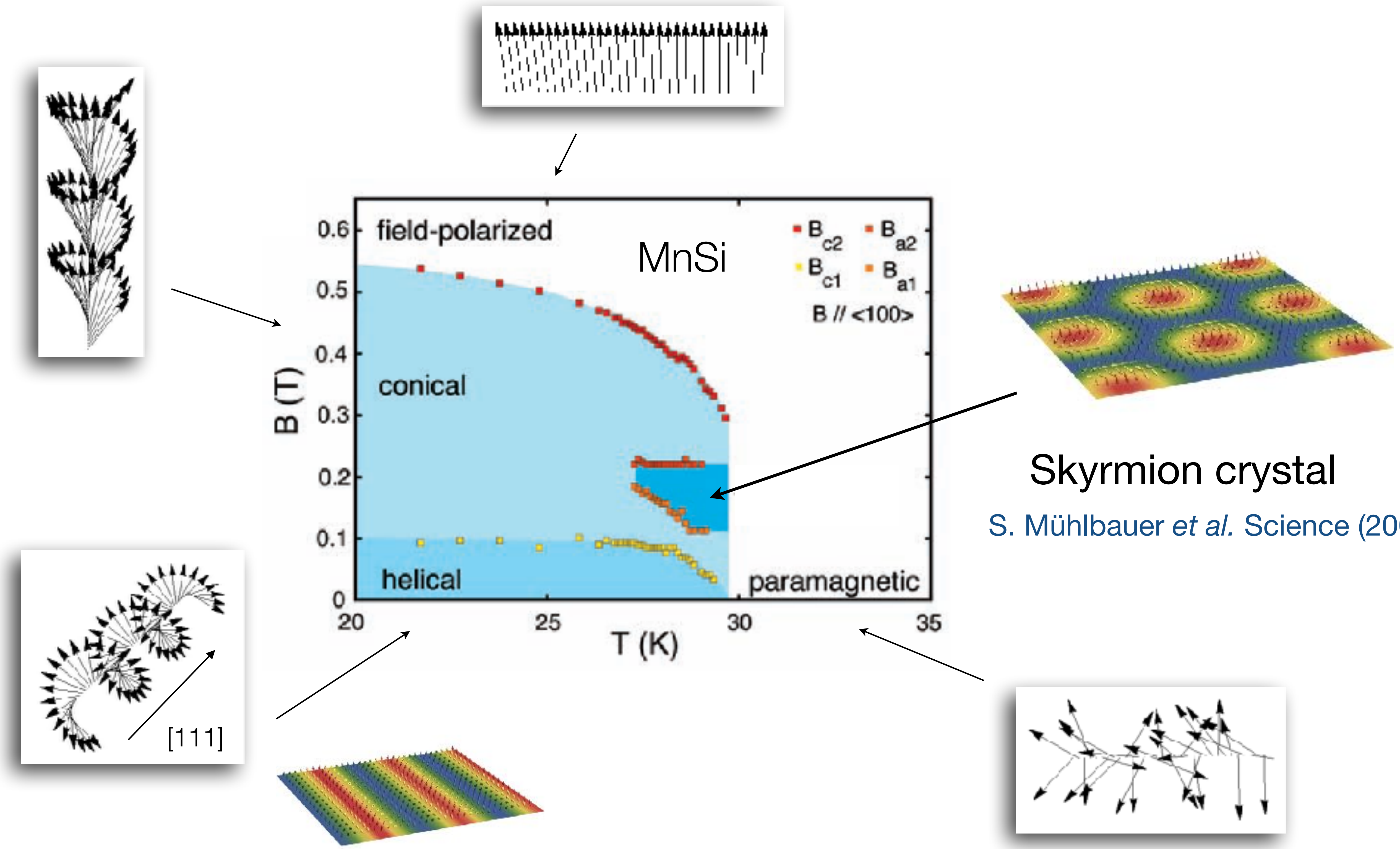

Skyrmion crystal

S. Mühlbauer *et al.* Science (2009)

Cubic chiral magnets

„universal“ magnetism shared by whole class of materials

metal MnSi

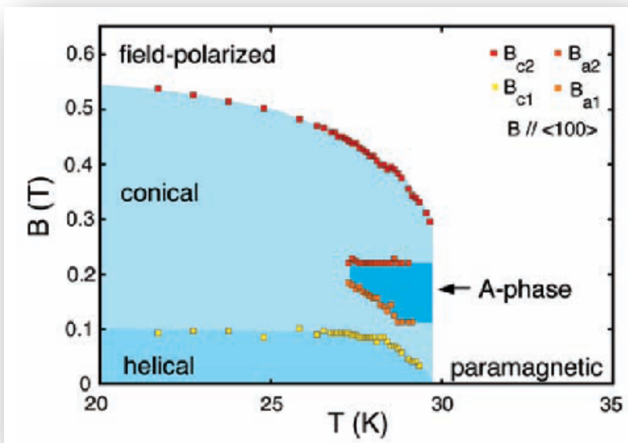

Mühlbauer et al. Science (2009)

insulator

Cu_2OSeO_3

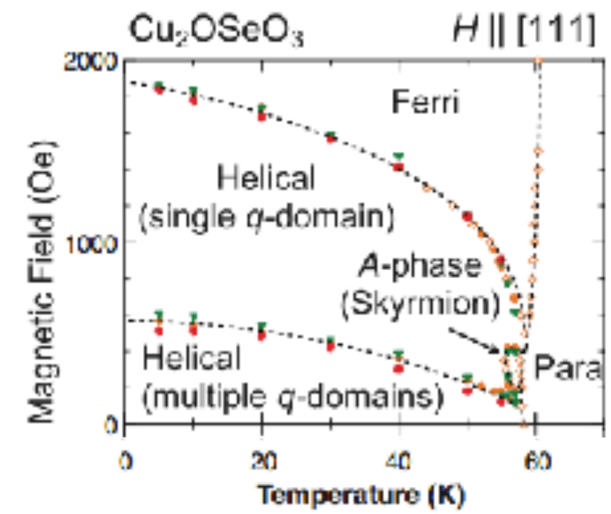

Seki et al. Science (2012)

semiconductor

$Fe_{0.5}Co_{0.5}Si$

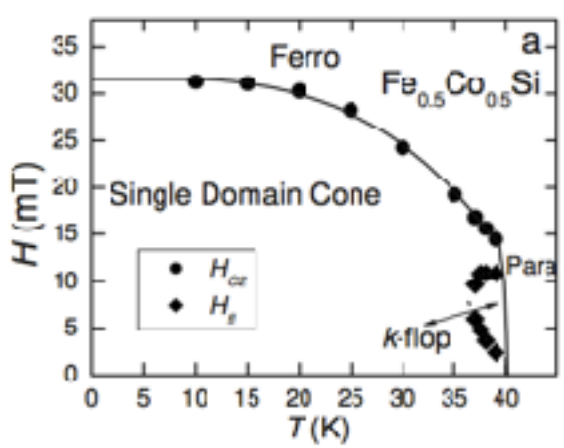

Grigoriev et al. PRB (2007)

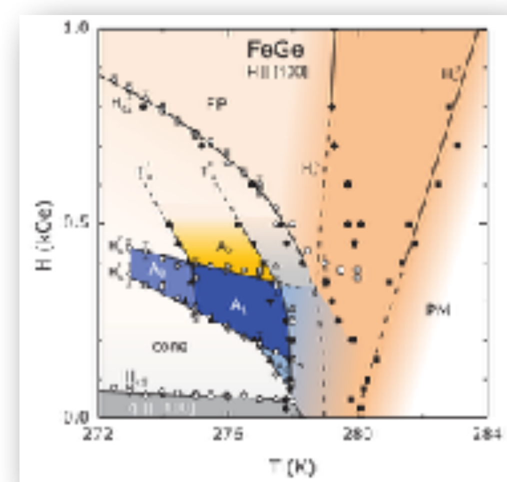

metal

FeGe

Wilhelm et al. PRL (2011)

Phase diagram of MnSi con‘t.

in a magnetic field

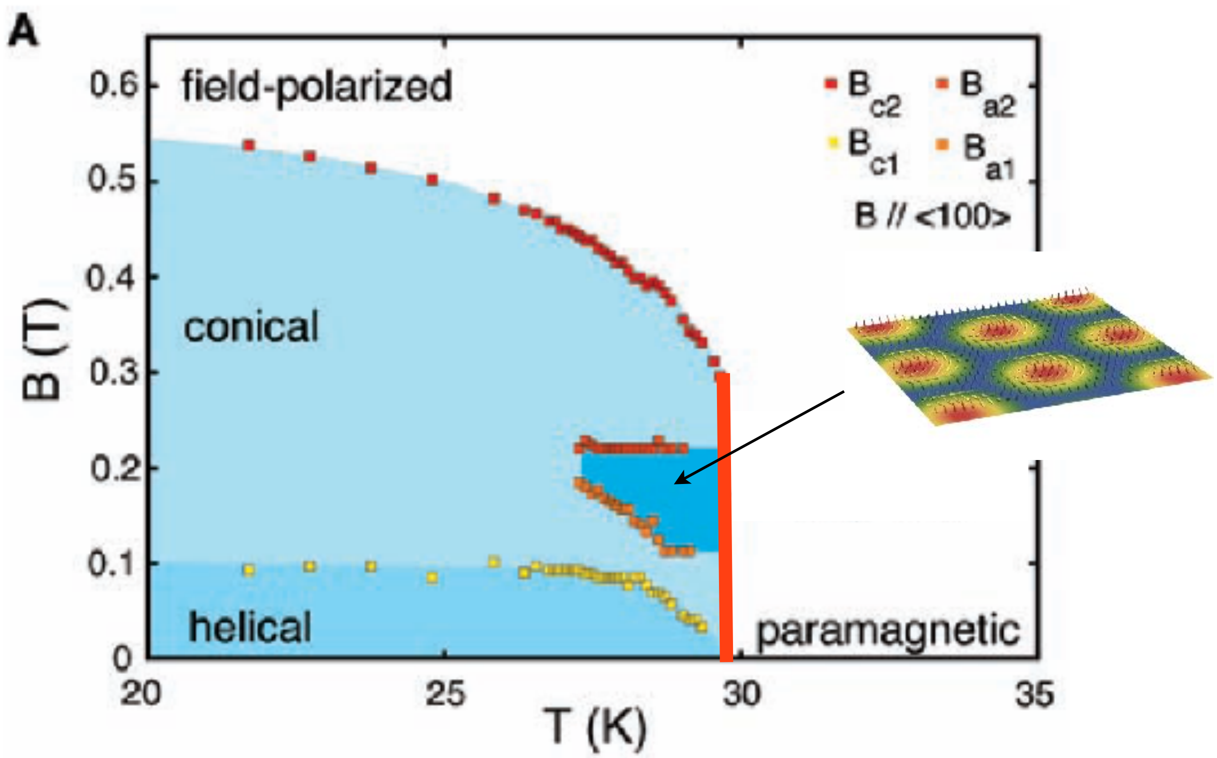

under pressure

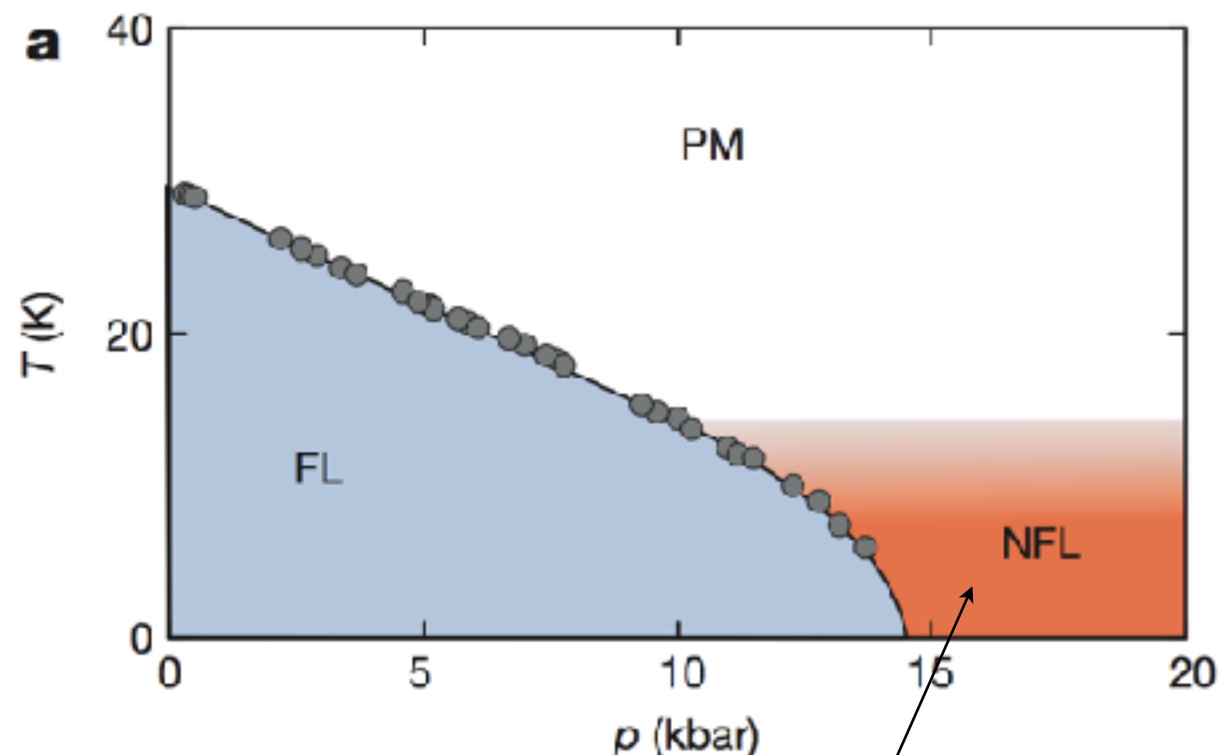

extended non-Fermi liquid regime
three (!) decades in temperature

Pfleiderer, Julian, Lonzarich, Nature 2001
Ritz … Pfleiderer, Nature 2013

holy-grail of MnSi $\delta\rho \sim T^{3/2}$

No comprehensive theoretical explanation of NFL behavior yet!

Chiral magnetic crystals

incommensurate periodic magnetic structures

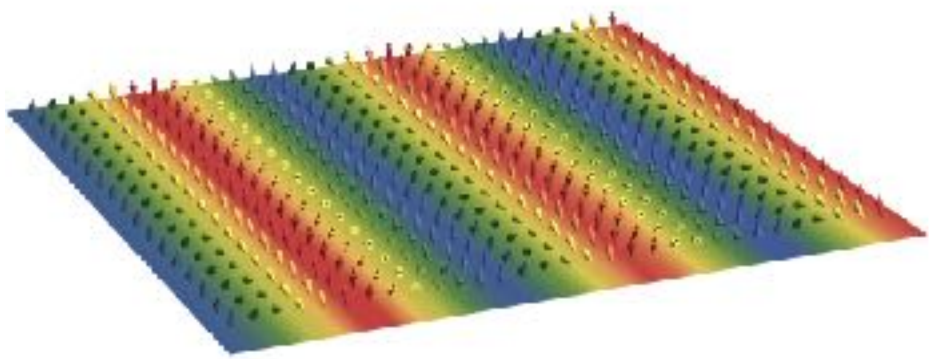

1d helix

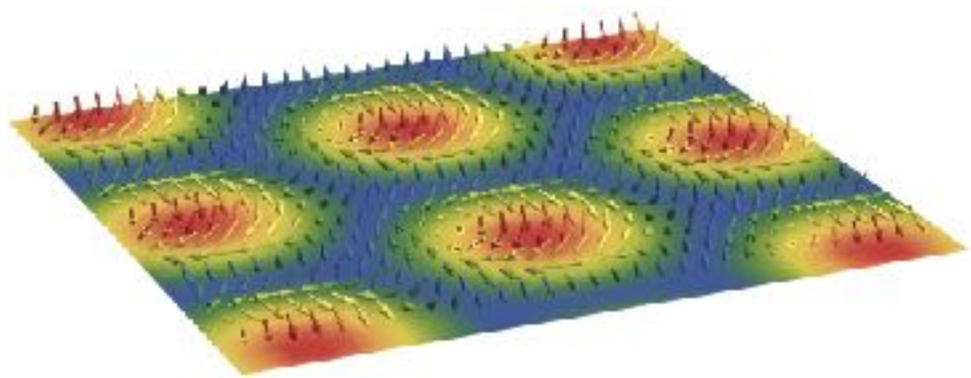

2d skyrmion crystal

share many aspect with crystalline order

lattice constant: $\lambda \approx$ 18 nm in MnSi
70 nm in FeGe

Chiral magnetic transition:
weak crystallization process

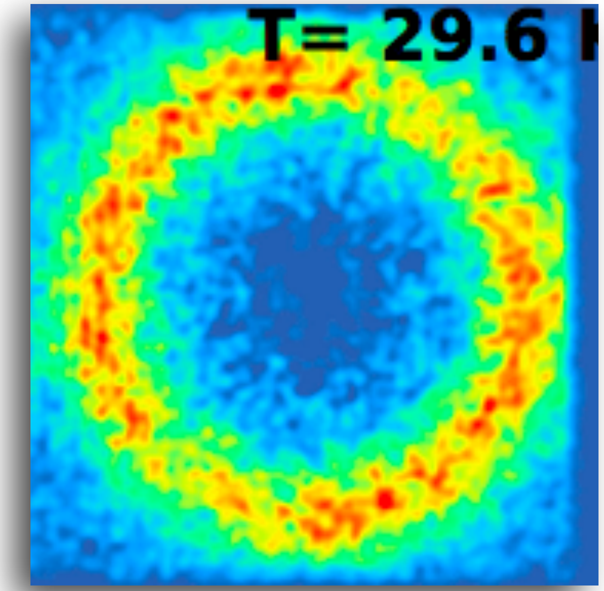

Weak crystallization process

crystal breaks translation symmetry and also isotropy of space!

⇨ critical mode becomes soft on a sphere in momentum space

$$\omega(\vec{q}) = \Delta + (|\vec{q}| - Q)^2$$

Brazovskii, JETP (1975)
Kats, Lebedev, Muratov, Phys. Rep, (1993)

⇨ one-dimensional divergence in density of states

$$\rho(\varepsilon) = \int d^3k \delta(\omega(\mathbf{k}) - \varepsilon) \sim \frac{1}{\sqrt{|\varepsilon - \Delta|}}$$

⇨ fluctuation-induced first-order transition to avoid the entropy of the critical state!

Paramagnons soften at finite momentum

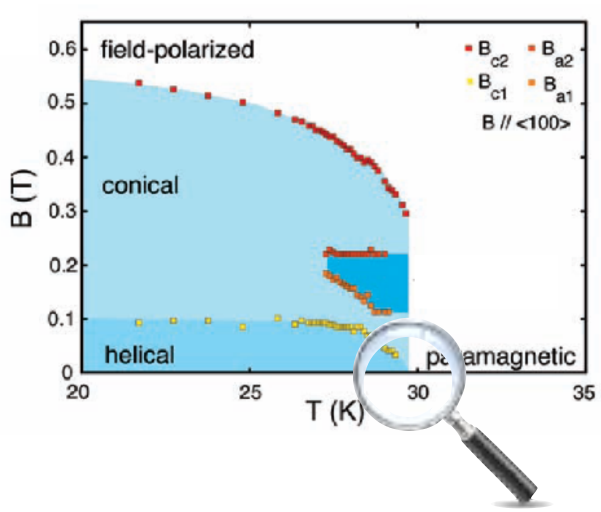

finite-T transition at zero field

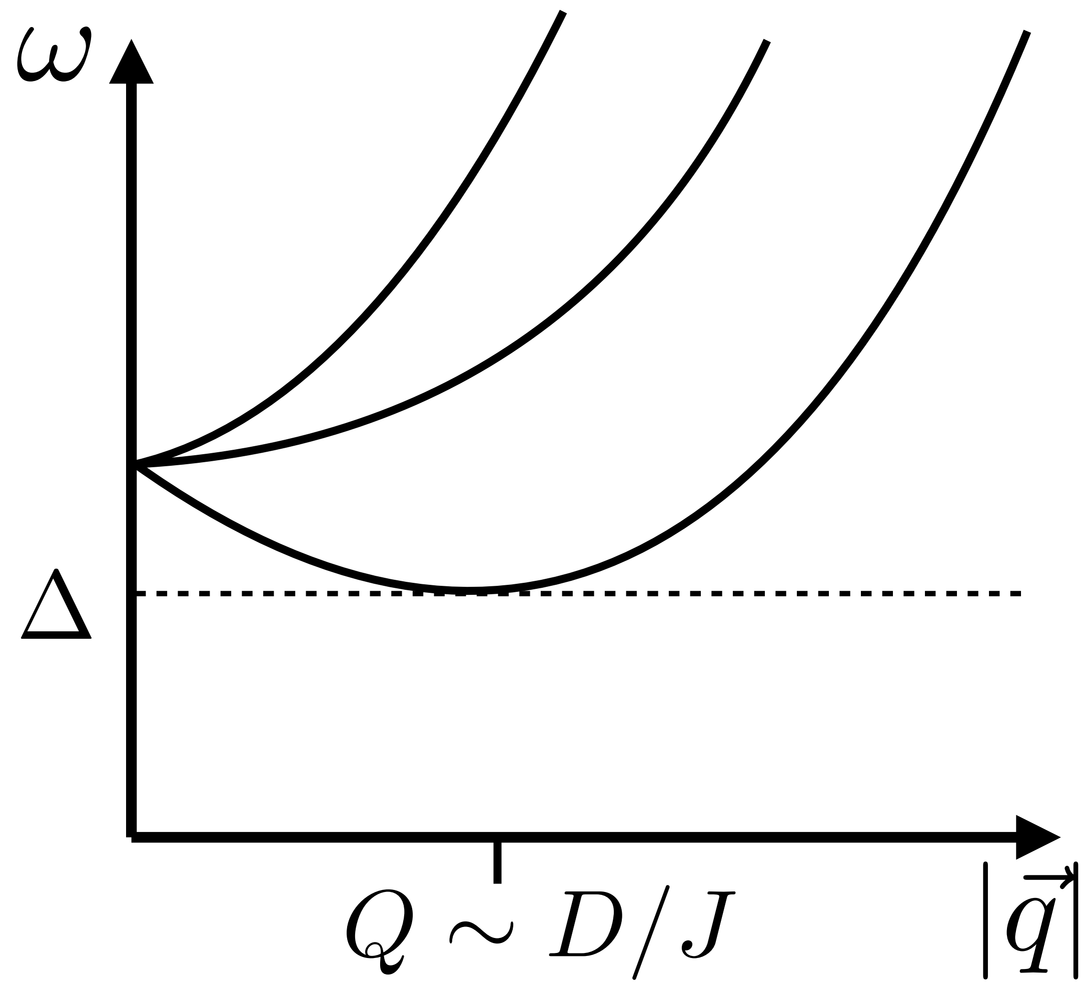

$$D\vec{M}(\nabla \times \vec{M})$$

Dzyaloshinskii-Moriya interaction

$$\omega(\vec{q}) = \Delta + (|\vec{q}| - Q)^2$$

Brazovskii spectrum!

critical mode becomes soft
on a sphere in momentum space

Strongly correlated critical paramagnet

strong correlations above T_c even at ambient pressure:

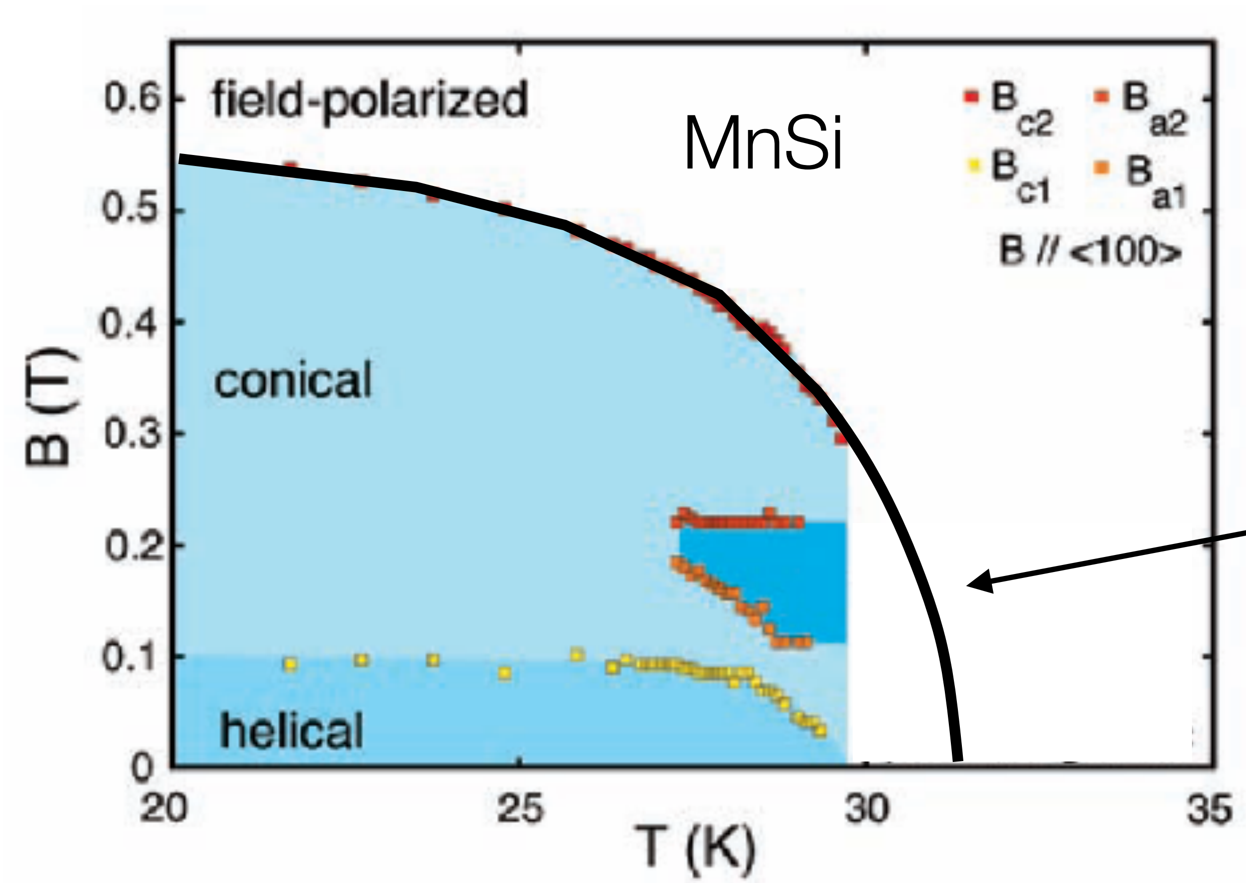

This is the prediction of mean-field theory!

2nd-order transition:

$$B_{c2} \propto \sqrt{T - T_c}$$

Strongly correlated critical paramagnet

strong correlations above T_c even at ambient pressure:

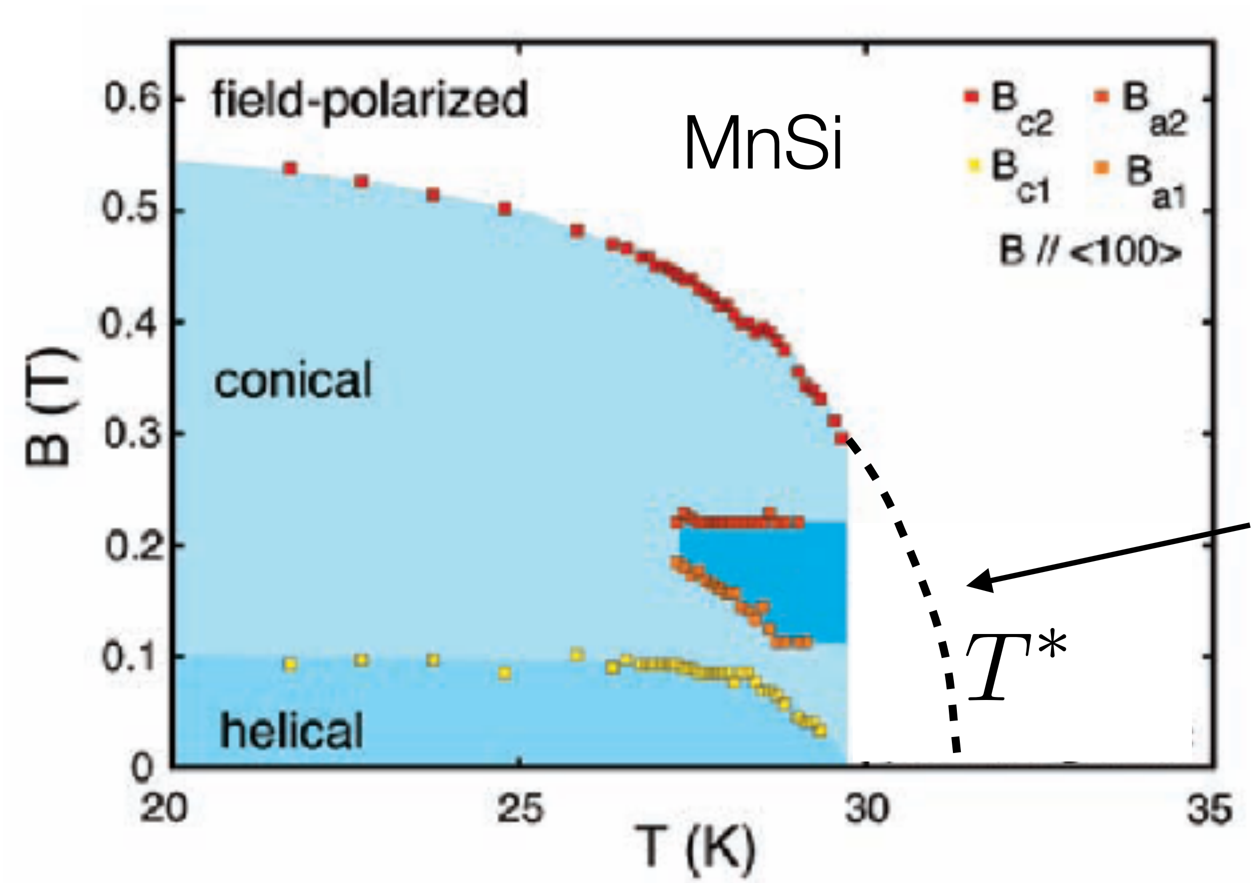

Instead:
fluctuations suppress the ordering - crossover

Fluctuation-induced first order transition

M. Janoschek, MG et al PRB (2013)
Bauer, MG, Pfleiderer, PRL (2013)
J. Kindervater, MG, et al PRB (2014)

fluctuation-induced
tricritical point

2nd order

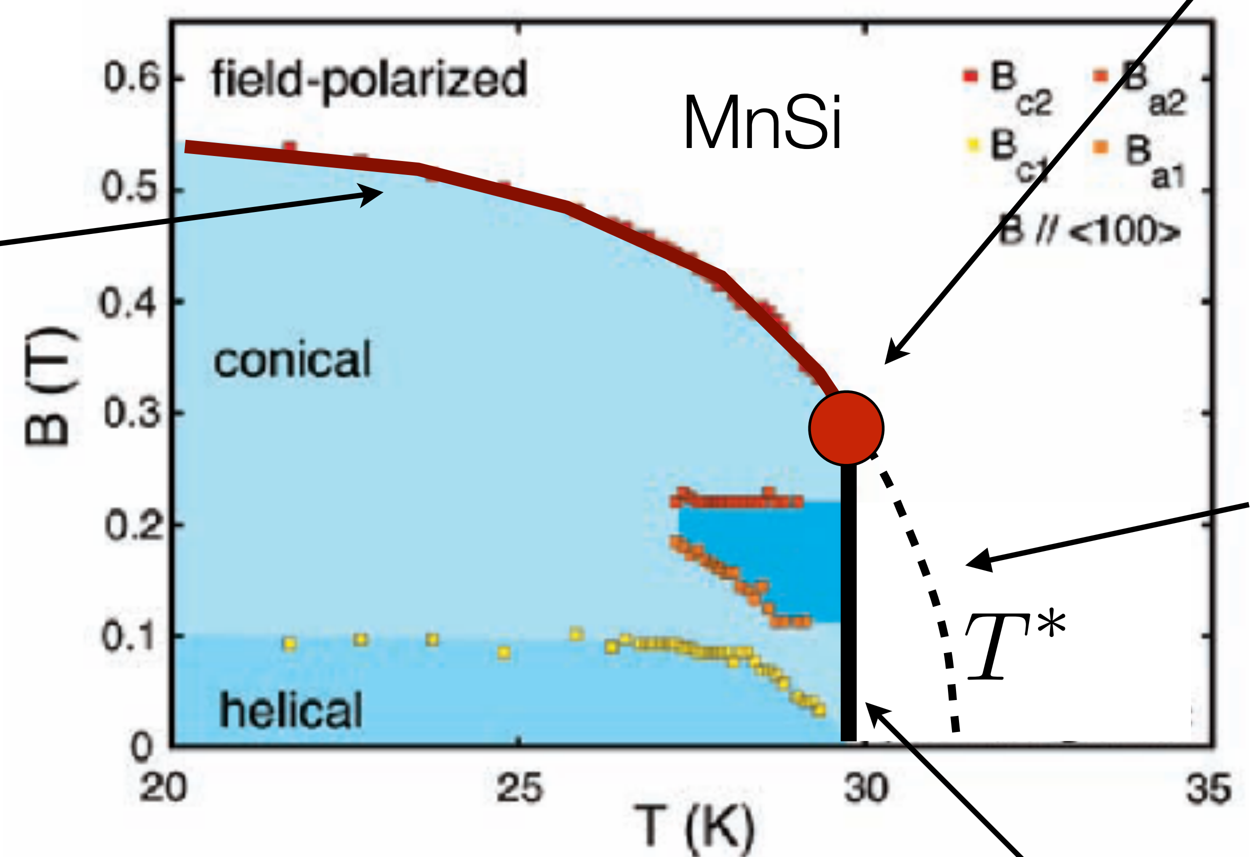

Instead:
fluctuations suppress
the ordering - crossover

fluctuation-induced first-order
weak crystallisation transition!

Fluctuation-induced first order transition

M. Janoschek, MG et al PRB (2013)
Bauer, MG, Pfleiderer, PRL (2013)
J. Kindervater, MG, et al PRB (2014)

fluctuation-induced tricritical point

2nd order

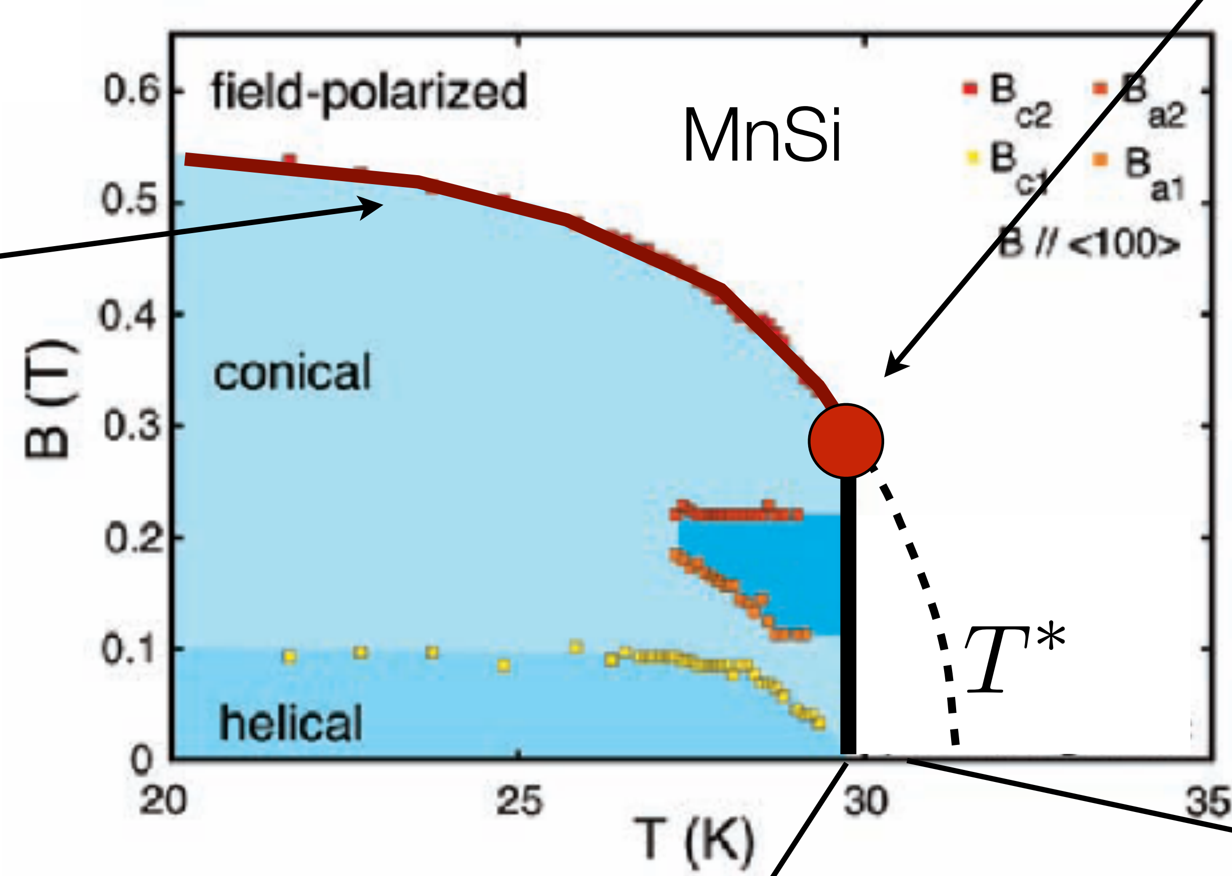

above T_c:

short-ranged ordered helices pointing in any direction

small angle neutron scattering:

softening on sphere in momentum space

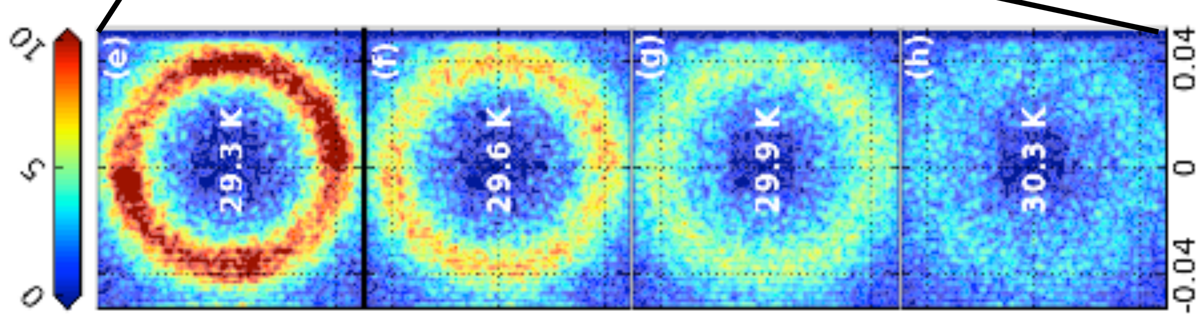

Brazovskii suppression of correlation length

temperature dependence of chiral correlation length $\kappa = 1/\xi$

Brazovskii renormalization

$\kappa^2 = \kappa_{\rm mf}^2 +$ 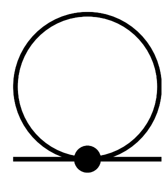

self-consistent loop

self-consistent HF

quasi-1d divergence

⇨ suppression of ξ ,

fluctuations inhibit the condensation of long-range order

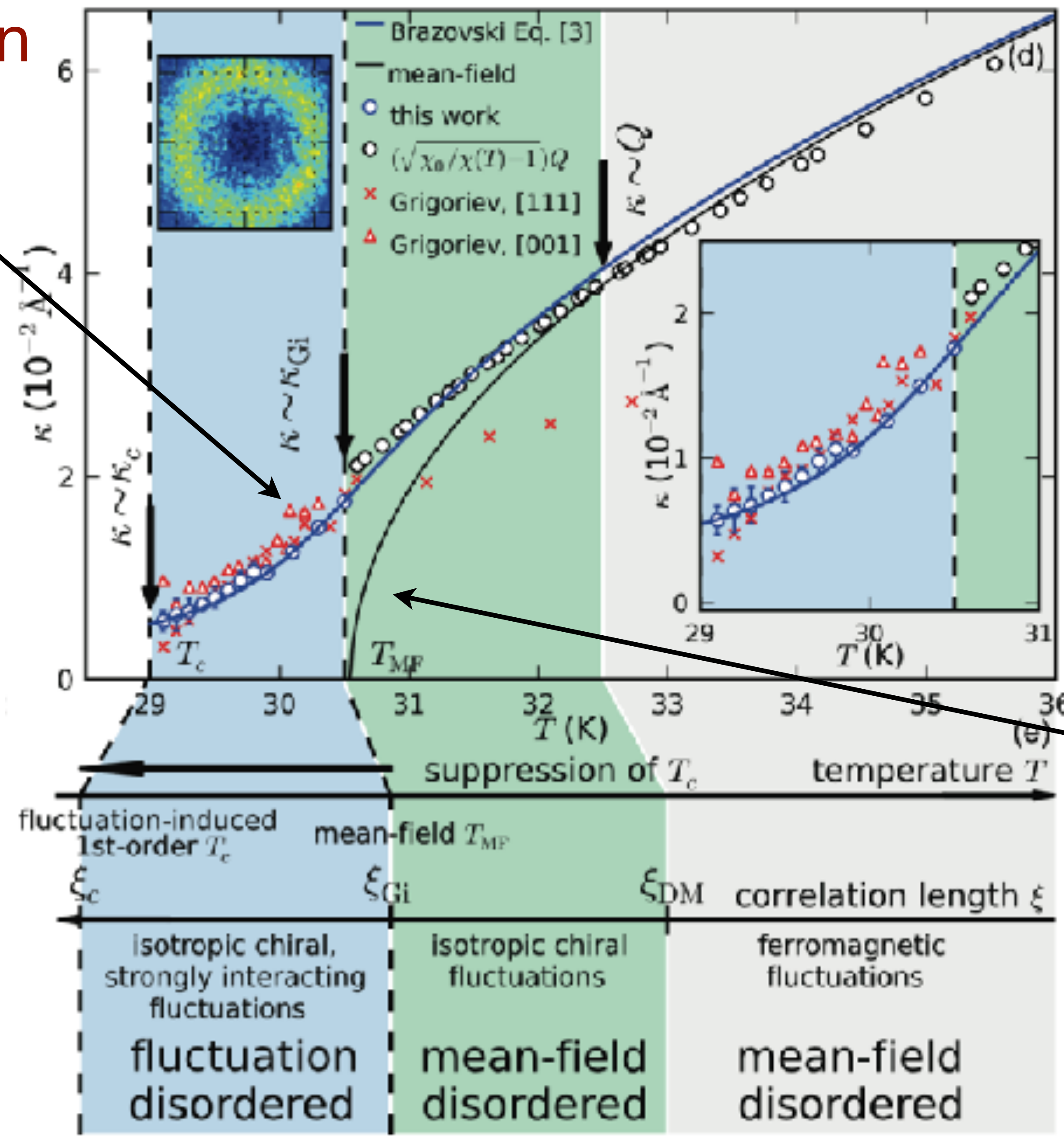

mean-field

$$1/\xi \sim \sqrt{T - T_{\rm mf}^{\rm hel}}$$

Janoschek et al. PRB (2013)

Brazovskii renormalization in thermodynamics

inverse correlation length

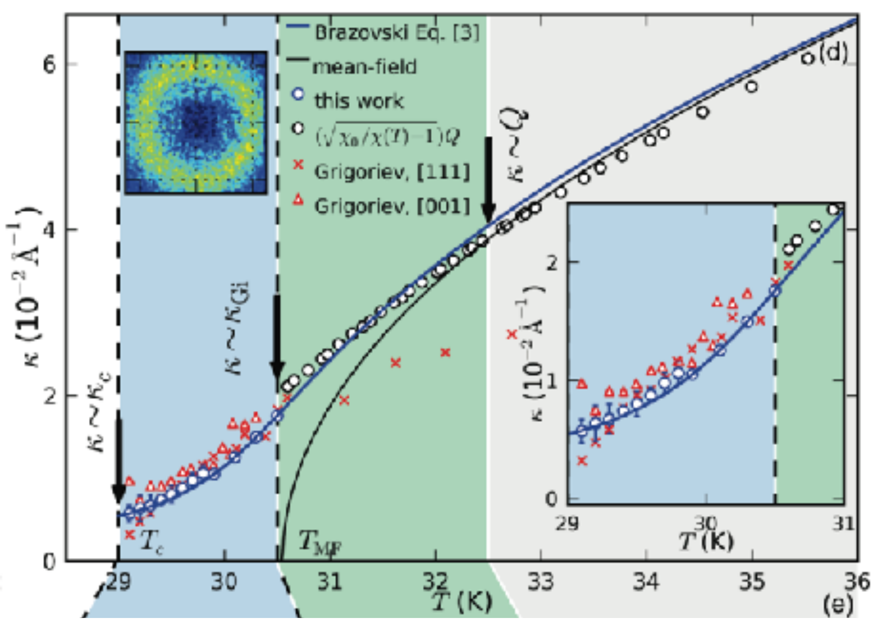

X

susceptibility

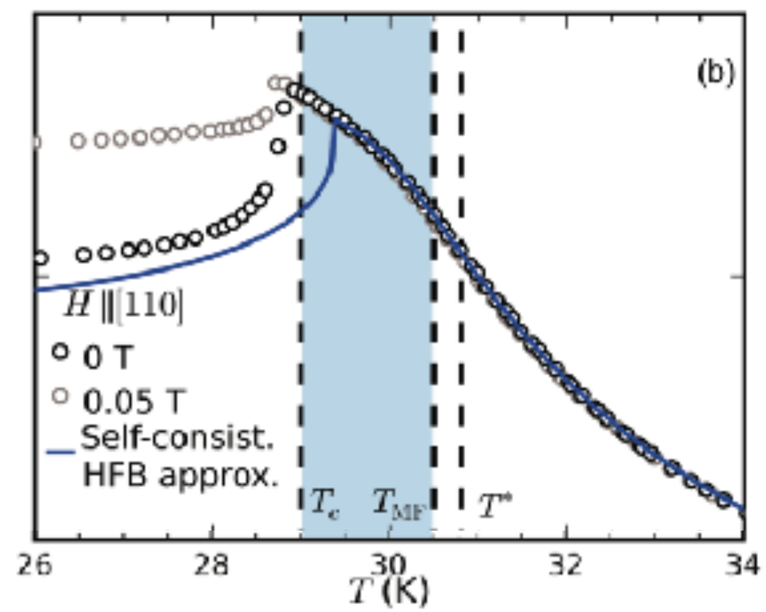

specific heat

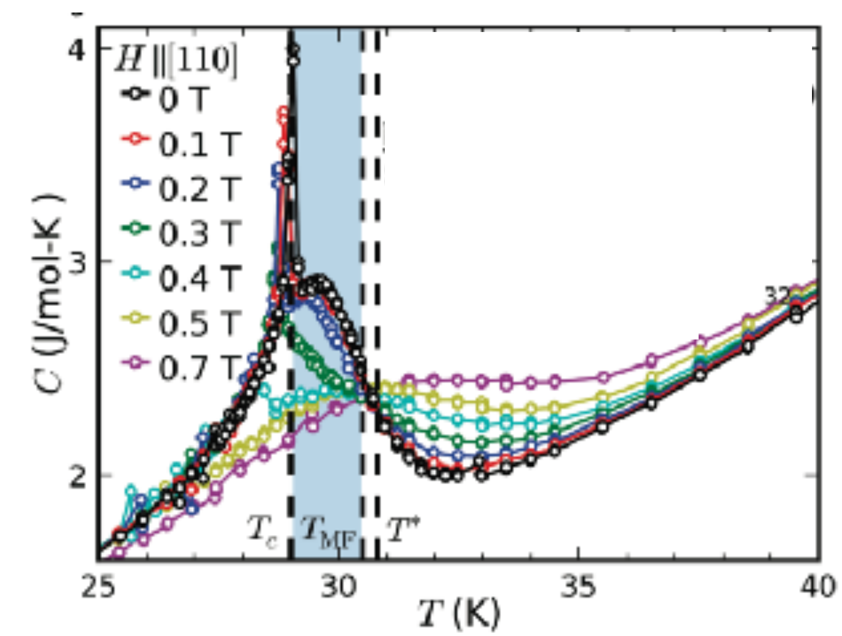

strongly correlated fluctuation-disordered regime

turning point

$$\chi^{-1} \propto \kappa(T)^2 + Q^2$$

crossing point
(Vollhardt invariance)

due to Maxwell relation

Janoschek et al. PRB (2013)

Helimagnon band structure

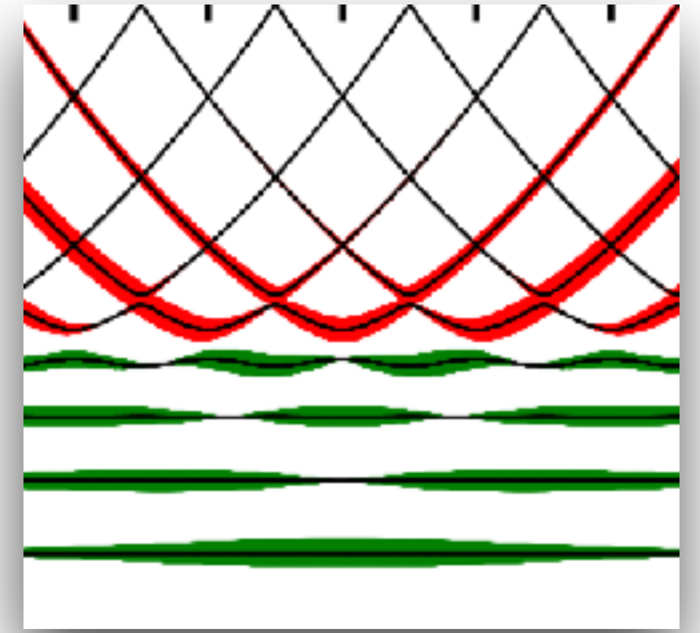

Magnetization dynamics

Landau-Lifshitz equation

wikipedia

$$\underbrace{\partial_t \vec{M} = -\gamma \vec{M} \times \vec{B}_{\mathrm{eff}}}_{\text{precession in effective field}} \quad \underbrace{+\ldots.}_{\text{damping, driving currents etc.}}$$

effective field is determined by the magnetic texture:

$\vec{B}_{\mathrm{eff}} = -\frac{\delta F}{\delta \vec{M}}$ with the Ginzburg-Landau functional F

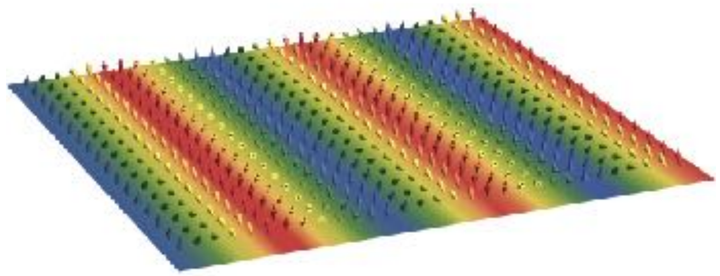

Magnon excitations:

expansion around the static magnetization $\hat{M} = \hat{M}_s \sqrt{1 - 2|\psi|^2} + \hat{e}^+ \psi + \hat{e}^- \psi^*$

⇨ Bogoliubov wave equation

$$\boxed{i\hbar\tau^z \partial_t \vec{\Psi} = H \vec{\Psi}}$$

with magnon spinor wave function

$$\vec{\Psi}^T = (\psi, \psi^*)$$

U(1) charge = spin angular momentum of magnon not conserved!

due to spin-orbit coupling, texture and dipolar interactions

Magnon excitations of the magnetic helix

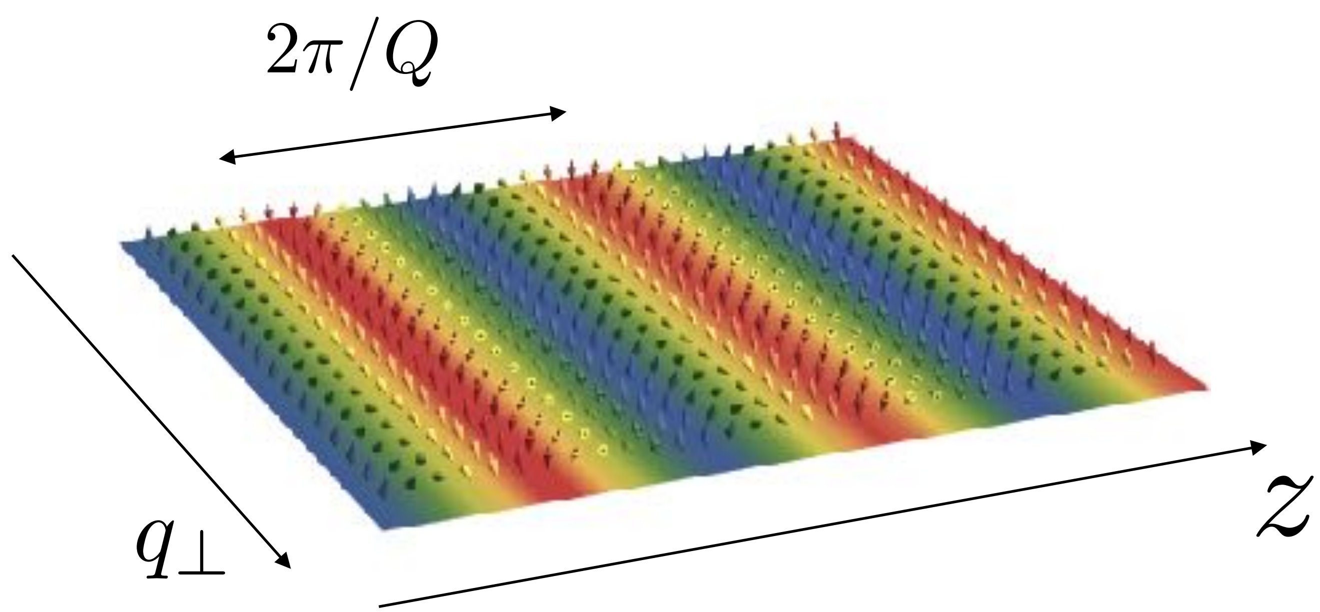

helix = 1d magnetic crystal

magnon excitations obey Bloch's theorem

⇨ magnon band structure

magnon Hamiltonian:

$$\mathcal{H}_0 = \mathcal{D}\left[\mathbb{1}(q_\perp^2 - \partial_z^2) - i2\tau^z Q q_\perp \cos(Qz) + \frac{Q^2}{2}(\mathbb{1} - \tau^x)\right]$$

variant of the Mathieu equation

⇨ particle in a one-dimensional periodic cosine potential

Kugler *et al* PRL (2015)
Weber, *et al* arXiv:1708.02098

Magnon excitations of the magnetic helix

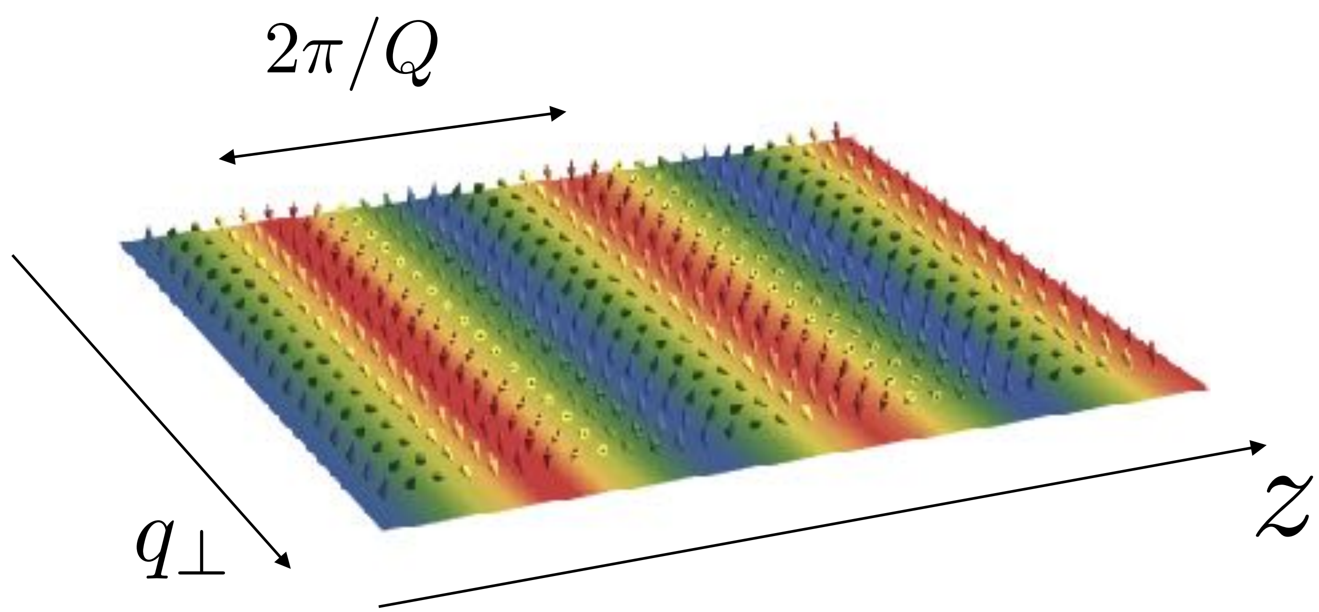

helix = 1d magnetic crystal

magnon excitations
obey Bloch's theorem

$\Rightarrow$ magnon band structure

transversal momentum $q_\perp$ tunes strength of periodic potential
crossover from weak to tight-binding limit

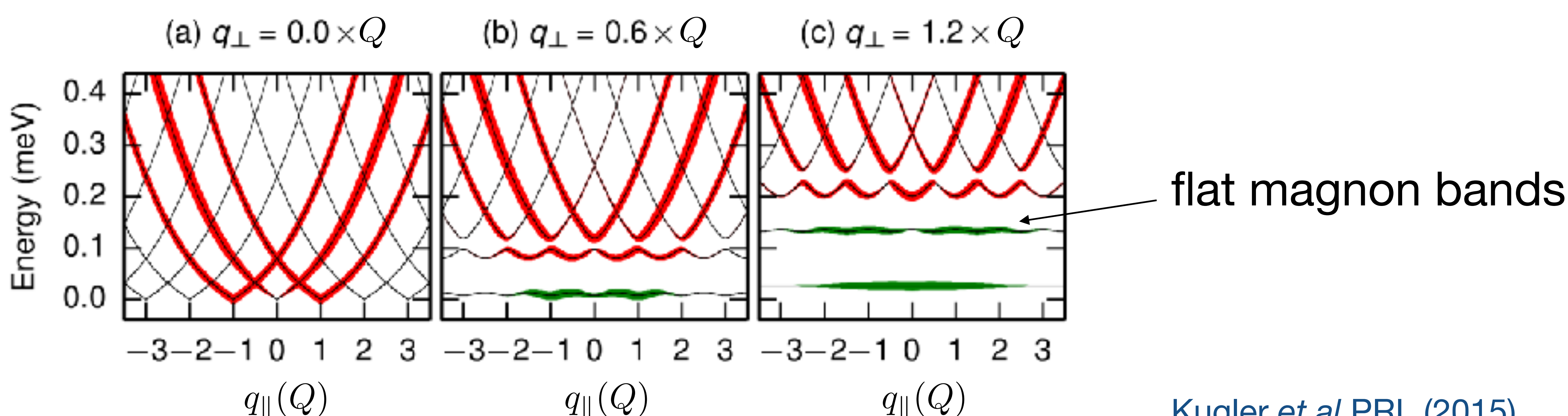

Kugler *et al* PRL (2015)
Weber, *et al* arXiv:1708.02098

Magnon excitations of the magnetic helix

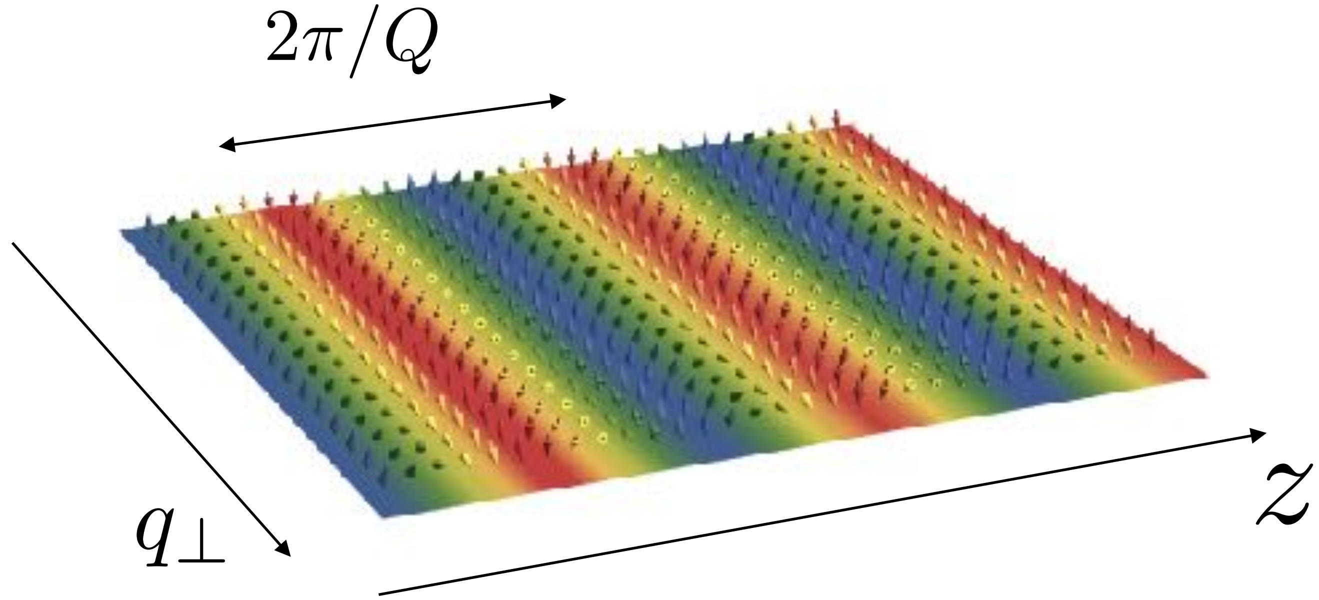

helix = 1d magnetic crystal

magnon excitations
obey Bloch's theorem

⇨ magnon band structure

Inelastic neutron scattering on MnSi:

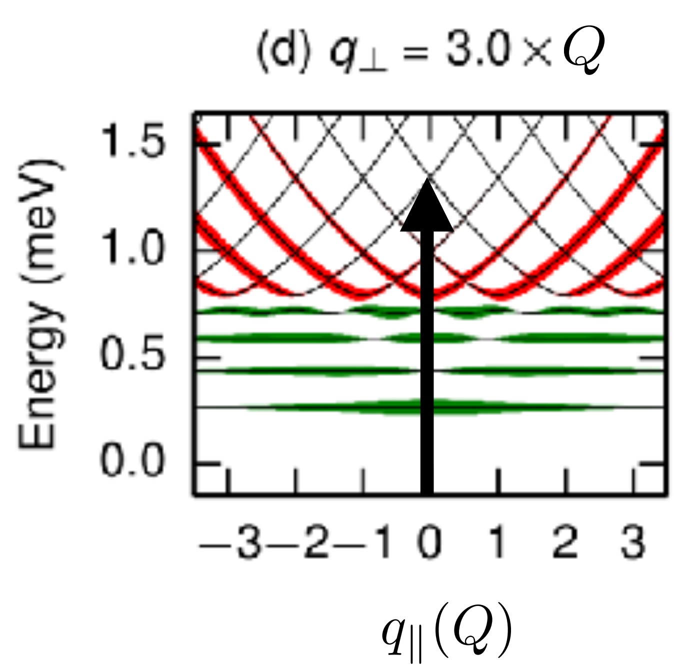

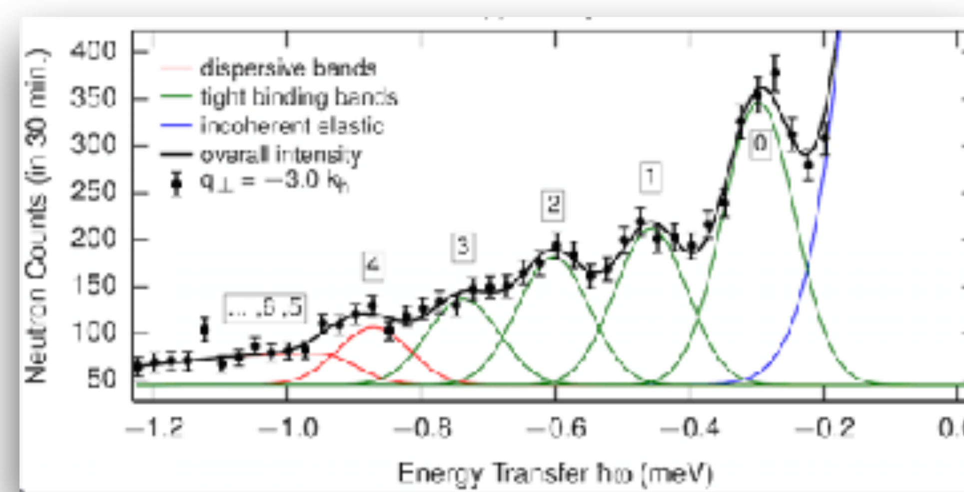

five magnon bands
well-resolved

Kugler *et al* PRL (2015)
Weber, *et al* arXiv:1708.02098

Skyrmions

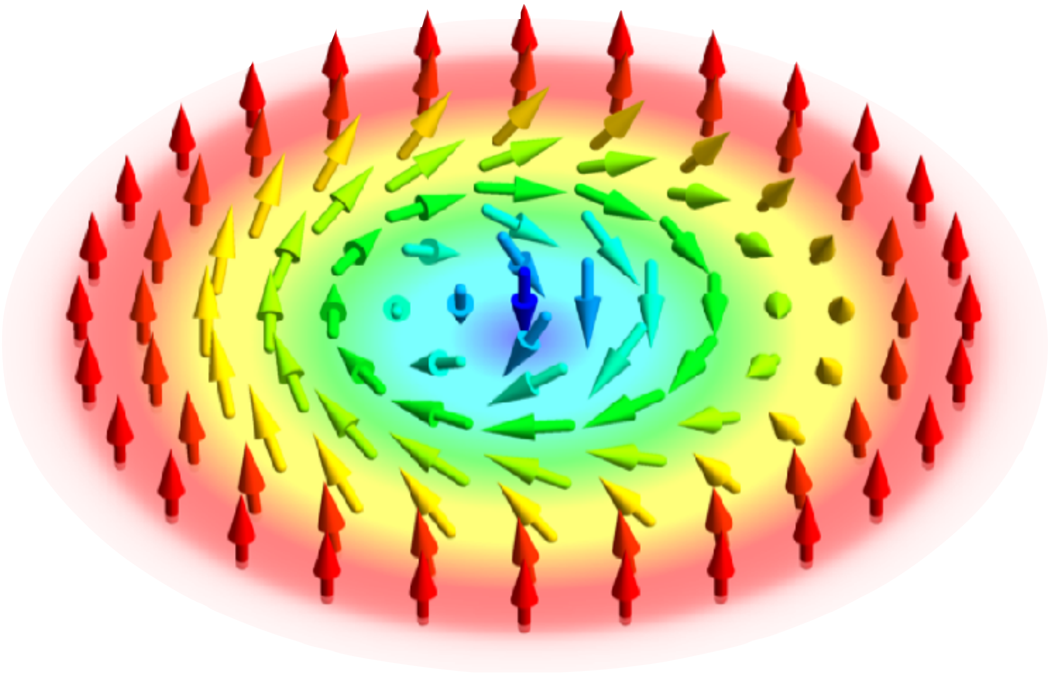

Skyrmions

Tony Skyrme (1961,1962)

solutions of a non-linear field theory,
model for baryons

B=3

(isospin doublet $^3H/^3He$)

stereographic projection from sphere to plane:

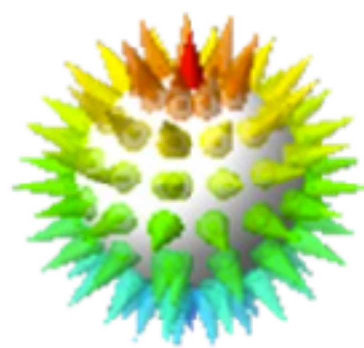

hedgehog

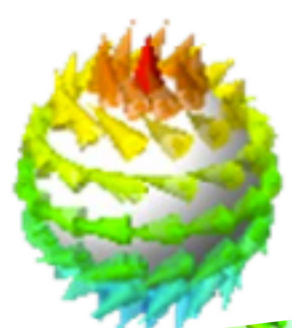

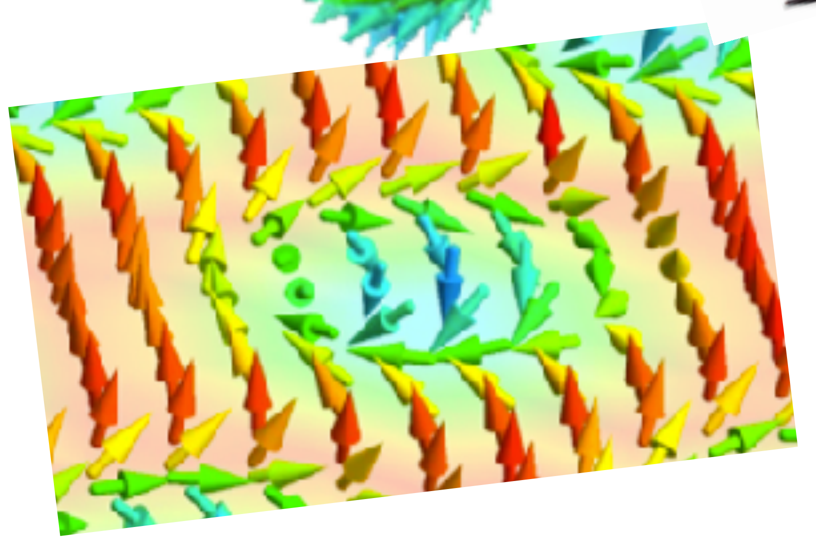

topologically stable object with quantized winding number

$$W = \frac{1}{4\pi}\int d^2\mathbf{r}\,\hat{M}\left(\partial_x\hat{M}\times\partial_y\hat{M}\right)$$

counts skyrmions!

$\Pi_2(S^2) = \mathbb{Z}$ baby-skyrmions

Observation of skyrmion crystals in B20 compounds

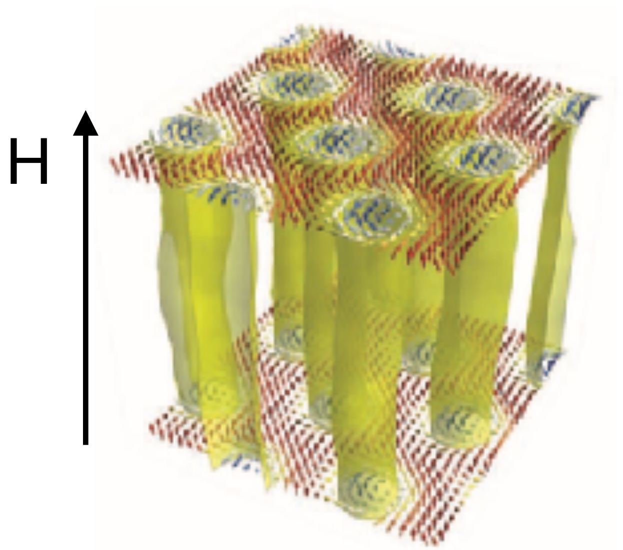

2d skyrmion crystal

First observation by neutron scatterin

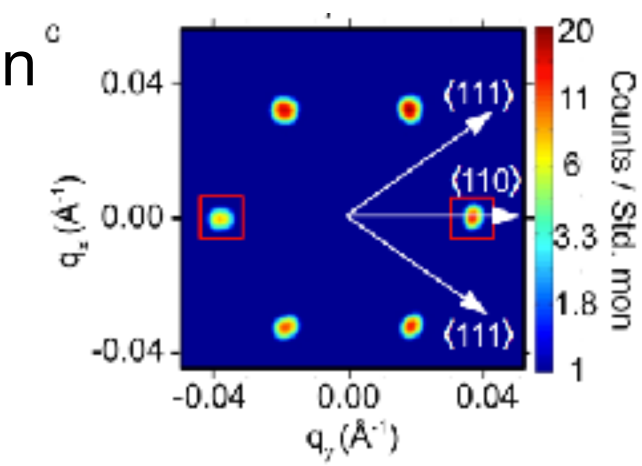

in MnSi

S. Mühlbauer *et al.* Science (2009)
T. Adams et al. PRL (2011)

in $Fe_{1-x}Co_xSi$

W. Münzer *et al.* PRB (2010)

6-fold symmetry

correlation length: ~100 μm !

transmission electron microscopy on films:

in $Fe_{0.5}Co_{0.5}Si$

X. Z. Yu *et al.* Nature (2010)

in FeGe

X. Z. Yu *et al.* Nature Materials (2011)

in Cu_2OSeO_3

S. Seki et al. Science (2012)

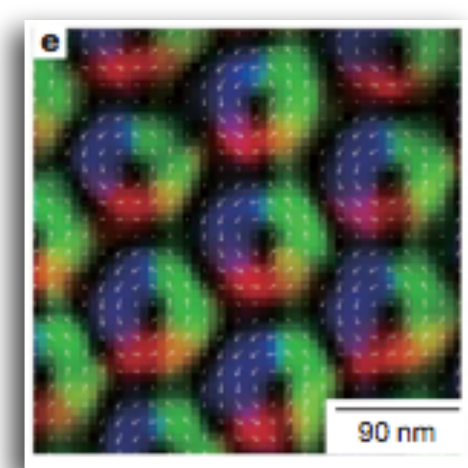

$Fe_{0.5}Co_{0.5}Si$

Magnetic force microscopy

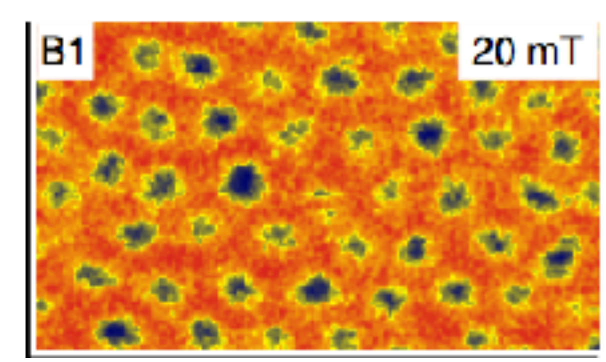

in $Fe_{0.5}Co_{0.5}Si$

P. Milde *et al.* Science (2013)

Consequences of non-trivial topology

Topological Hall effect

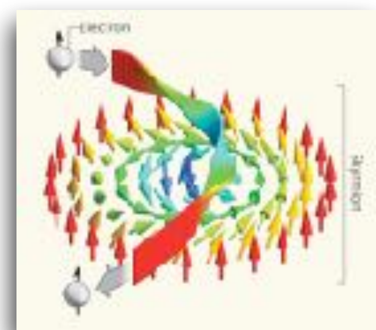

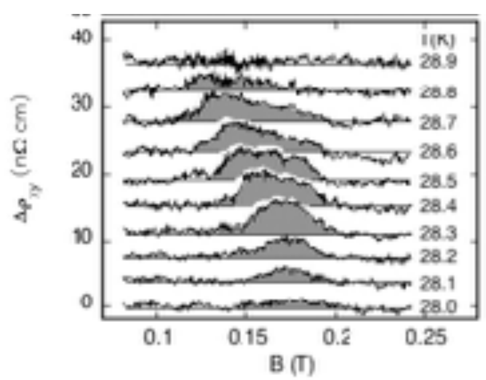

A. Neubauer *et al.* PRL (2009)

Spin Magnus force

moving skyrmions are deflected

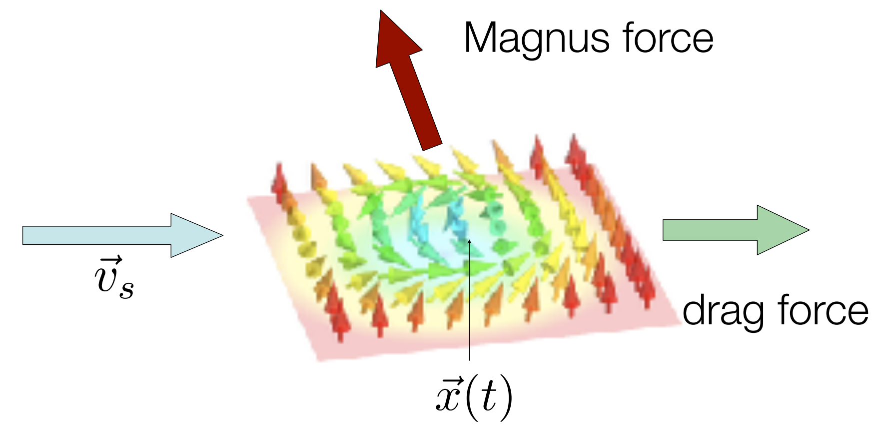

Jonietz et al., Science (2010)

Skyrmion-flow Hall effect

emergent electrodynamics

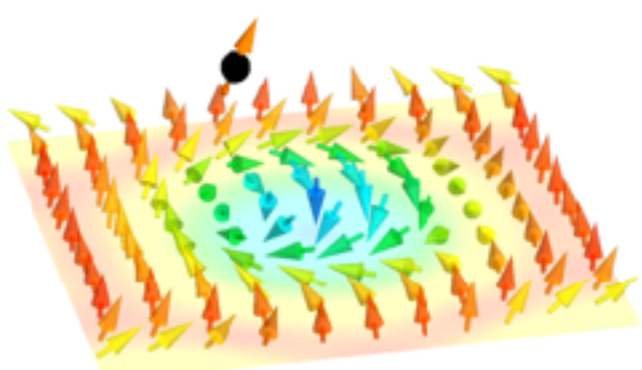

Schulz et al, Nature Physics (2012)

Spintronics with ultralow threshold current

$$j_c \sim 10^6 A/m^2$$

Skyrmion hosting materials

Néel 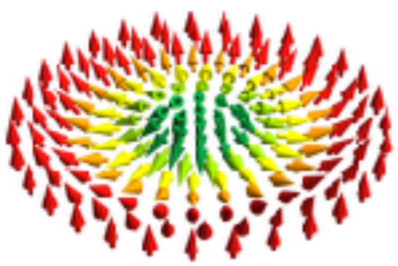 Bloch 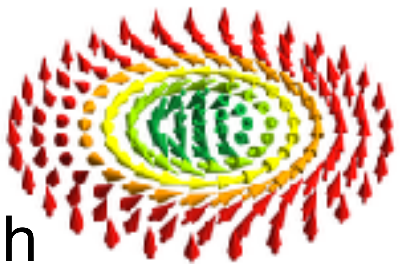

Material	Crys. Class	SG	Skyrm. Type	T_c	λ (nm)	Trans.	References
MnSi	*T*	$P2_13$	Bloch	30 K	18	Metal	S. Mühlbauer *et al.*, Science **323**, 915 (2009)
FeGe	*T*	$P2_13$	Bloch	279 K	70	Metal	X.Z. Yu *et al.*, Nat. Mater. **10**, 106 (2010)
$\mathbf{Fe_{1-x}Co_x}$Si	*T*	$P2_13$	Bloch	< 36 K	40-230	Semi-cond.	W. Münzer *et al.*, PRB **81**, 041203(R) (2010) X.Z. Yu *et al.*, Nature **465**, 901 (2010)
$\mathbf{Mn_{1-x}Fe_x}$Si	*T*	$P2_13$	Bloch	< 17 K	10-12	Metal	S.V. Grigoriev *et al.*, PRB **79**, 144417 (2009)
$\mathbf{Mn_{1-x}Fe_x}$Ge	*T*	$P2_13$	Bloch	< 220 K	5–220	Metal	K. Shibata *et al.*, Nat. Nanotech. **8**, 723–728 (2013)
$\mathbf{Cu_2}OSeO_3$	*T*	$P2_13$	Bloch	58 K	60	**Insulator**	S. Seki *et al.*, Science **336**, 198 (2012) T. Adams *et al.*, PRL **108**, 237204 (2012)
$\mathbf{Co_x}Zn_y\mathbf{Mn_z}$	O	$P4_132$ / $P4_332$	Bloch	**150 K – 500 K**	120 – 200	Metal	Y. Tokunaga *et al.*, Nat. Commun. **6**, 7638 (2015)
(**Fe,Co**)$_2$Mo$_3$N	O	$P4_132$ / $P4_332$	Bloch	< 36 K	110	Metal	W. Li *et al.*, Phys. Rev. B **93**, 060409(R) (2016)
Ga$\mathbf{V_4}$S$_8$	C_{3v}	R3m	**Néel**	13 K	17	Semicond/ Insulator	I. Kézsmárki *et al.*, Nat. Mater. **14**, 1116 (2015)

Table from Jonathan White

Skyrmions in magnetic multilayers

lack of inversion at interfaces:

interfacial Dzyaloshinskii-Moriya interaction

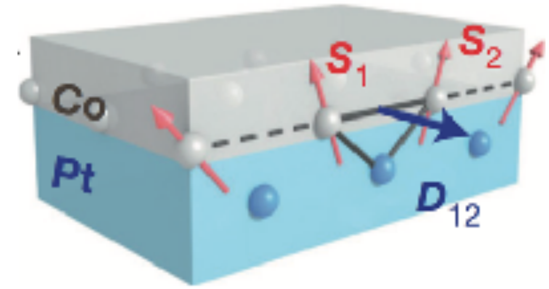

Fert & Levy, PRL (1980)

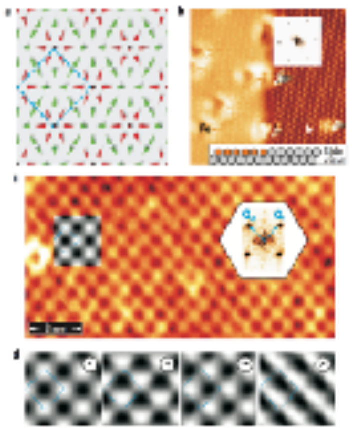

small Neel skyrmions in Fe monolayer on Ir(111)

S. Heinze et al, Nat Phys. (2011)

controlled creation and annihilation in a PdFe bilayer

N. Romming et al, Science (2013)

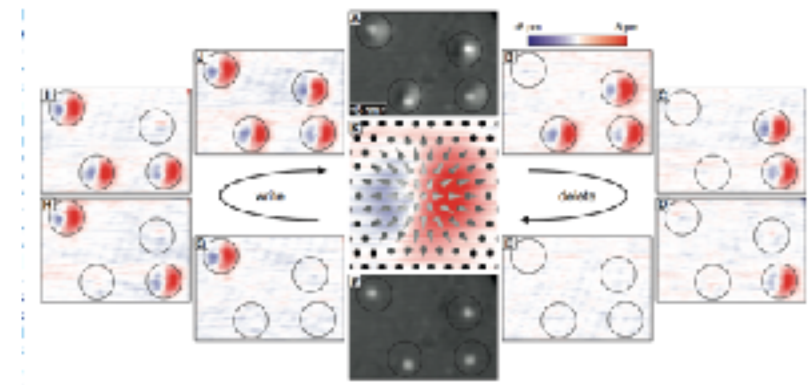

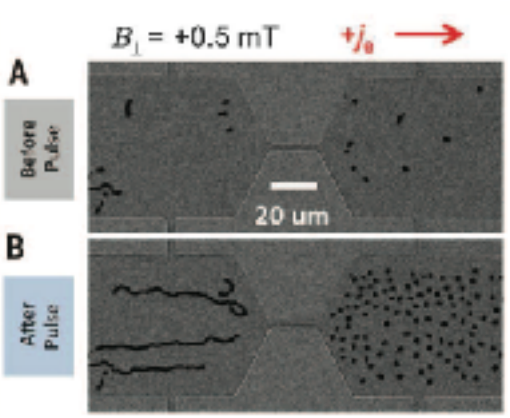

W. Jiang et al, Science (2015)

HM/F/I trilayer

Ir/Co/Pt multilayer with additive interfacial chiral interactions → strong DMI at RT

C. Moreau-Luchaire *et al.*, Nat. Nanotech. **11**, 444 (2016)

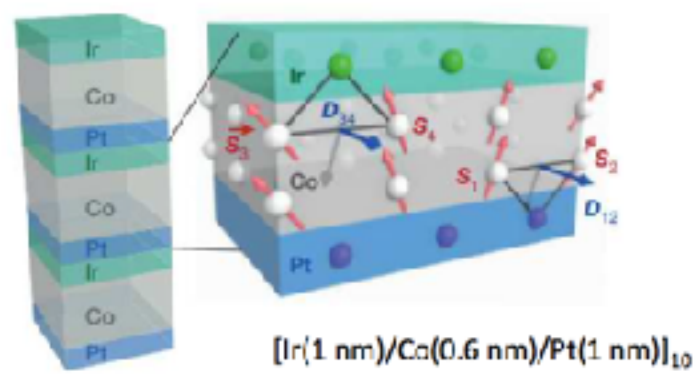

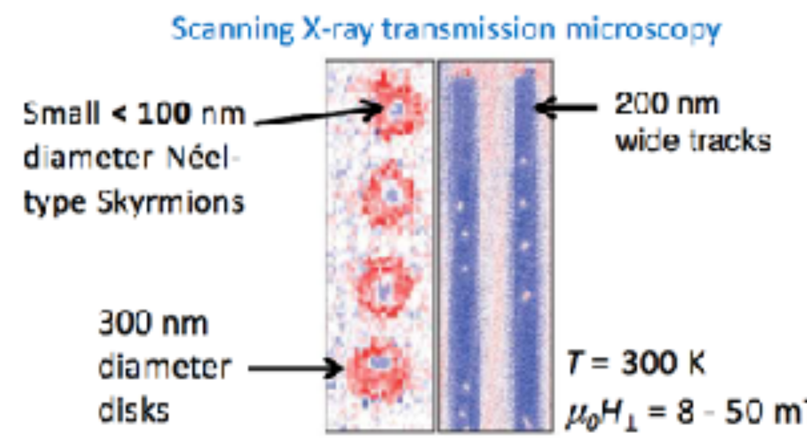

reviews: A. Soumyanarayanan *et al.* Nature 539, 509 (2016).
R. Wiesendanger, Nat. Rev. Mater. 1, 16044 (2016).
W. Jiang *et al.* AIP Advances **6**, 055602 (2016)

Skyrmion in a field-polarised background

standard model for chiral magnets:

$$\mathcal{L} = A(\nabla \hat{M})^2 + D\hat{M}(\nabla \times \hat{M}) - M_s \hat{M} \mu_0 \vec{H}$$

Dzyaloshinskii-Moriya
interaction

static soliton solution $\hat{M}_s(\mathbf{r})$

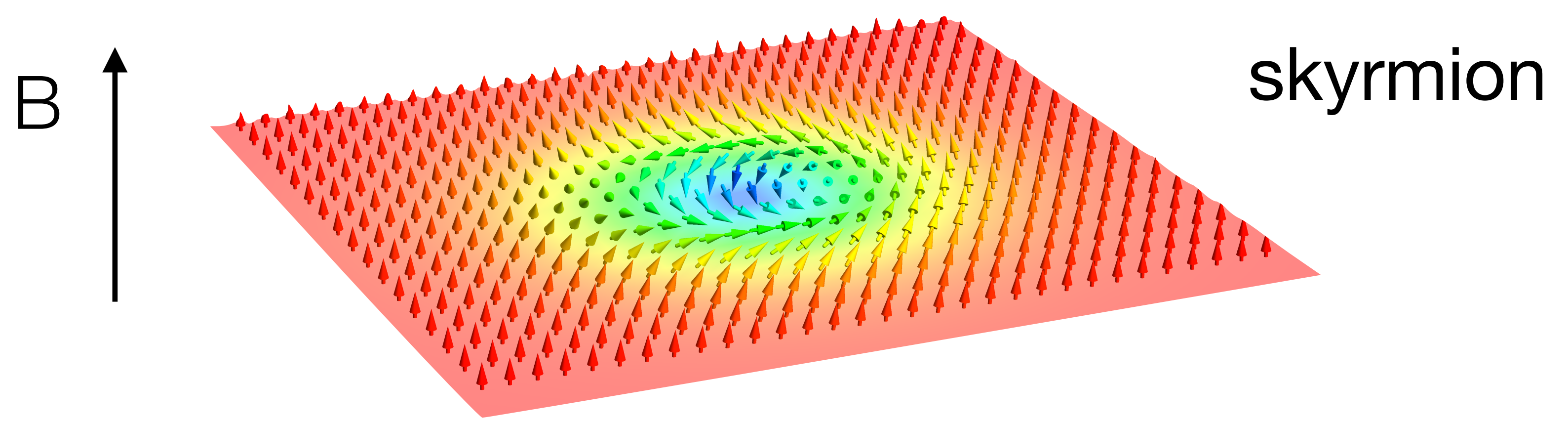

Bogdanov & Hubert (1994)

Equation of motion for the skyrmion

Thiele approach:

project Landau-Lifshitz equation onto translational zero mode

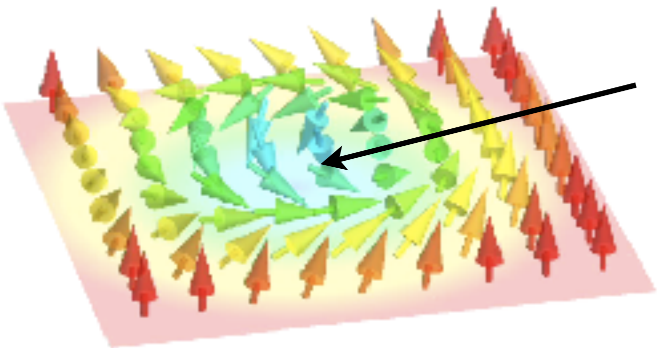

$\vec{R}(t)$ center-coordinate of a skyrmion

A. A. Thiele, PRL (1973)

$$\partial_t \vec{M} = -\gamma \vec{M} \times \vec{B}_{\text{eff}} \quad + \ldots . \quad \Rightarrow \quad \vec{G} \times \partial_t \vec{R}(t) = \vec{F}$$

F: damping, disorder, driving currents etc.

effective equation of motion:

massless particle in an effective magnetic field G

$$\vec{G} = \mathcal{S} \hat{z} \int d^2\mathbf{r} \hat{M} (\partial_x \hat{M} \times \partial_y \hat{M}) \quad \Leftarrow \text{ topological winding number}$$

gyrocoupling vector

S: spin density

Skyrmion topology ⇨ spin magnus force $\vec{G}$

$$\boxed{\vec{G} \times \partial_t \vec{R}(t) = \vec{F}}$$

massless particle in an effective magnetic field

(on tree-level)

magnetization dynamics of a skyrmion:

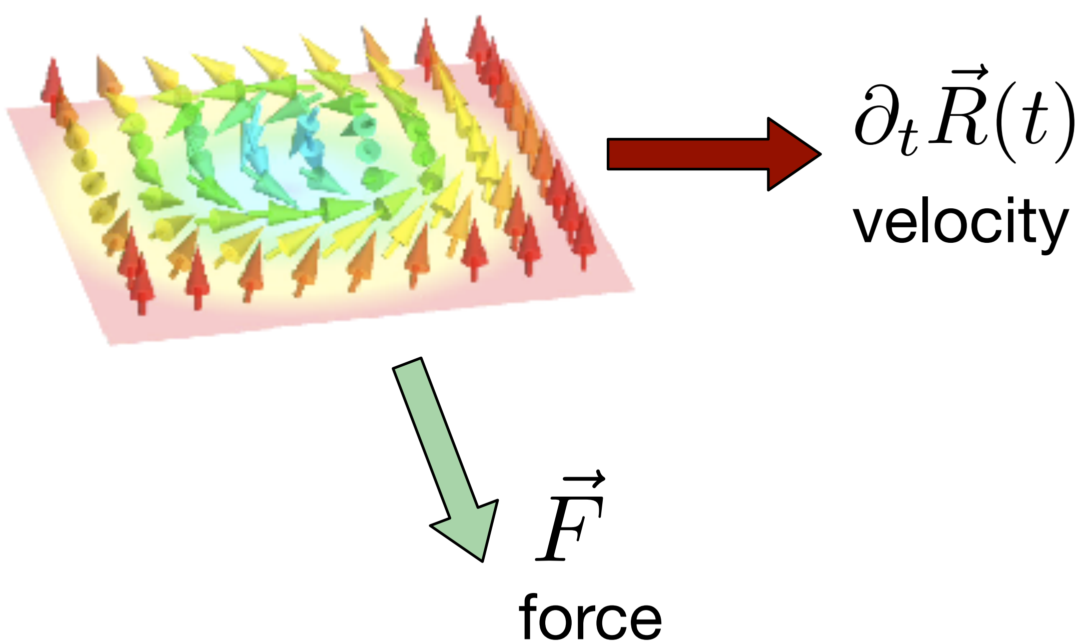

skyrmion moves perpendicular to the force!

similar to the guiding center of electrons in a strong magnetic field (lowest Landau level)

Magnons in the presence of a skyrmion

static skyrmion-soliton solution

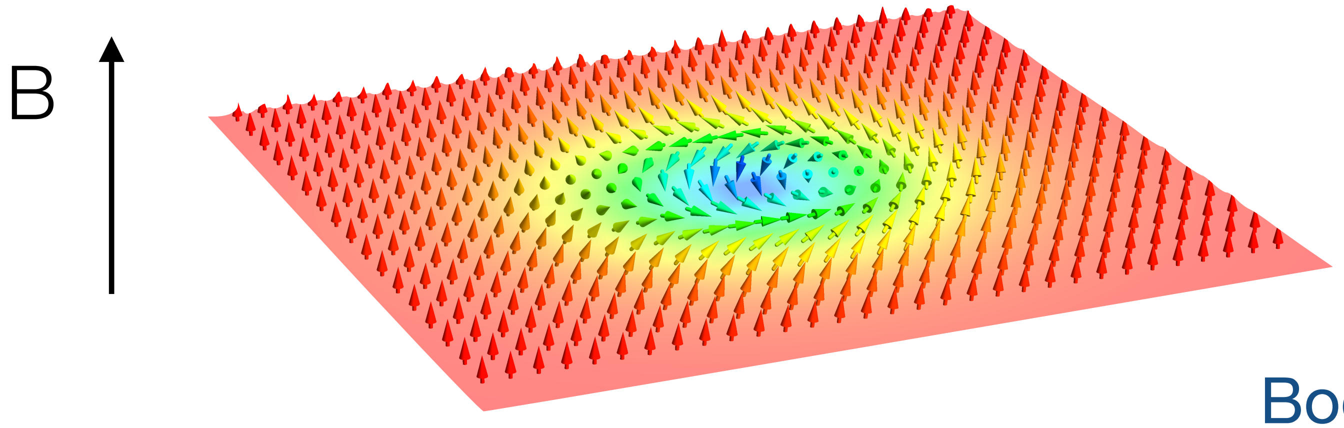

Bogdanov & Hubert (1994)

spin-waves scatter off the skyrmion ⇨ magnon scattering problem

Bogoliubov Hamiltonian

$$\mathcal{H} = \frac{\hbar^2(-i\tau^z\vec{\nabla} - \mathbf{1}\vec{a})^2}{2M_{\rm mag}} + \mathbf{1}\mathcal{V}_0 + \tau^x\mathcal{V}_x$$

scattering vector potential

scattering potentials

Magnon-skyrmion bound states

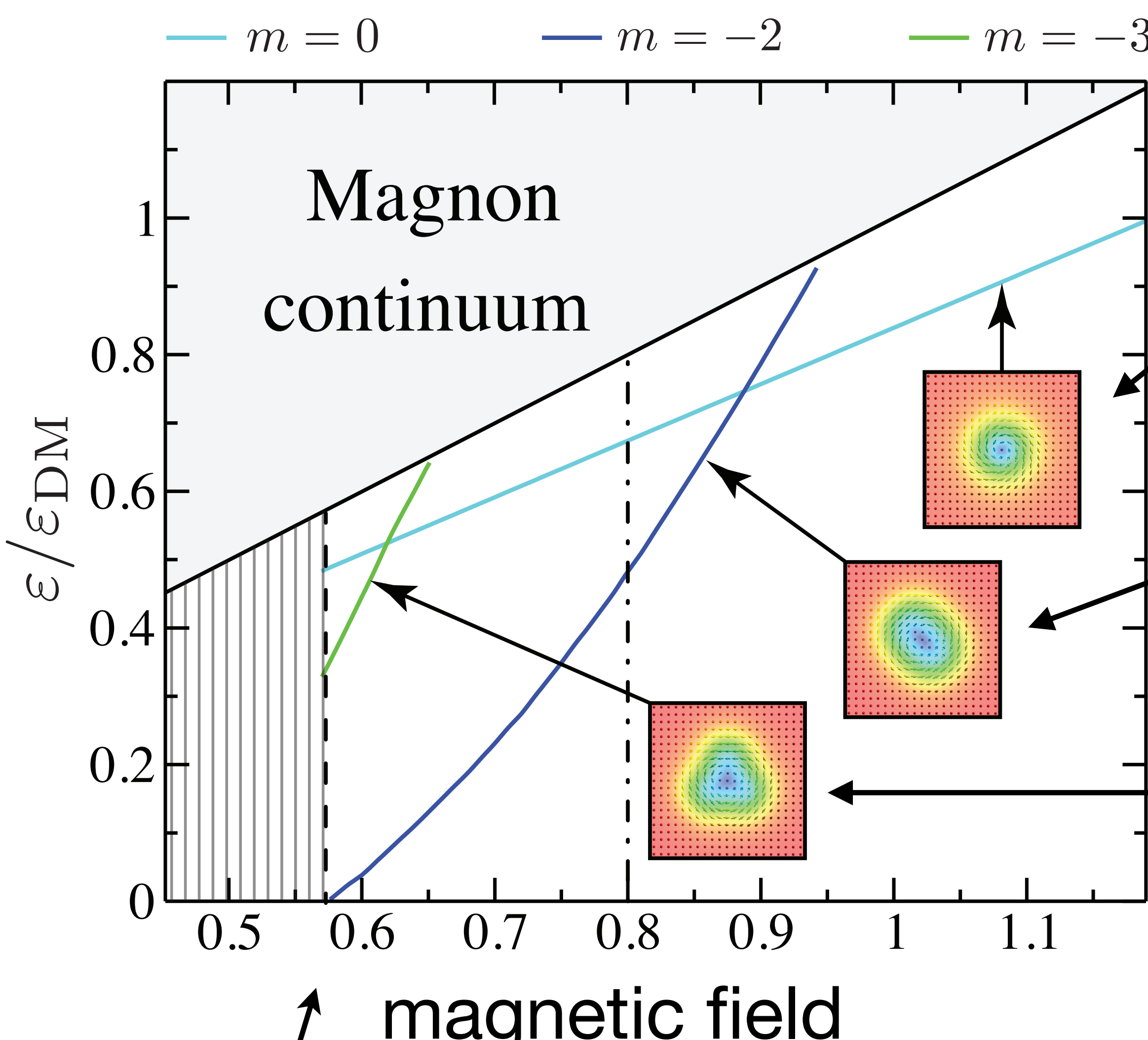

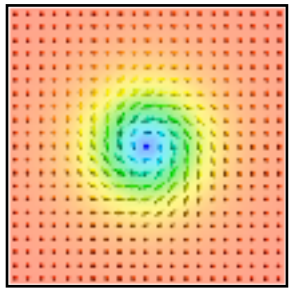

breathing mode

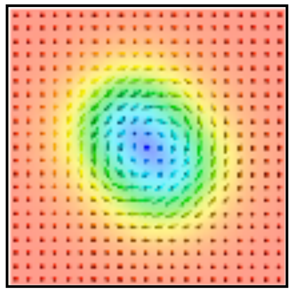

quadrupolar mode

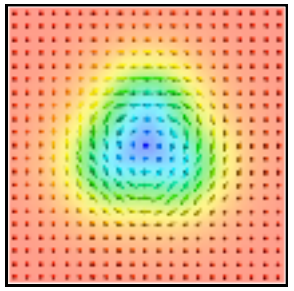

sextupolar mode

local elliptical instability

global instability

magnon-skyrmion bound states

⇨ thermally excited subgap states!

see also Lin, Batista & Saxena PRB (2014)

Schütte & MG PRB (2014)

Emergent magnon Lorentz force

adiabatic adjustment of local frame

⇨ Berry phase

vector scattering potential $\vec{a}$

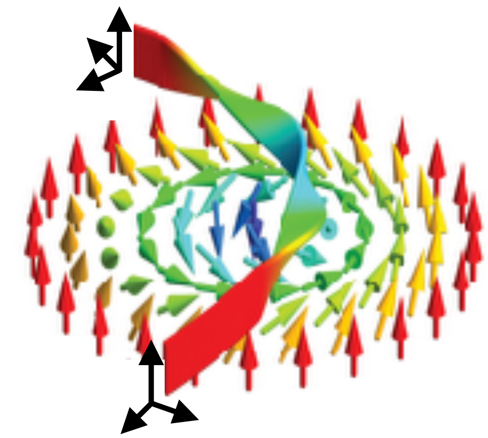

with quantised total flux

$$\int d^2\mathbf{r}(\nabla \times \vec{a}) = \int d^2\mathbf{r}\hat{M}(\partial_x\hat{M} \times \partial_y\hat{M})$$

⇦ topological winding number

magnon scatter off a localised emergent magnetic flux

due to non-trivial topology of skyrmion

⇨ emergent Lorentz force

Topological magnon skew scattering

WKB wave function

incoming
magnon wave

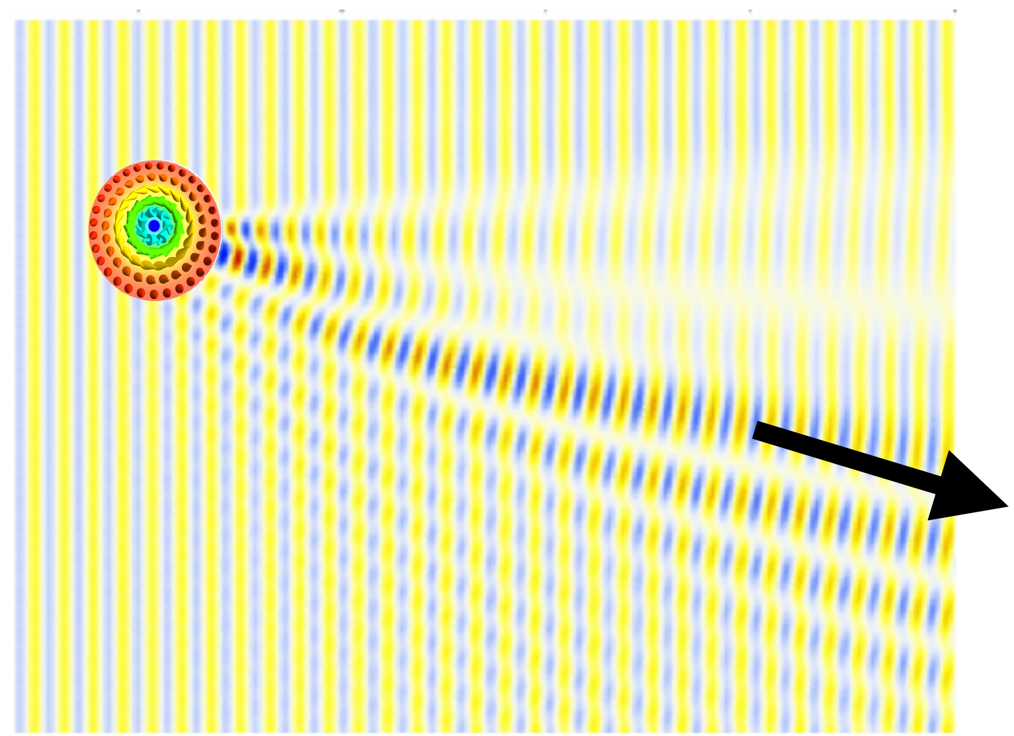

scattered to the
right-hand side

emergent Lorentz force leads to skew scattering for high-energy magnons!

⇨ topological magnon Hall effect!

see also Iwasaki, Beekman & Nagaosa PRB (2014)
Mochizuki *et al.* Nat. Mat. (2014)

Schütte & MG PRB (2014)
Schroeter & MG LTP (2015)

Skew & rainbow scattering

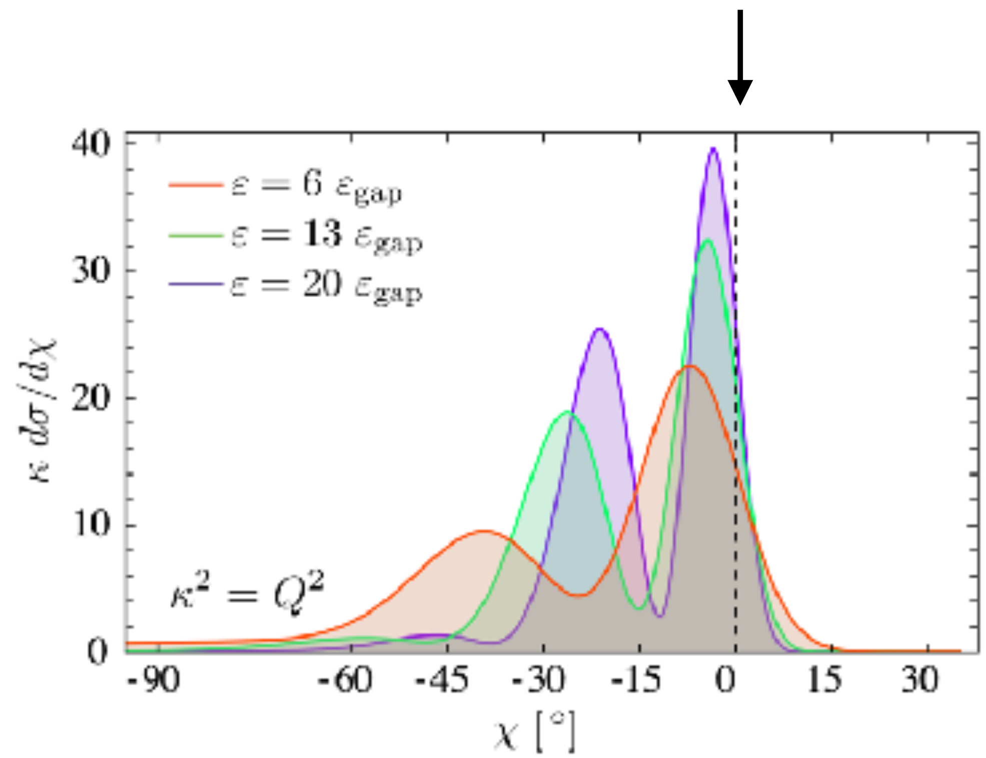

magnon differential cross section

asymmetric & oscillations

Different classical trajectories contribute and interfere!

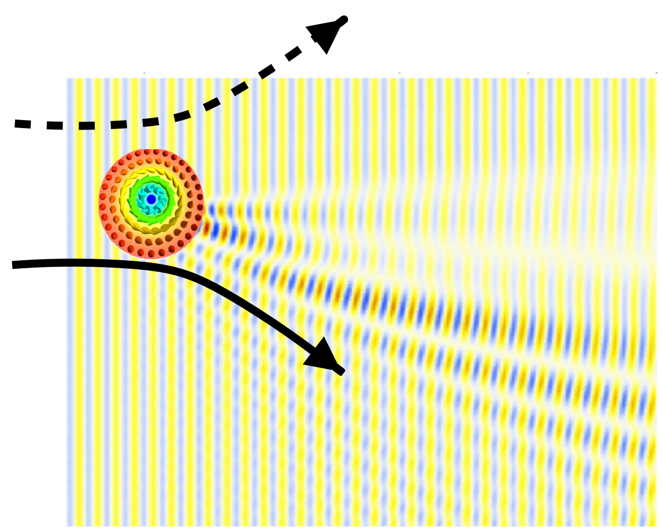

rainbow scattering!

Schütte & MG PRB (2014)
Schroeter & MG LTP (2015)

Skew & rainbow scattering

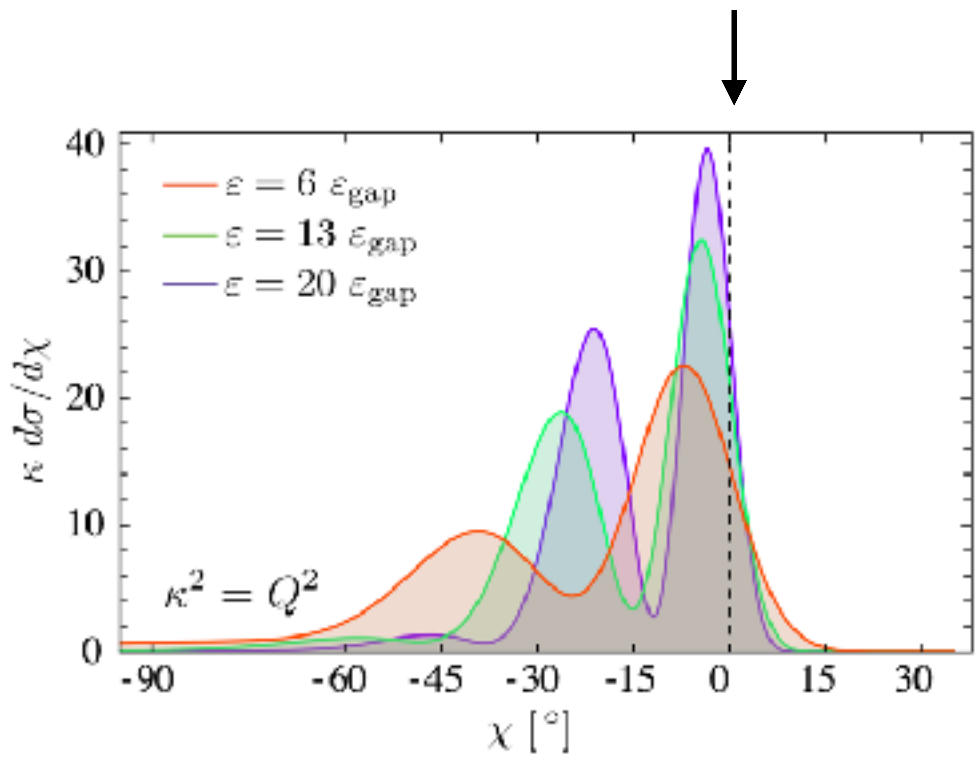

magnon differential cross section

asymmetric & oscillations

Different classical trajectories contribute and interfere!

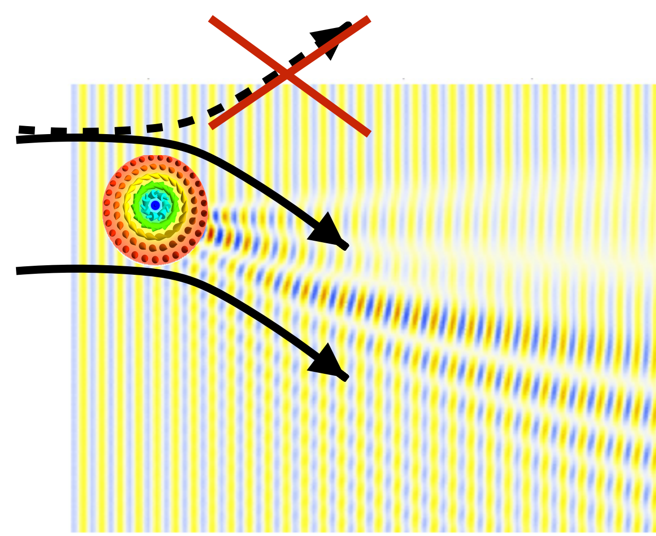

rainbow scattering!

Schütte & MG PRB (2014)
Schroeter & MG LTP (2015)

How to drive skyrmions with magnon currents?

incoming momentum

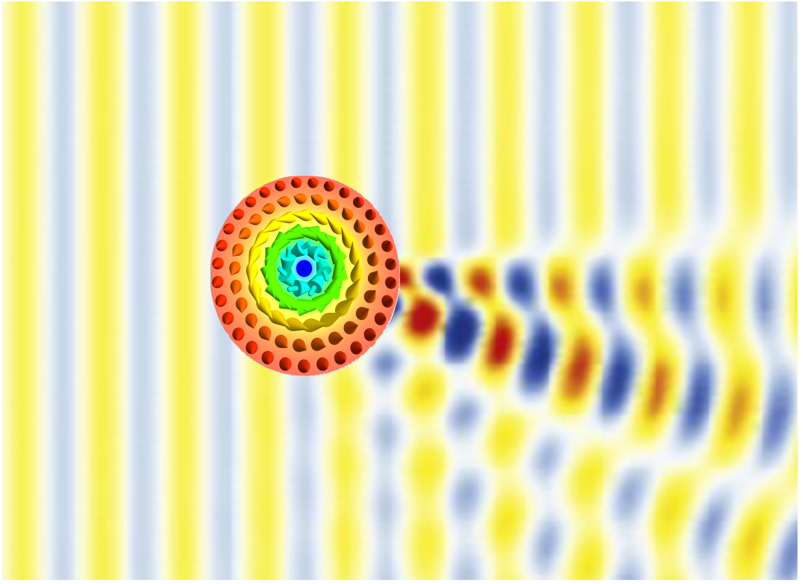

magnon wave exerts a pressure on the skyrmion…

in which direction will it move?

momentum conservation?

Driving skyrmions with magnon currents

incoming magnon wave transfers momentum to the skyrmion

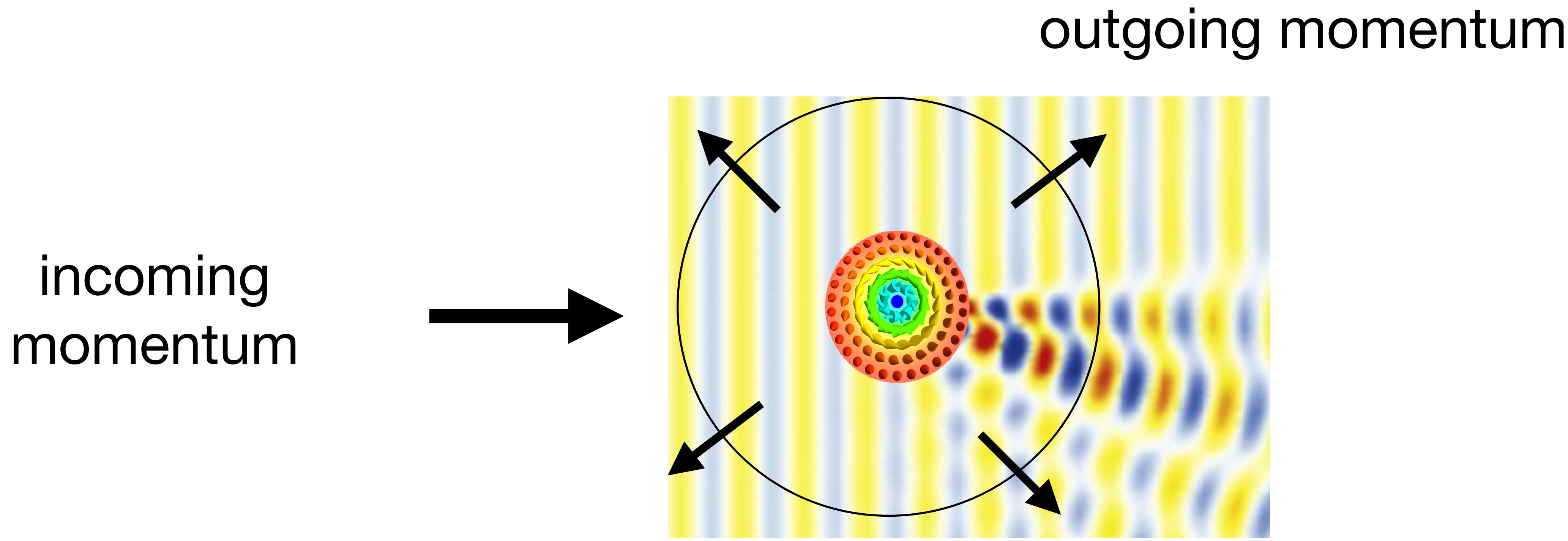

counting net flux of incoming & outgoing momentum
using conservation of energy-momentum tensor

$$\partial_\mu T_{\mu\nu} = 0$$

⇨ force in the Thiele equation

$$\boxed{\vec{G} \times \partial_t \vec{R}(t) = \vec{F}}$$

Linear response approximation

Thiele equation with a magnon force

$$\vec{G} \times \partial_t \vec{R}(t) = \vec{F}$$

Linear response: evaluate force F for skyrmion at rest $\dot{R} = 0$

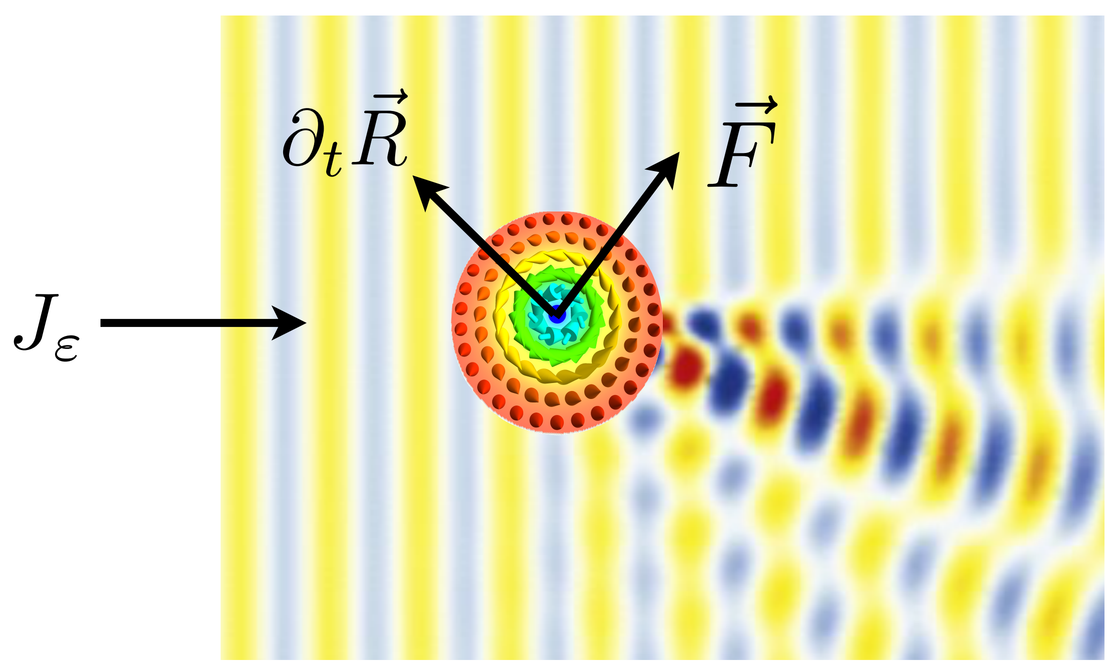

momentum-transfer force

after some algebra using optical theorem:

$$\vec{F} = J_\varepsilon\, k \begin{pmatrix} \sigma_{\parallel}(\varepsilon) \\ \sigma_{\perp}(\varepsilon) \end{pmatrix}$$

magnon force determined by transport scattering cross sections:

with

$$\begin{pmatrix} \sigma_{\parallel}(\varepsilon) \\ \sigma_{\perp}(\varepsilon) \end{pmatrix} = \int_0^{2\pi} d\chi \begin{pmatrix} 1 - \cos\chi \\ -\sin\chi \end{pmatrix} \frac{d\sigma(\varepsilon)}{d\chi}.$$

skew scattering $\rightarrow$ finite transversal force

Skyrmion caloritronics

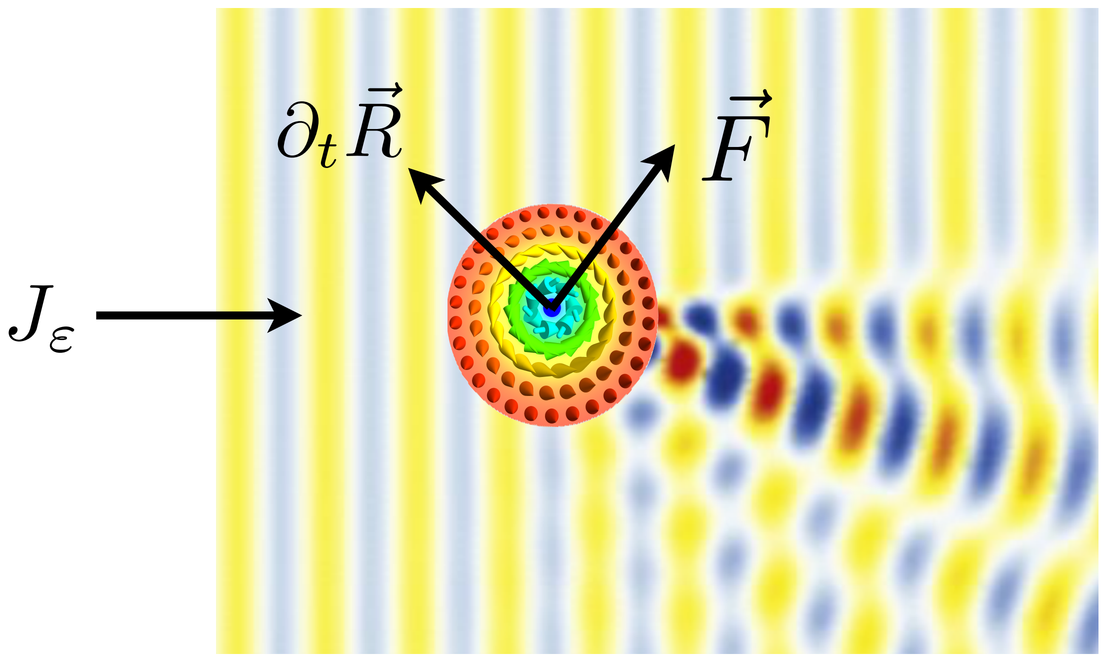

skyrmion velocity:

towards the
magnon source

$$\partial_t \vec{R} = J_\varepsilon k \begin{pmatrix} -\sigma_\perp(\varepsilon) \\ \sigma_\parallel(\varepsilon) \end{pmatrix}$$

in the presence of a temperature gradient:

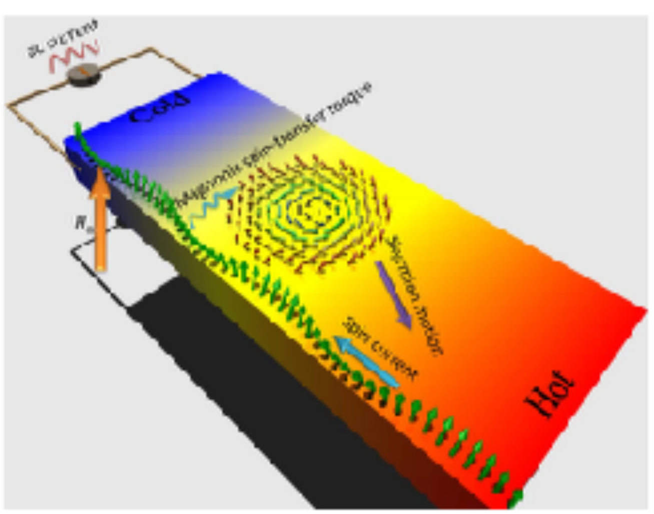

skyrmion moves
towards hot region!

numerical Langevin dynamics:

Lin, Batista, Reichhardt, & Saxena, PRL (2014)
Kong and Zang PRL (2013)

Experiment: thermal ratchet

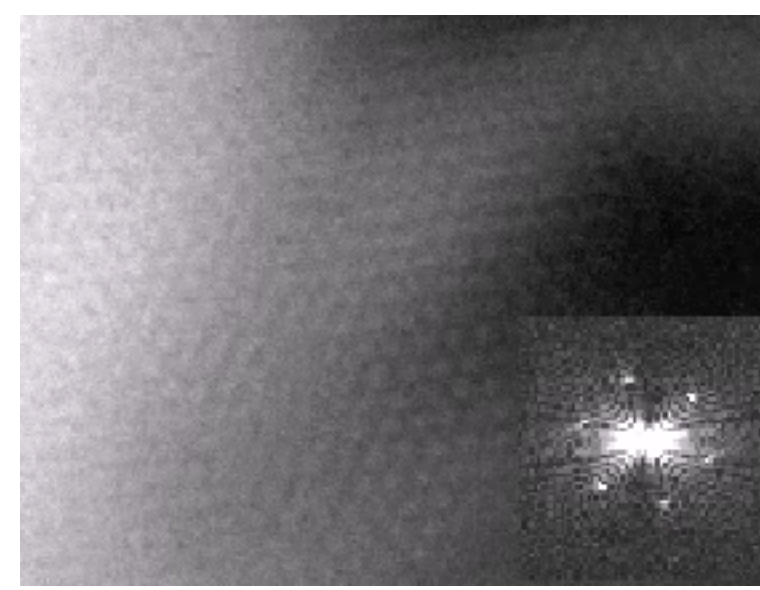

Mochizuki *et al.* Nat. Mat. (2014)

Magnon band structure of skyrmion lattices

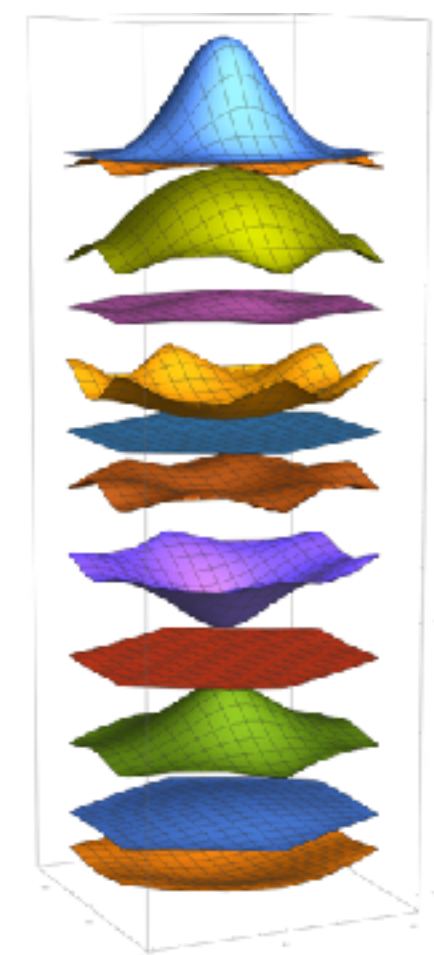

Magnon-band structure of skyrmion lattice

magnon dispersion for in-plane momenta

skyrmion lattice

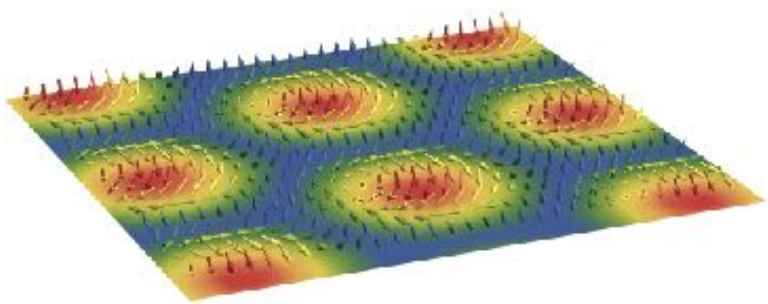

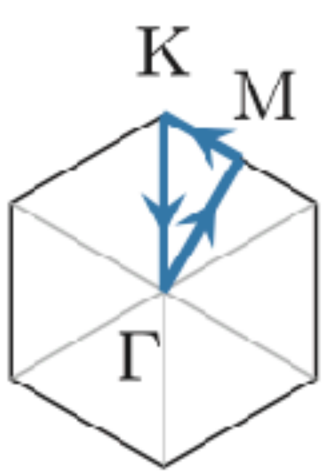

2d magnetic
Brillouin zone

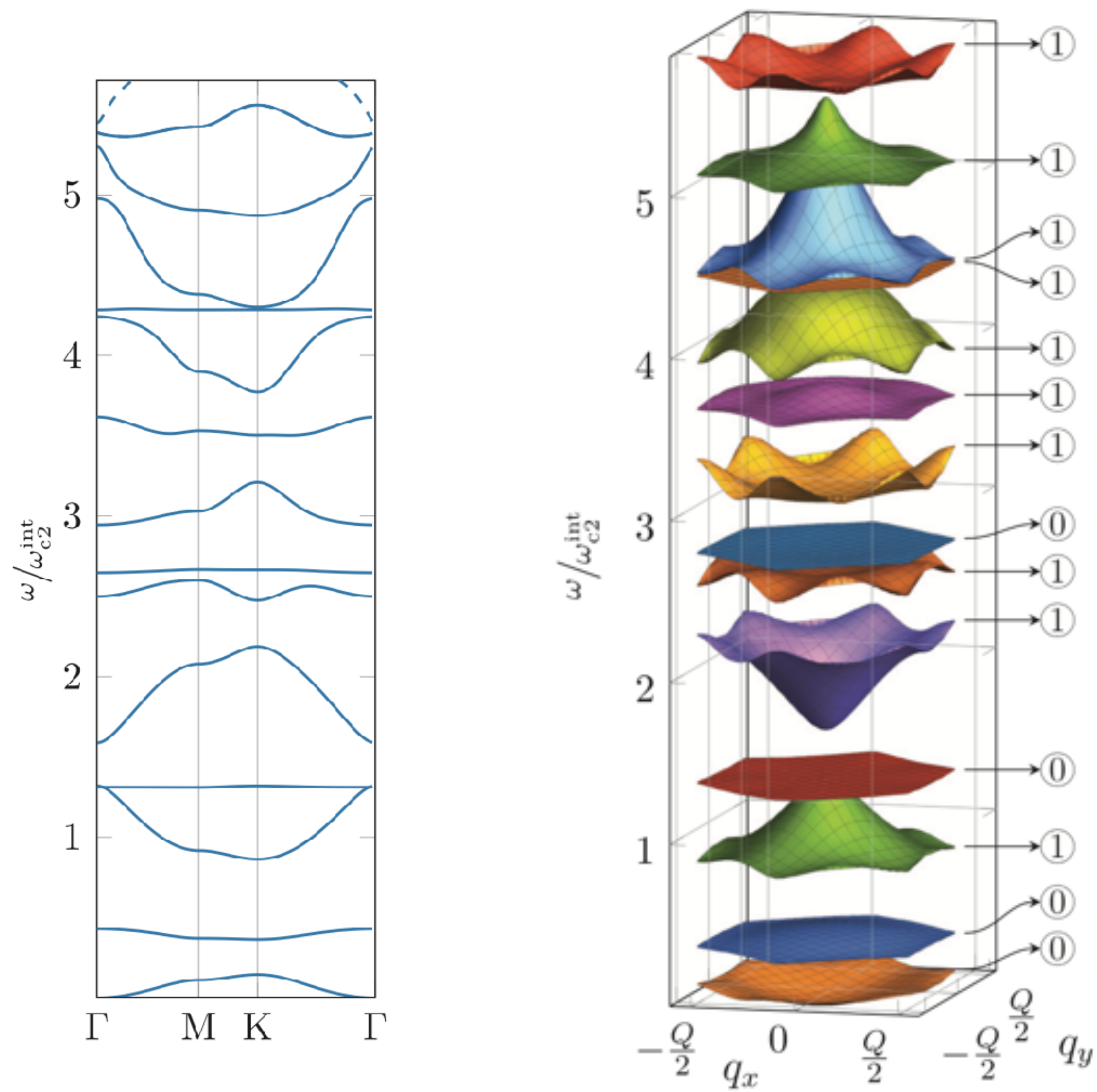

MG, J. Waizner, D. Grundler, J. Phys. D: Appl. Phys. 50, 293002 (2017)

Topological magnon-band structure

non-trivial topology of skyrmions ⇨ topological magnon band structure

each skyrmion acts like a source of emergent magnetic flux

⇩

emergent magnon electrodynamics

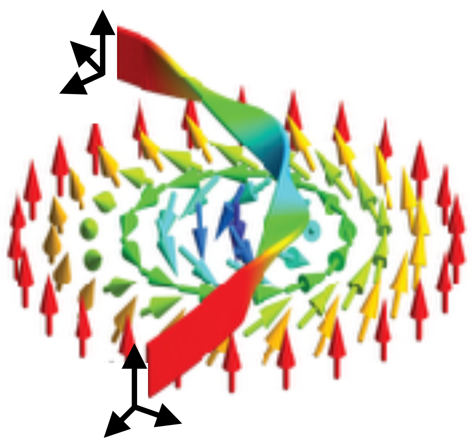

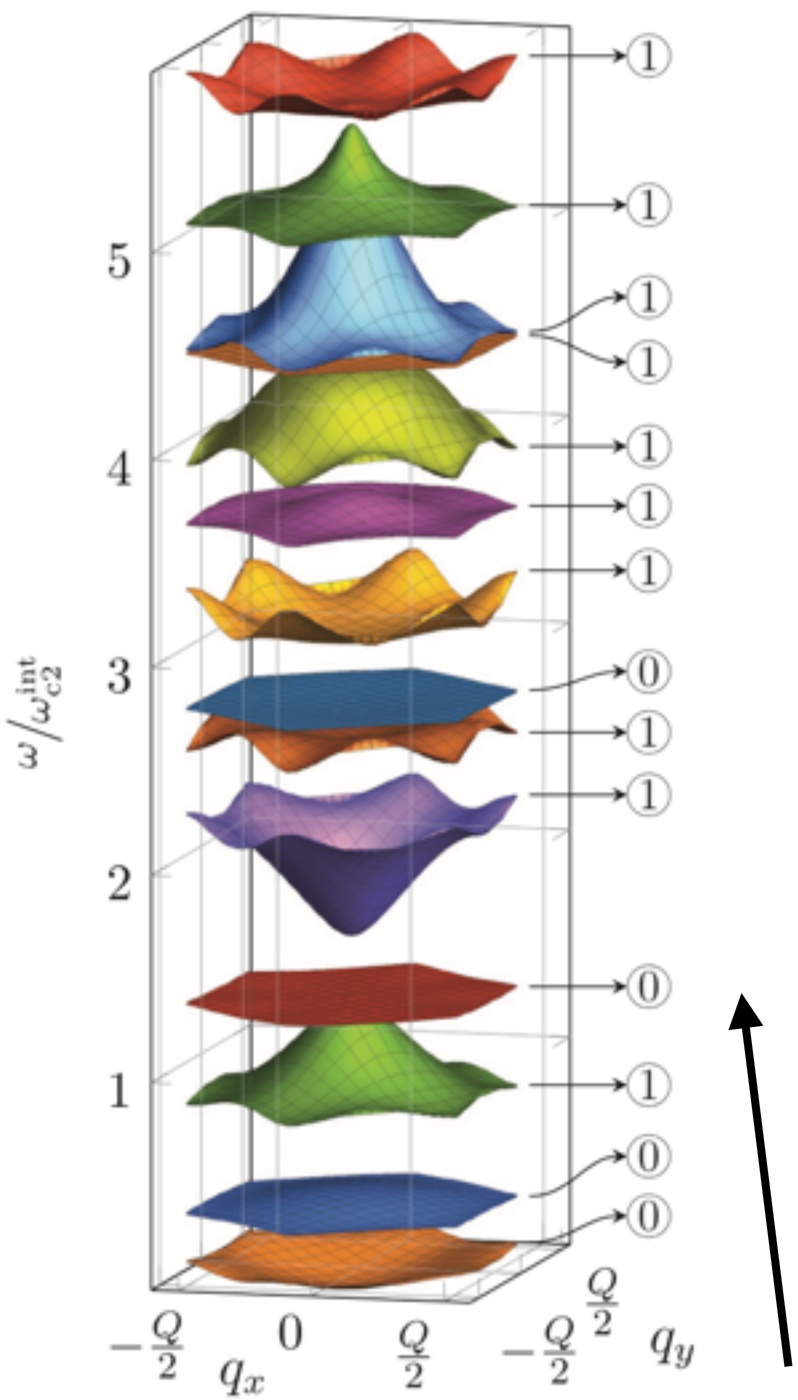

Chern numbers

- emergent magnon Landau levels
- bands with finite Chern numbers
- topologically protected magnon edge states

Magnon normal modes with finite frequency

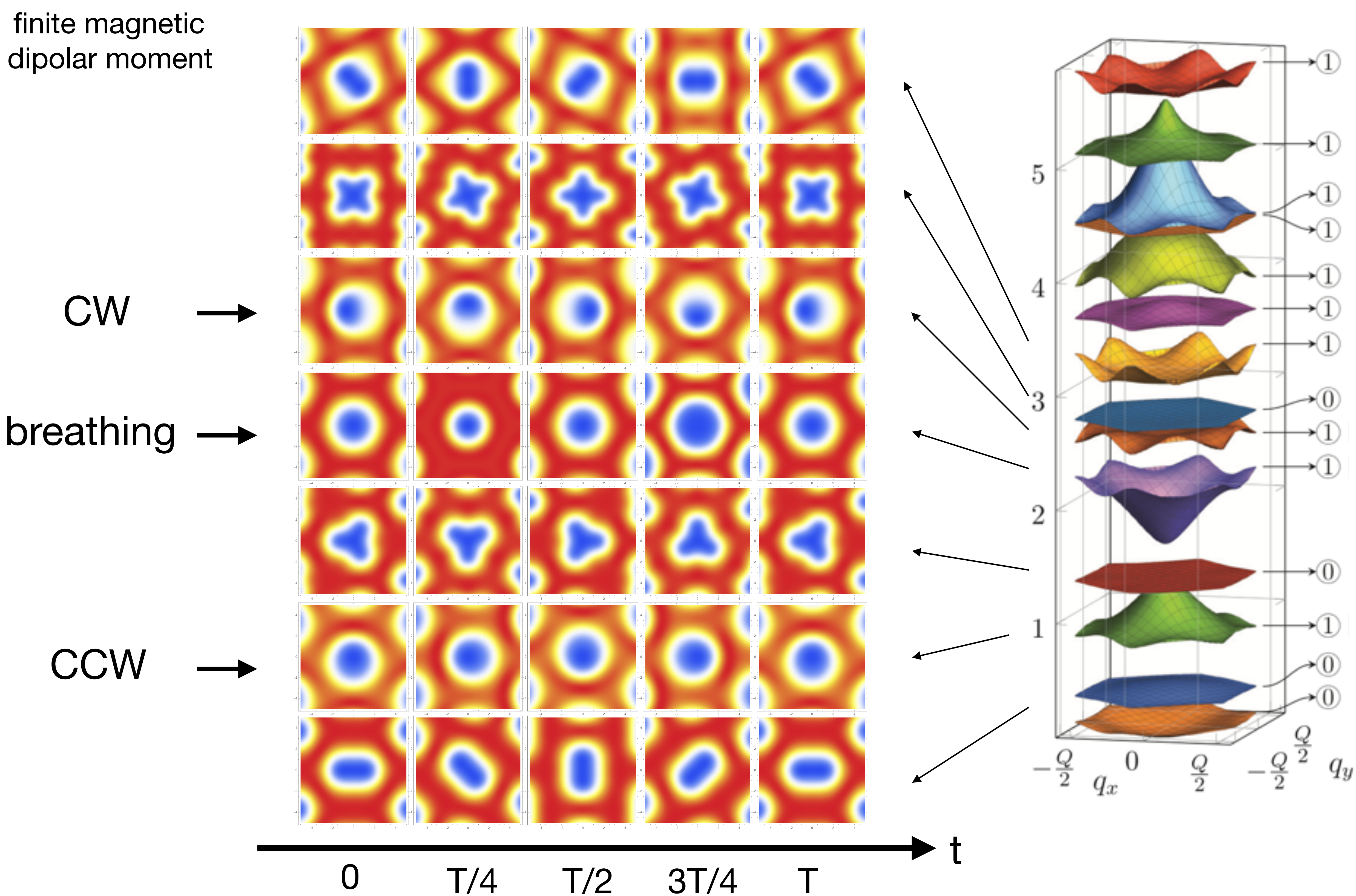

Magnetic resonances

ac magnetic field ⇨ exciting magnons at zero momentum

spectrum:

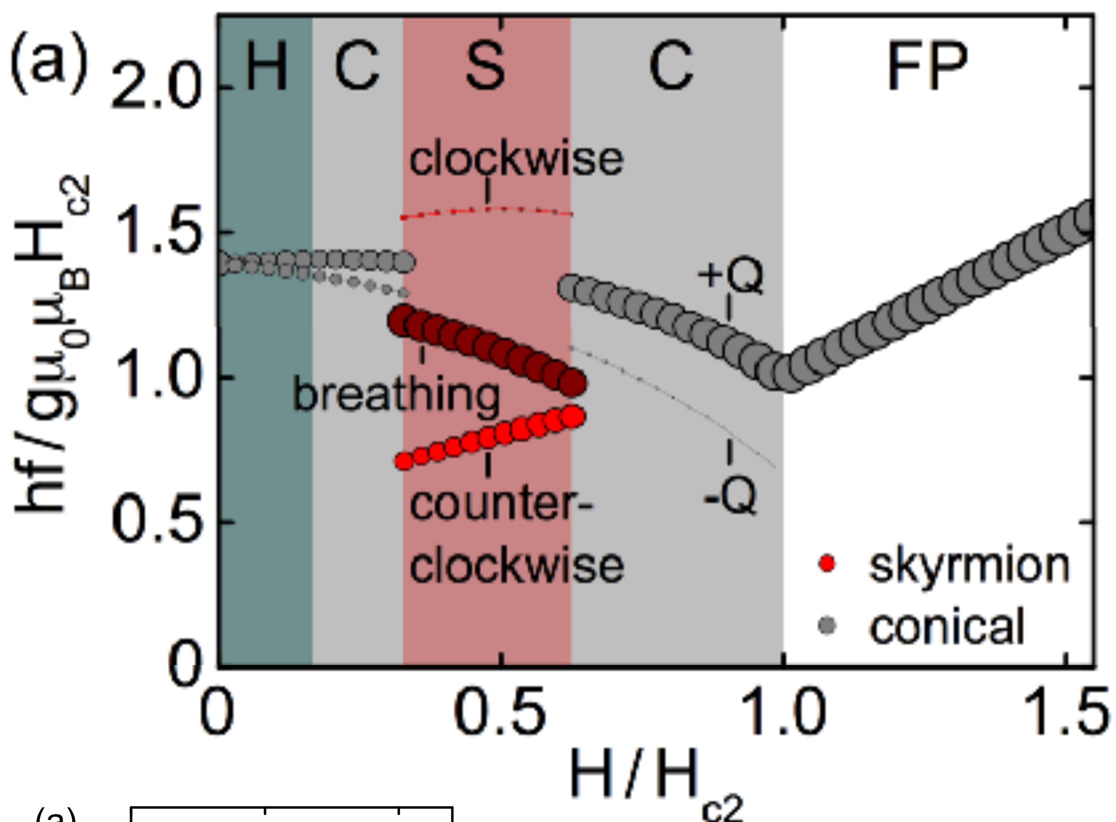

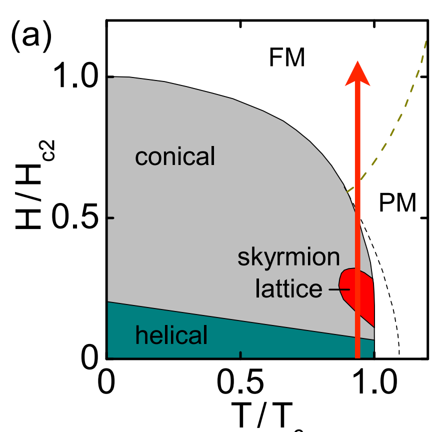

for a field sweep

T. Schwarze, *et al.* Nature Materials (2015)

Two resonances of the helix:

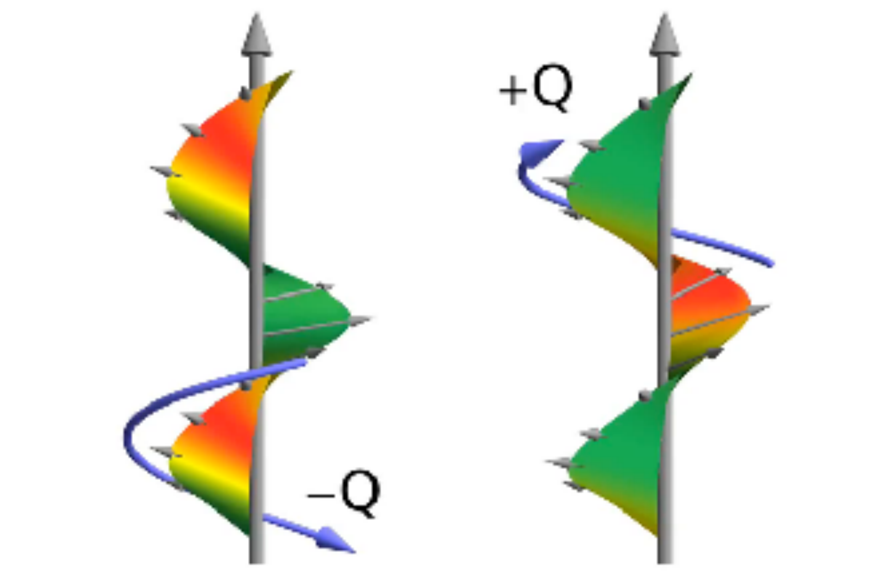

Three resonances of the skyrmion crystal:

clockwise

counter clockwise

breathing

Comparison experiment & theory

different field sweeps normalized with $H_{c2}(T)$

three different materials

MnSi, $Fe_{0.8}Co_{0.2}Si$ and Cu_2OSeO_3

with three different shapes

(demagnization factors)

„universal" chiral magnetism

excellent parameter-free theoretical description

T. Schwarze, *et al.* Nature Materials (2015)

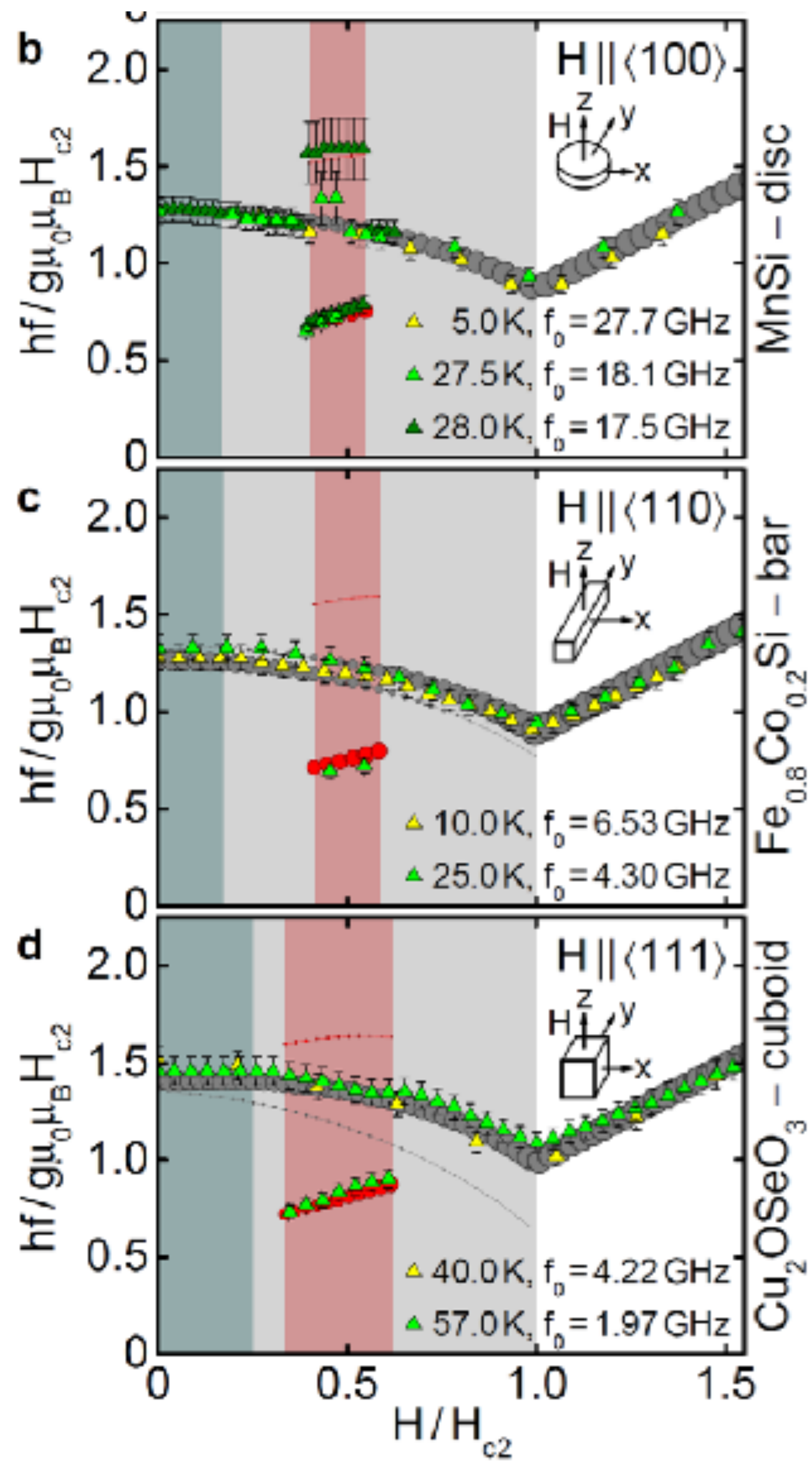

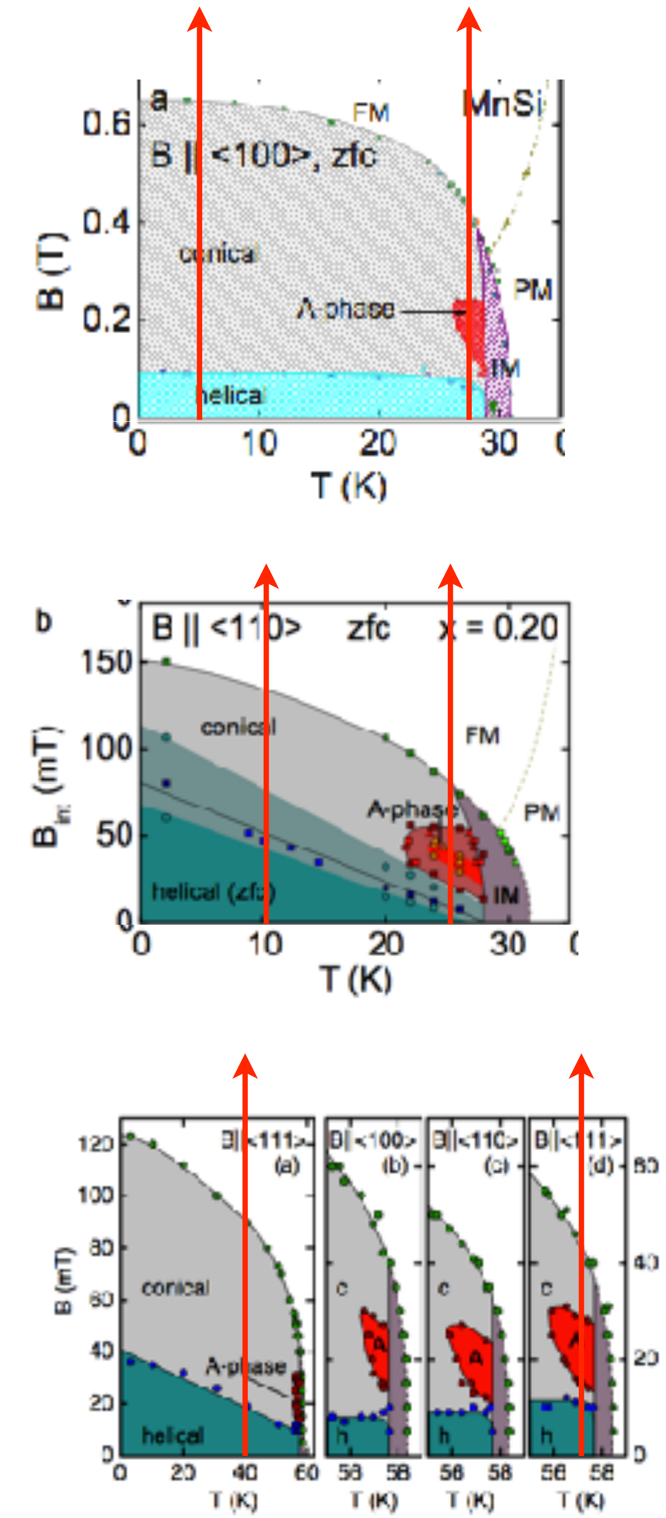

Orientation of the skyrmion crystal

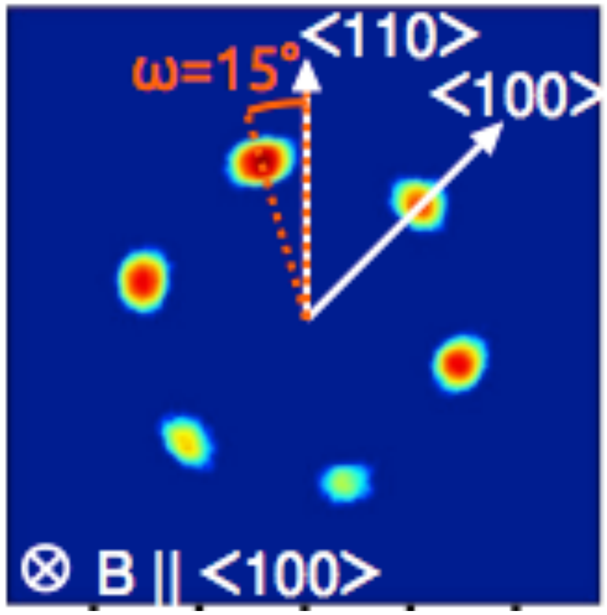

Orientation of the skyrmion lattice

real space

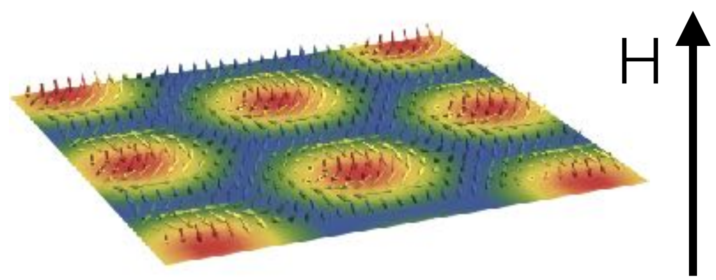

hexagonal skyrmion lattice

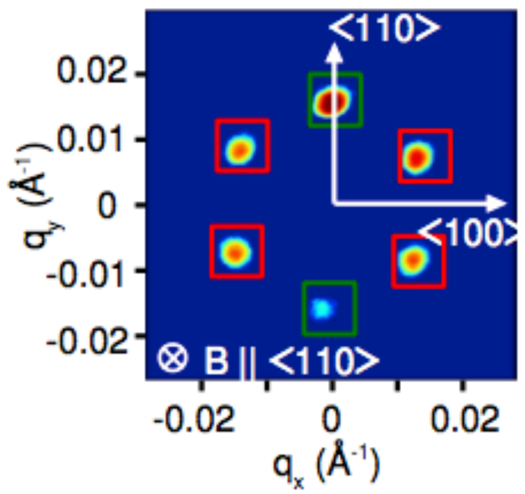

momentum space

six-fold symmetric Bragg peaks

orientation determined by weak cubic magnetic anisotropies!

How does the scattering pattern orient within the plane normal to H?

Bragg pattern defines six-fold symmetric tangent vector field on the H-unit sphere:

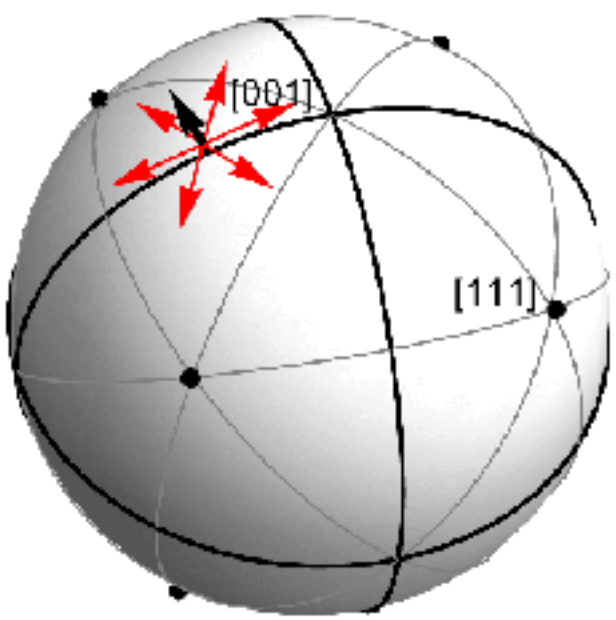

Effective theory for skyrmion lattice orientation

define local frame for
each point on the unit sphere

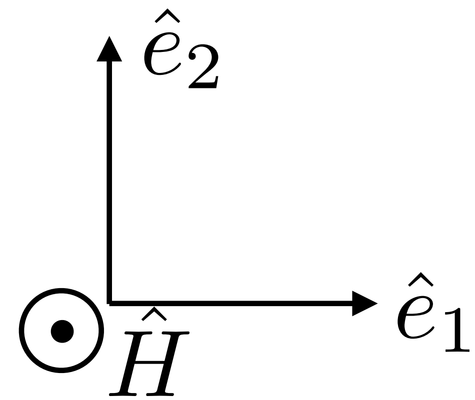

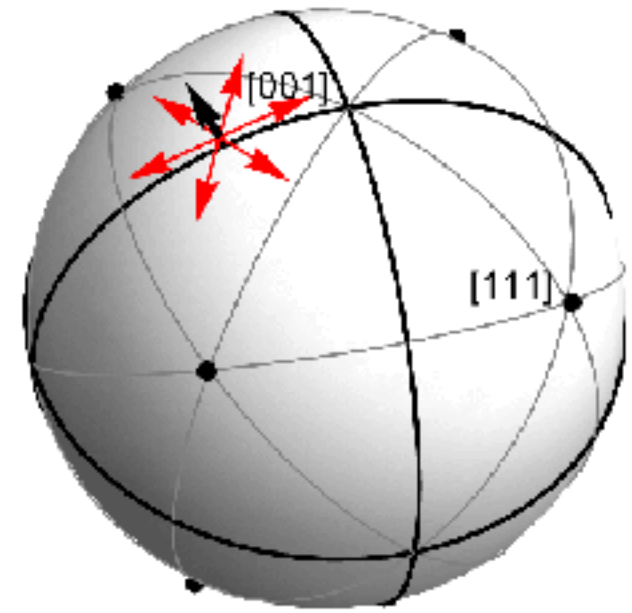

six-fold star:

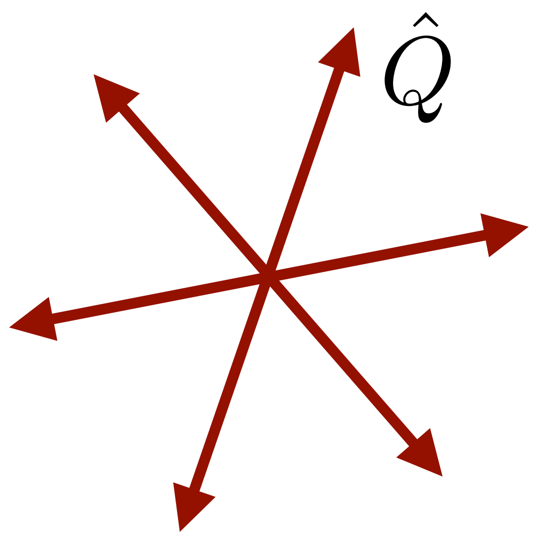

$$\hat{Q} = \cos\omega\hat{e}_1 + \sin\omega\hat{e}_2$$

order parameter: angle ω

effective potential: $\mathcal{V}(\hat{Q}) = \hat{Q}_x^6 + \hat{Q}_y^6 + \hat{Q}_z^6 + \lambda(\hat{Q}_x^2\hat{Q}_y^4 + \hat{Q}_y^2\hat{Q}_z^4 + \hat{Q}_z^2\hat{Q}_x^4)$

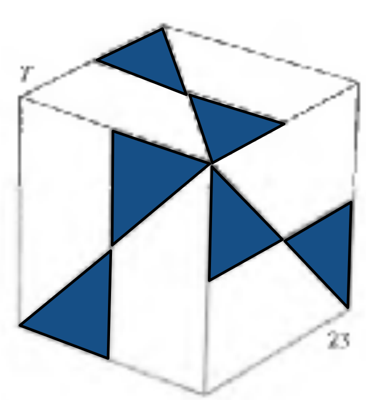

two anisotropy terms
of sixth-order

single fitting parameter

tetrahedral point group

A. Bauer, et al. submitted

Experiment: skyrmion orientation

experimental setup

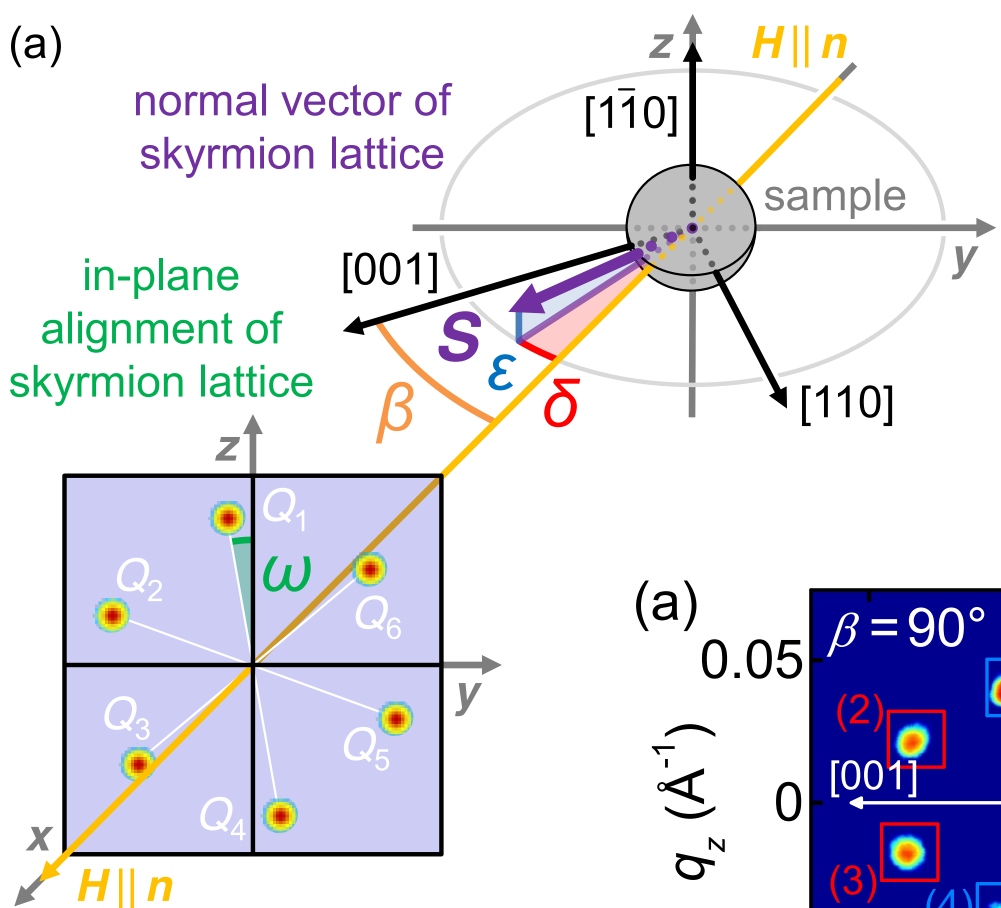

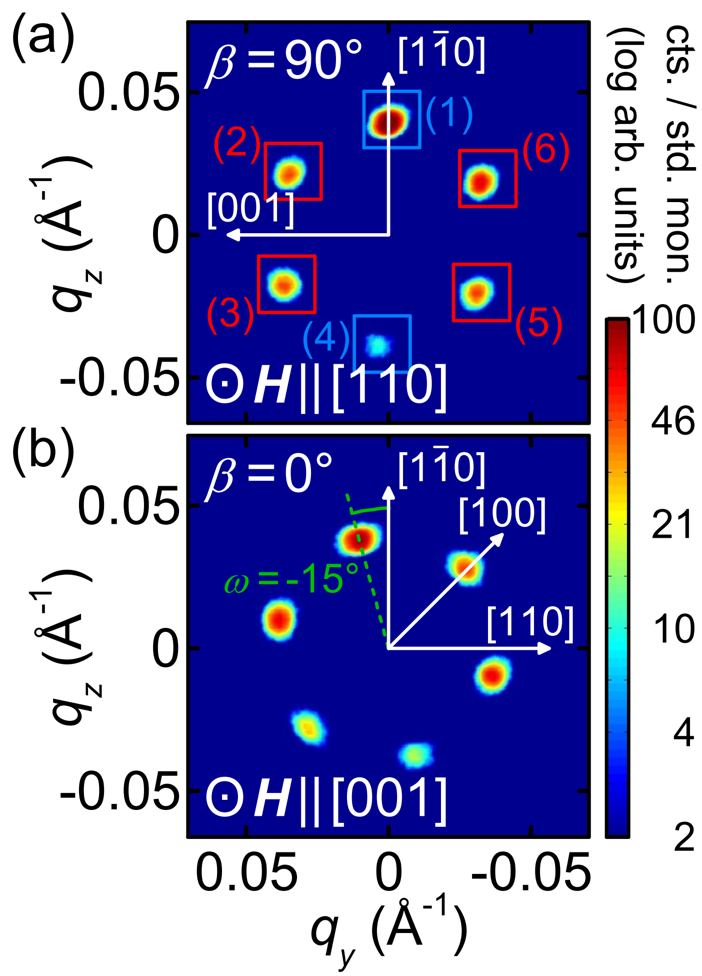

experiment excellently described by theory

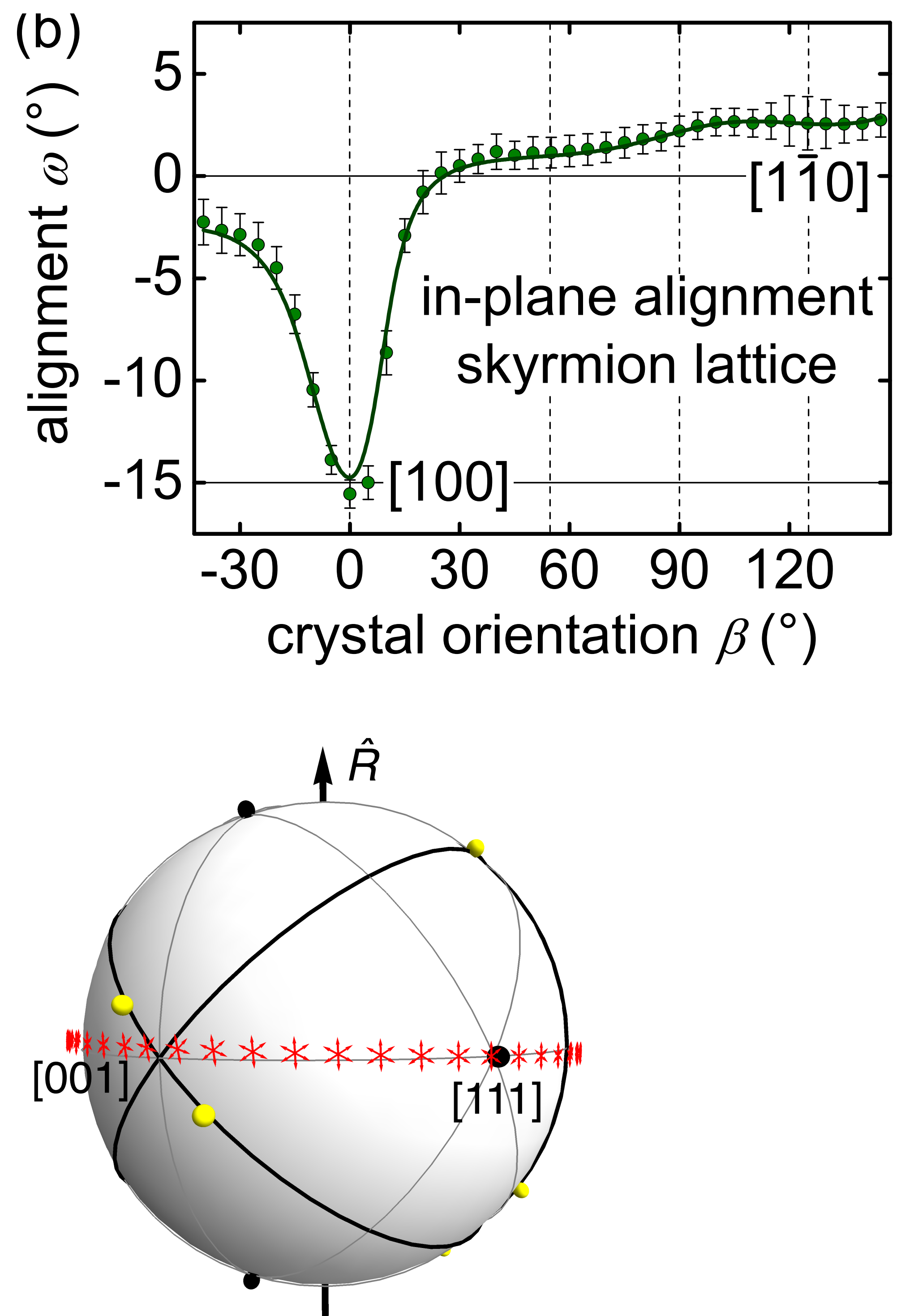

A. Bauer, et al. submitted

Topology of wind patterns and skyrmion lattices

Hairy-Ball theorem (Poincare-Hopf): continuous non-vanishing tangent vector cannot exist everywhere on the sphere

wind velocity has to vanish at least twice

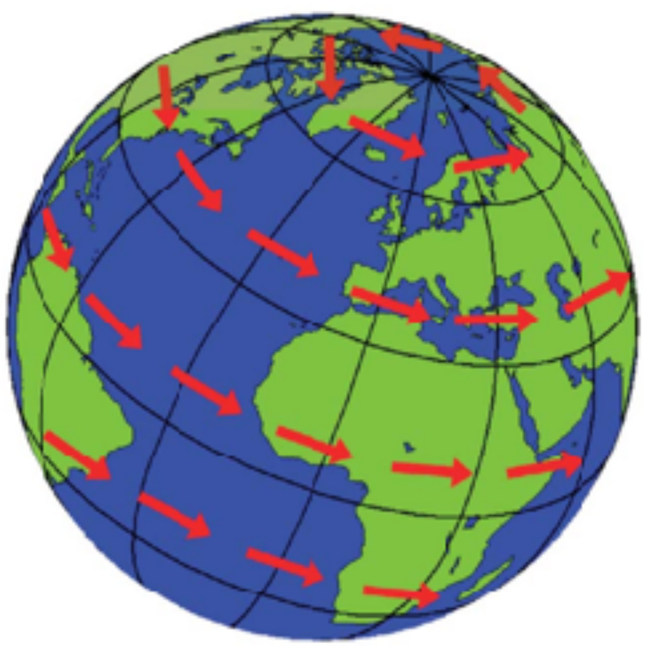

eg. singularity on the north and south pole

also relevant for
Abrikosov vortex lattice in type II SC

Larver & Forgan, Nat. Comm. (2010).

skyrmion lattice in MnSi

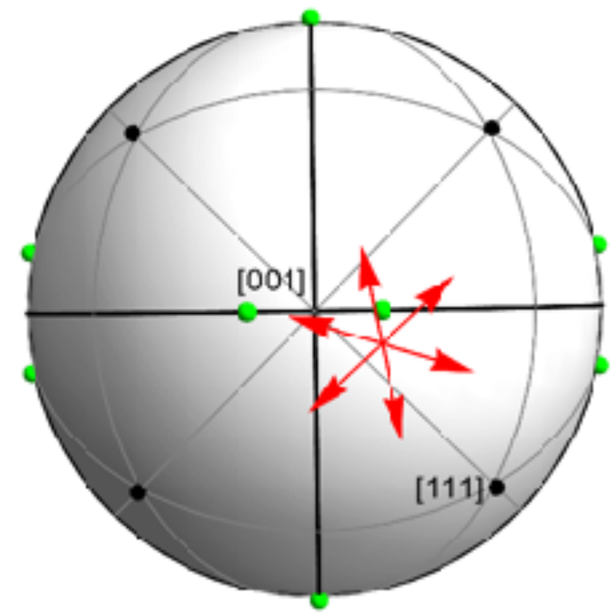

singularities of strengths 1/6
winding of the pattern by π/3

A. Bauer, et al. submitted

Topological domain walls of helimagnetic order

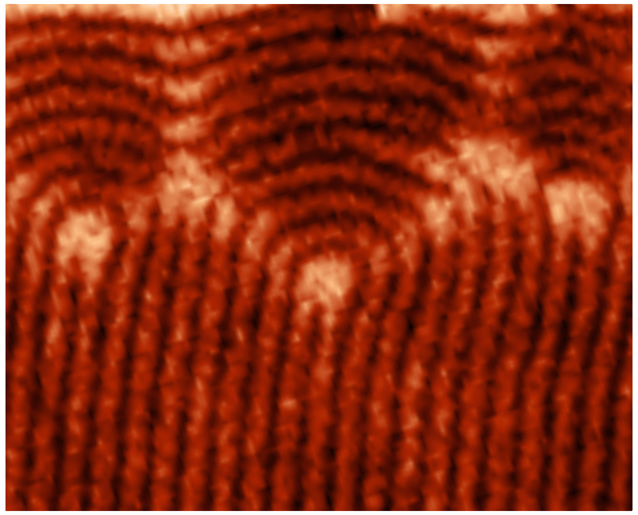

Domain walls in helimagnets

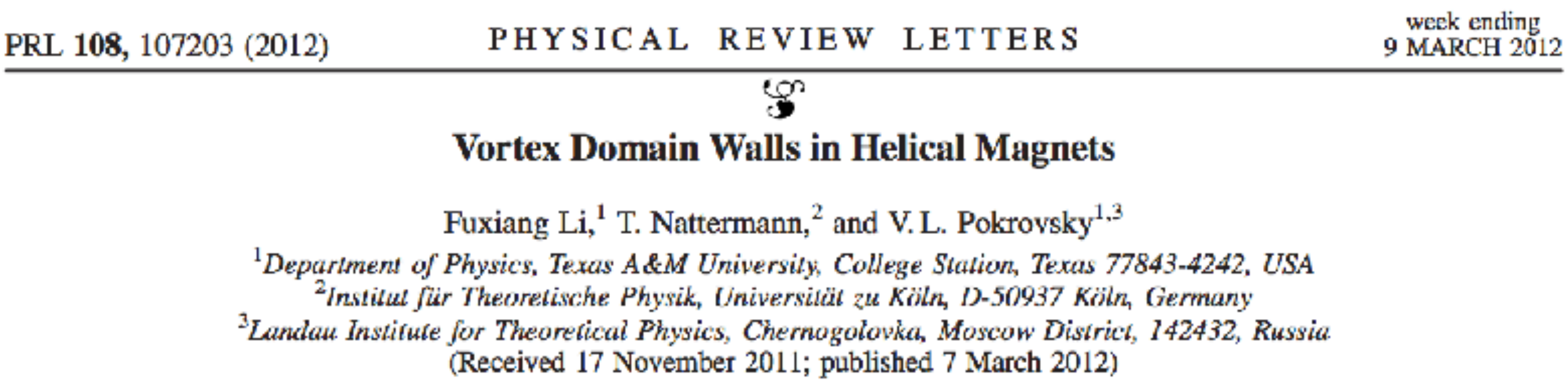
PRL **108**, 107203 (2012) PHYSICAL REVIEW LETTERS week ending 9 MARCH 2012

Vortex Domain Walls in Helical Magnets

Fuxiang Li,[1] T. Nattermann,[2] and V. L. Pokrovsky[1,3]
[1]*Department of Physics, Texas A&M University, College Station, Texas 77843-4242, USA*
[2]*Institut für Theoretische Physik, Universität zu Köln, D-50937 Köln, Germany*
[3]*Landau Institute for Theoretical Physics, Chernogolovka, Moscow District, 142432, Russia*
(Received 17 November 2011; published 7 March 2012)

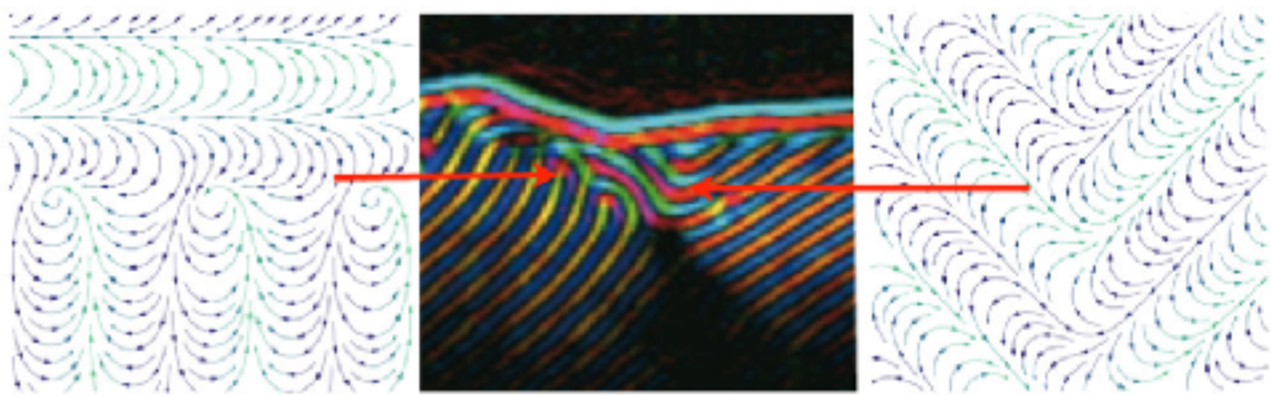

FIG. 3 (color online). DWs in noncentrosymmetric helical magnets. A detail of Fig. 1(g) of Ref. [29] (center) showing two types of DWs in the ferromagnet FeGe; the left one includes vortices, the right one is vortex-free. The panels are theoretically calculated DWs, right without vortices, left with vortices.

Domain walls in helimagnets

similar to grain boundaries in cholesteric liquid crystals

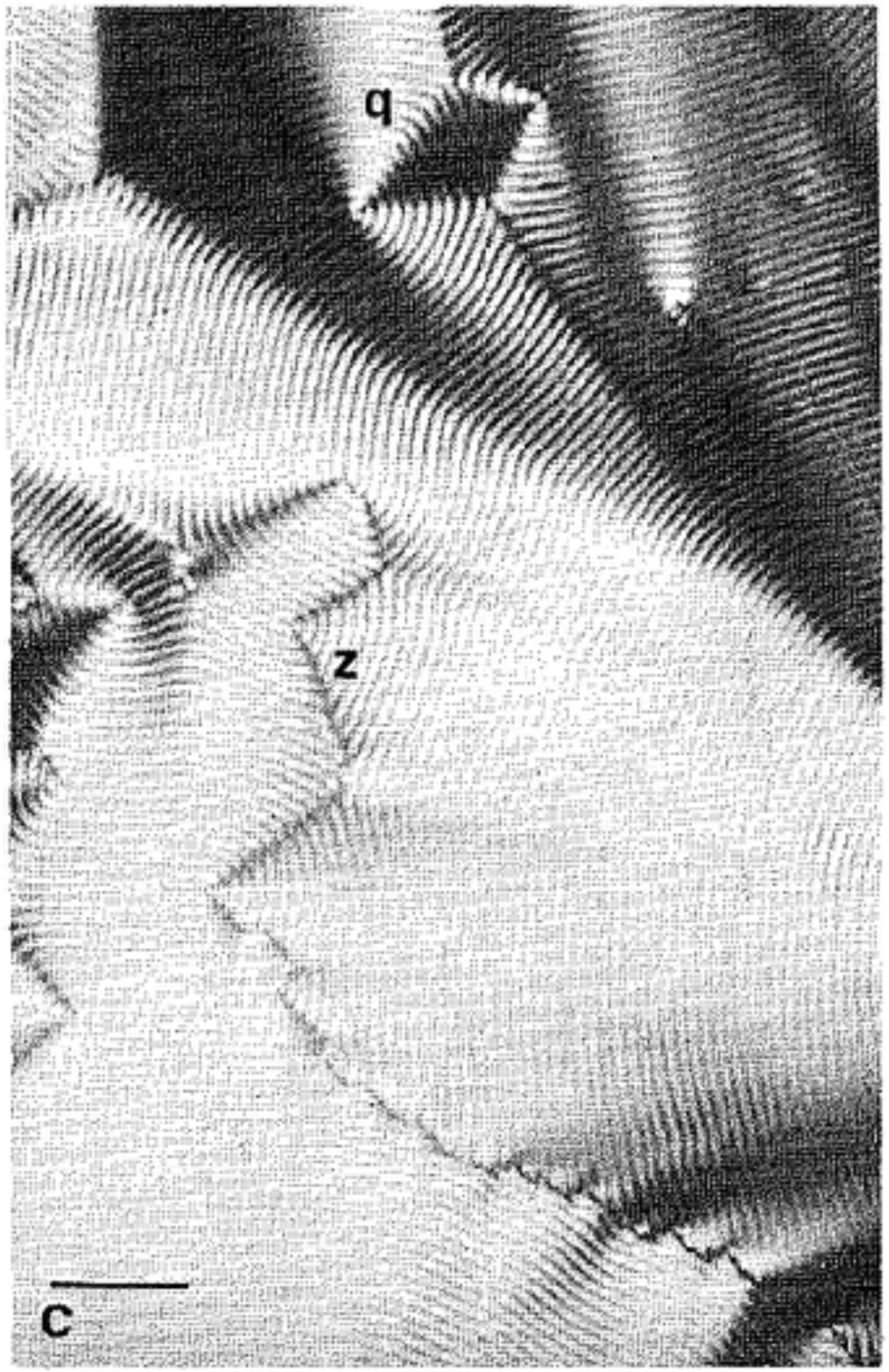

Y. Bouligand 1970ies

Topological defects of helimagnetic order

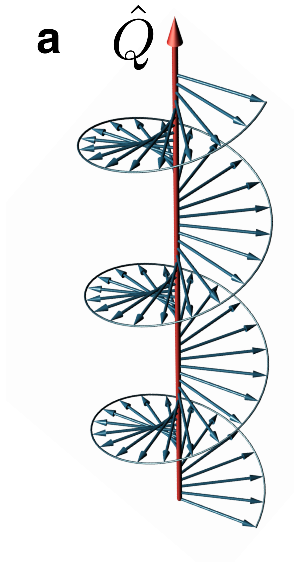

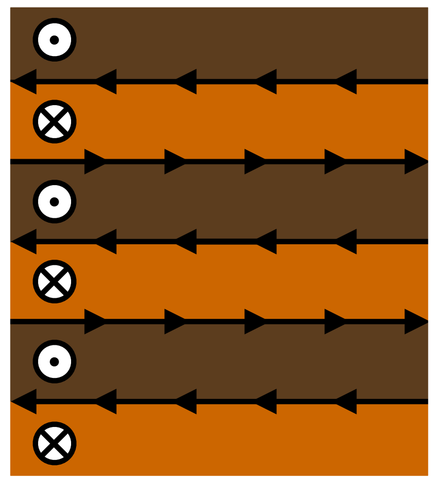

magnetic helix = lamellar structure similar to cholesteric liquid crystals

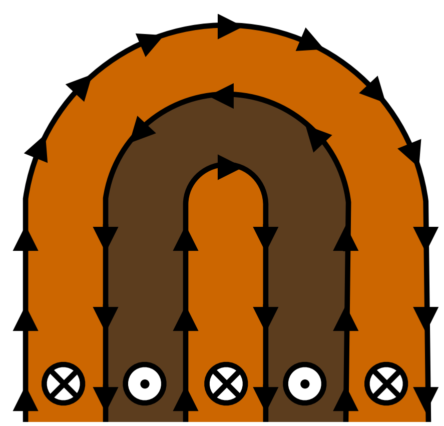

pitch $\hat{Q}$ is a director

$\Rightarrow$ $\pm\pi$ vortices are possible

= disclinations defects

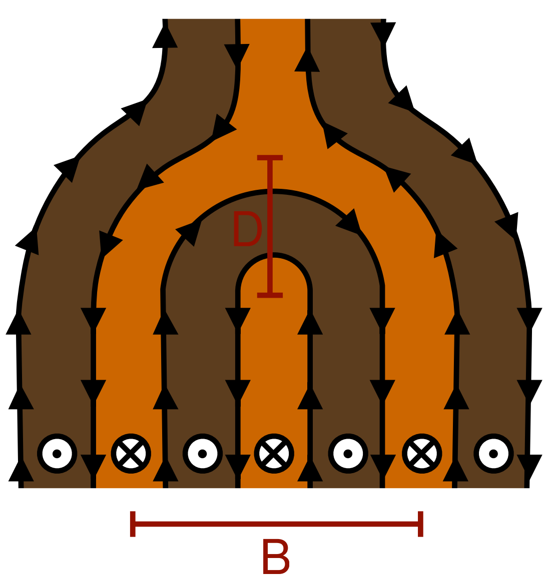

disclinations combine to form a dislocation with Burgers vector B

Relaxation by climb motion of dislocations

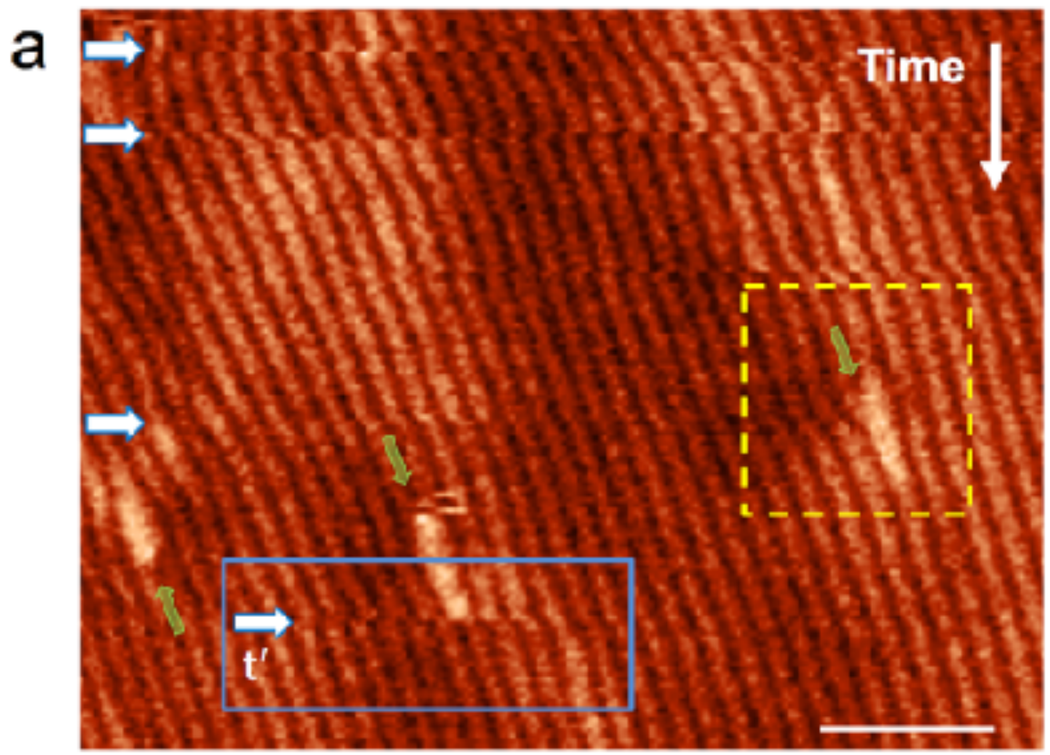

MFM: surface of FeGe

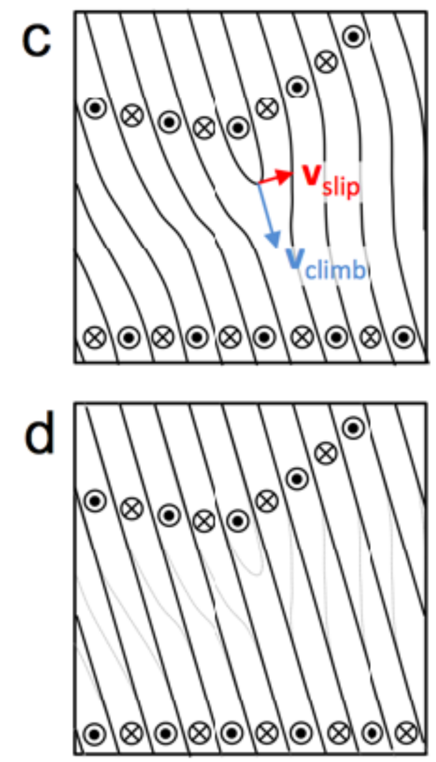

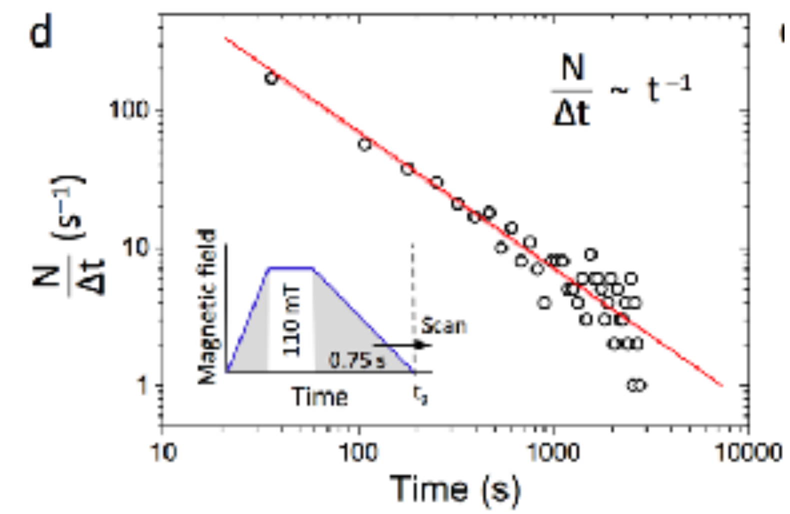

slow power-law relaxation

climb motion of dislocations $\Rightarrow$ 180° phase shift

A. Dussaux *et al.*, Nat Comm 2016

Topological domain walls

depending on relative angle: three types of domain walls

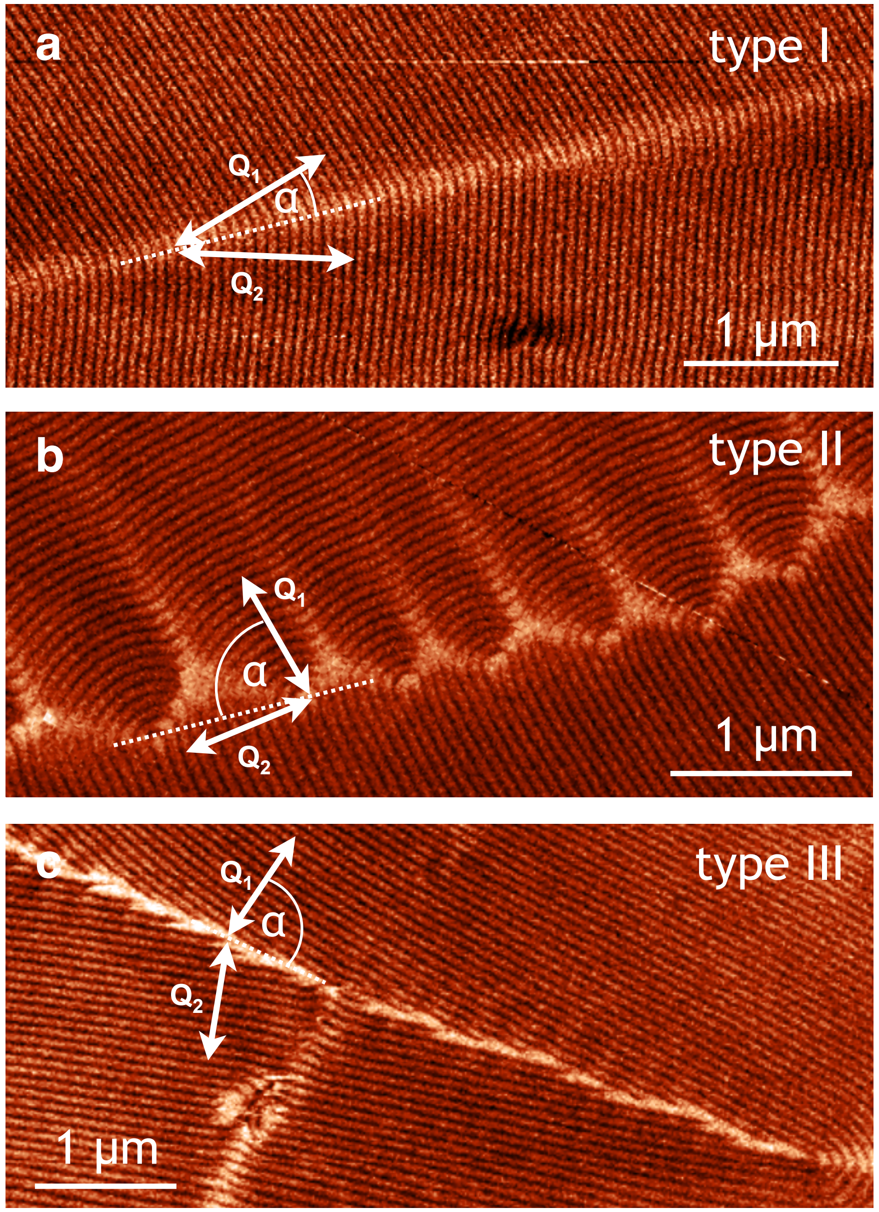

curvature wall

zig-zag
disclination wall

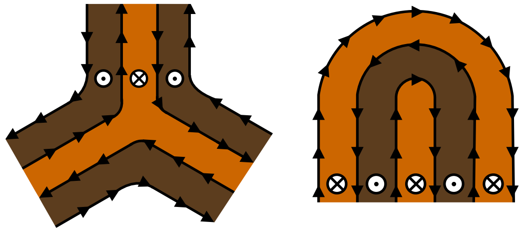

dislocation wall

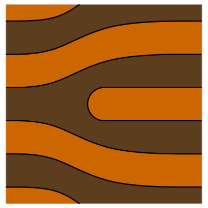

MFM: surface of FeGe

P. Schoenherr et al, Nat. Phys. (2018)

Domain wall angles

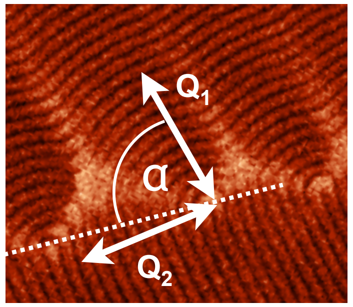

experiment:

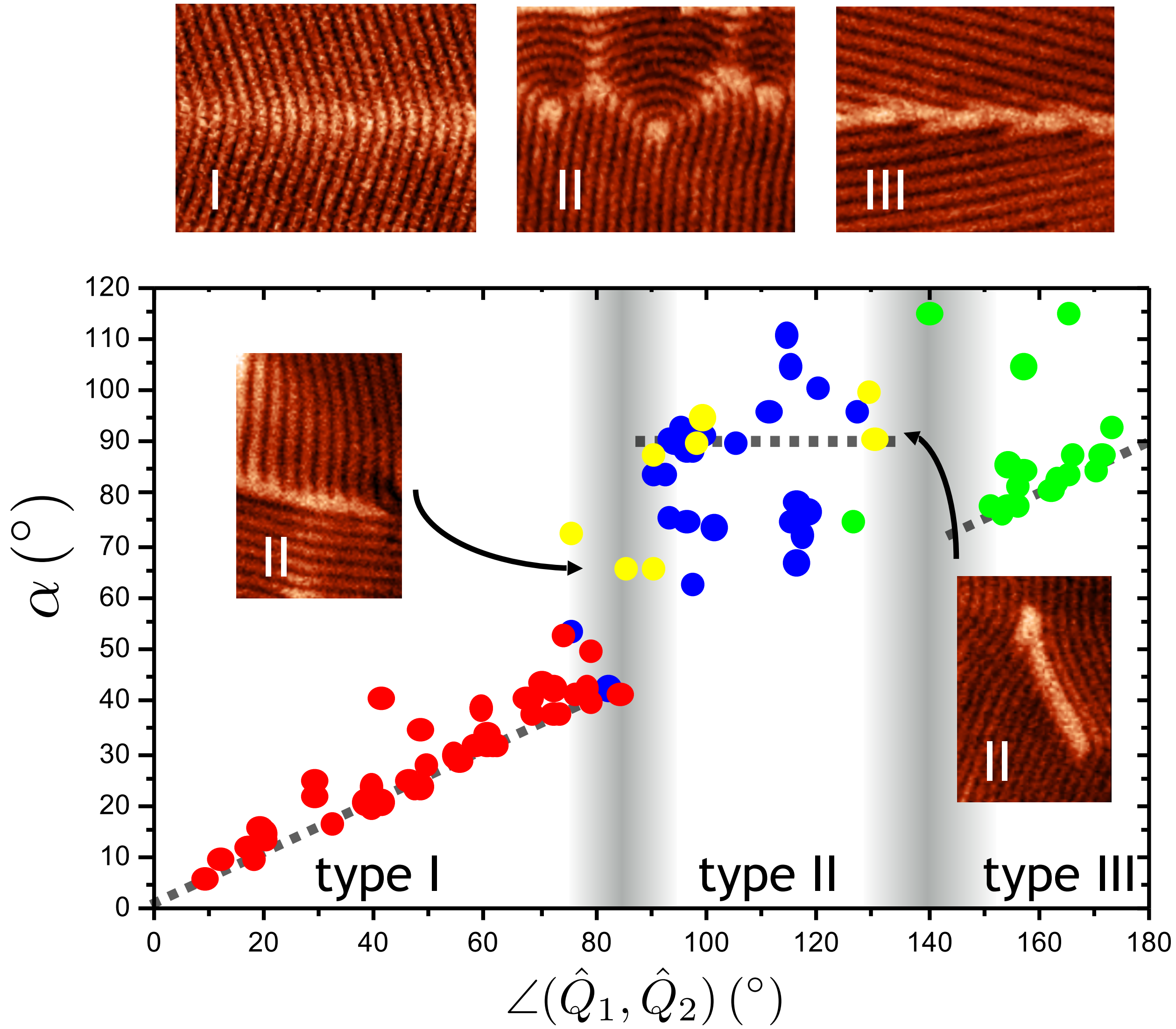

P. Schoenherr et al, Nat. Phys. (2018)

Domain wall angles

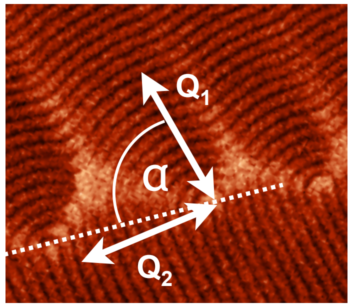

experiment:

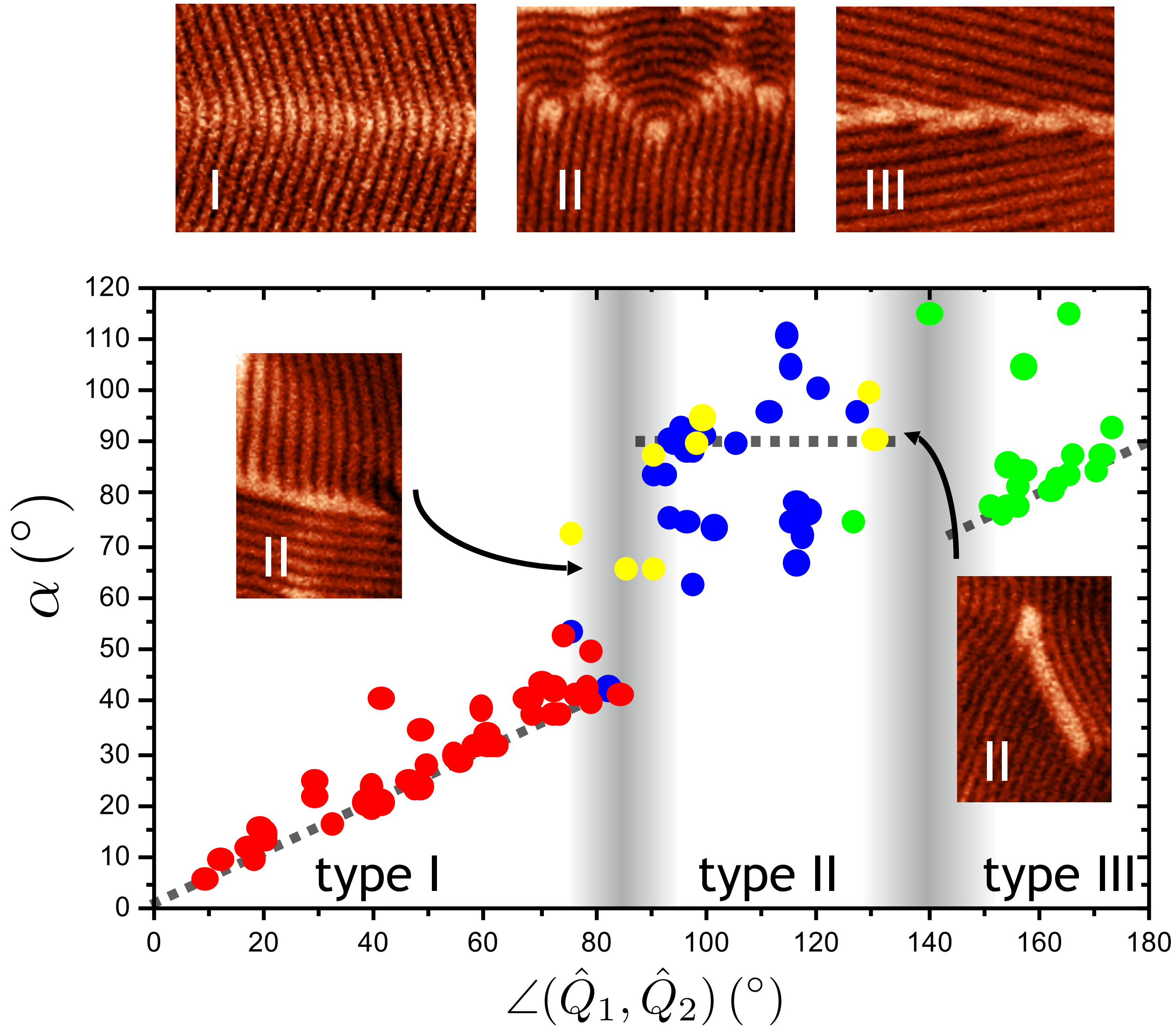

micromagnetic simulations:

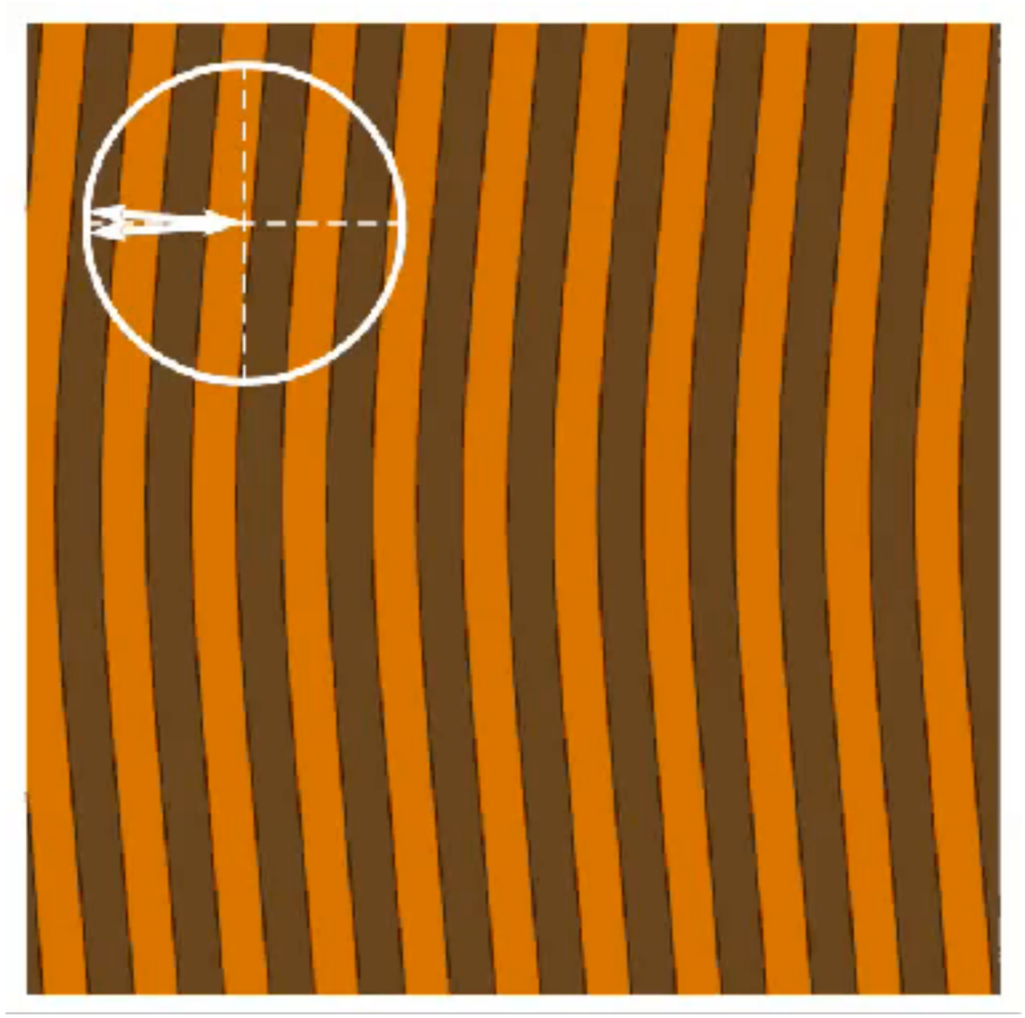

P. Schoenherr et al, Nat. Phys. (2018)

Domain wall angles

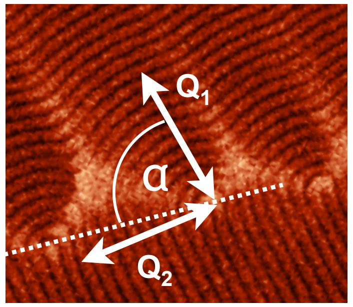

experiment:

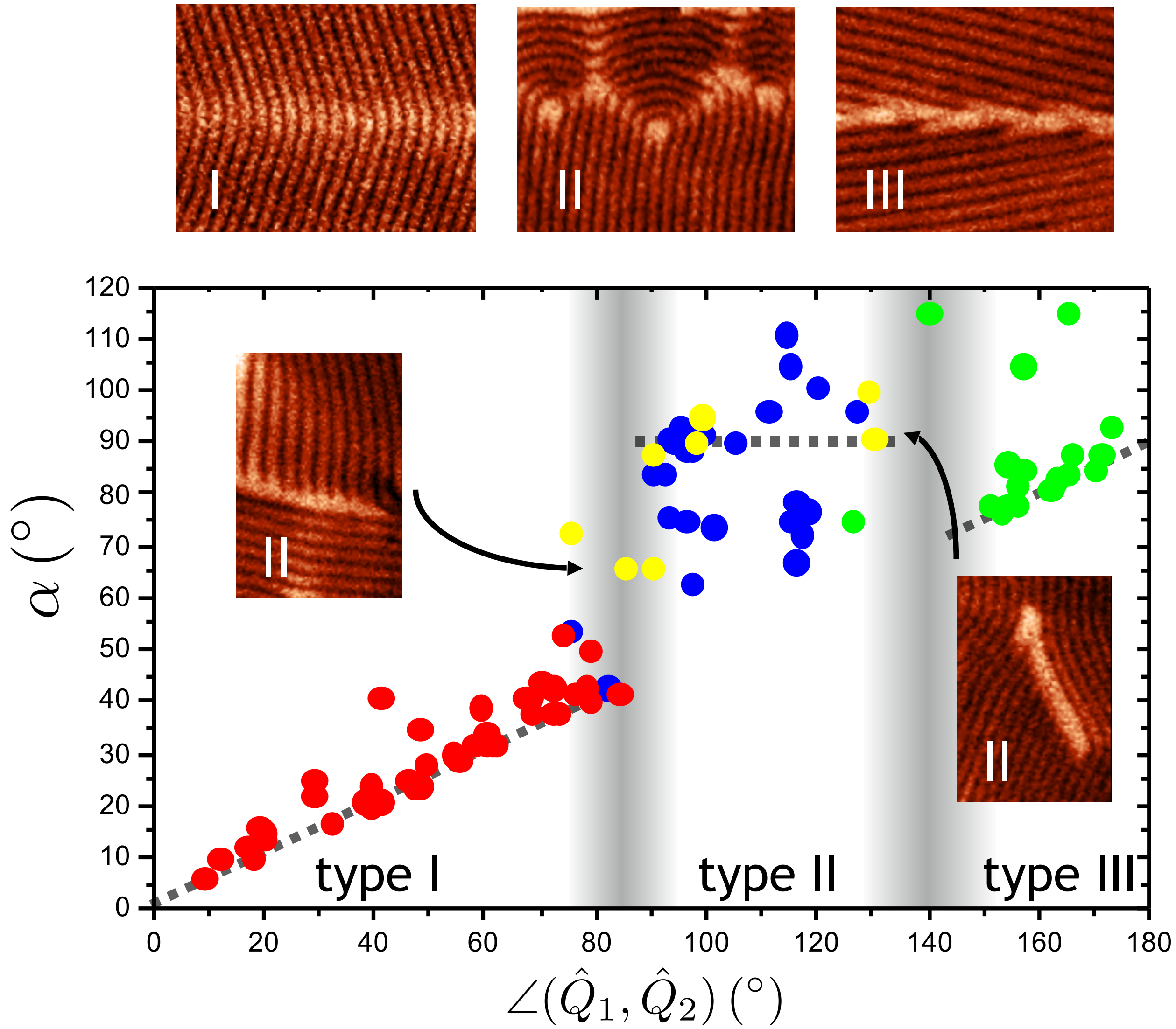

micromagnetic simulations:

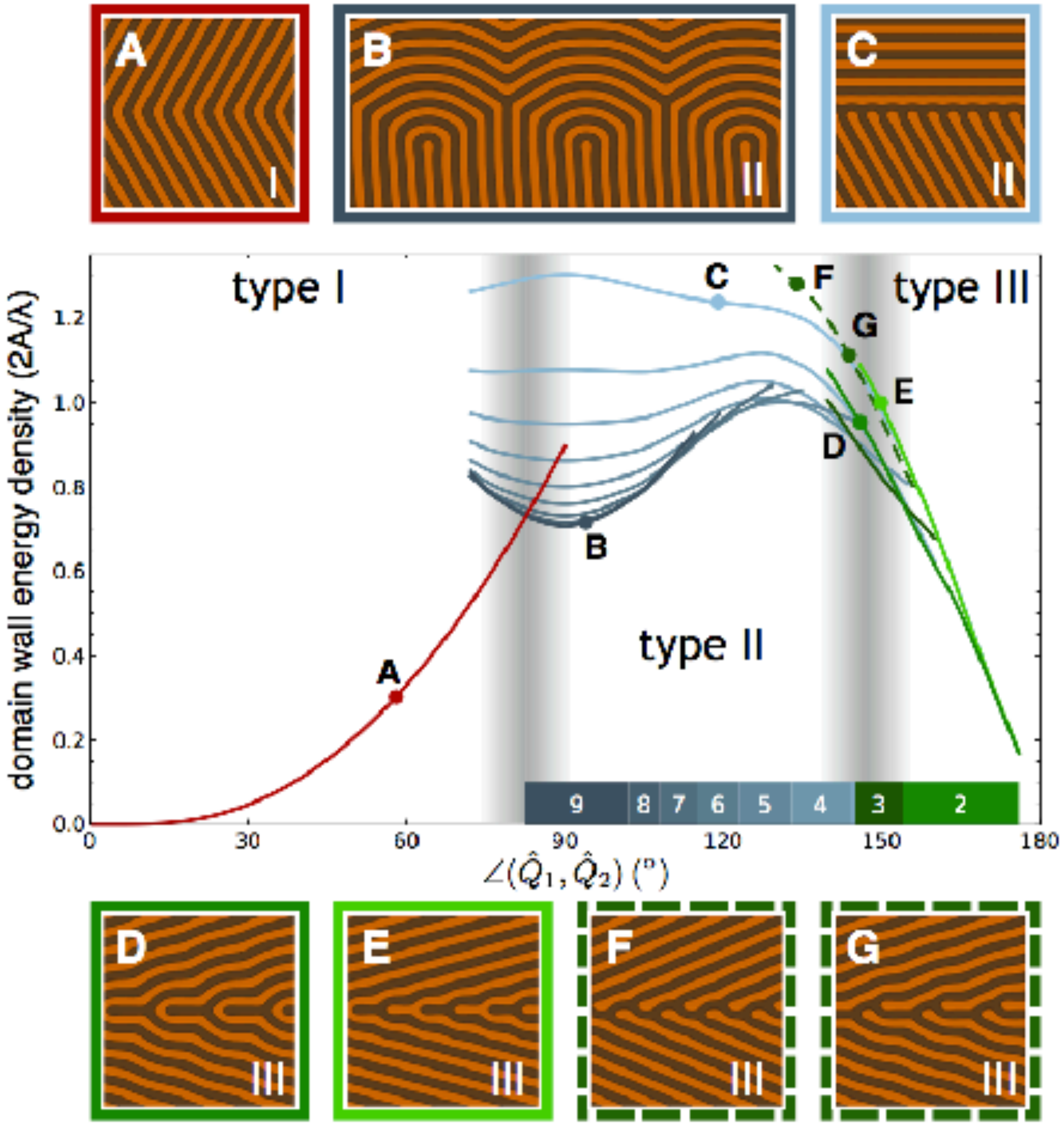

P. Schoenherr et al, Nat. Phys. (2018)

Skyrmion charge of dislocations

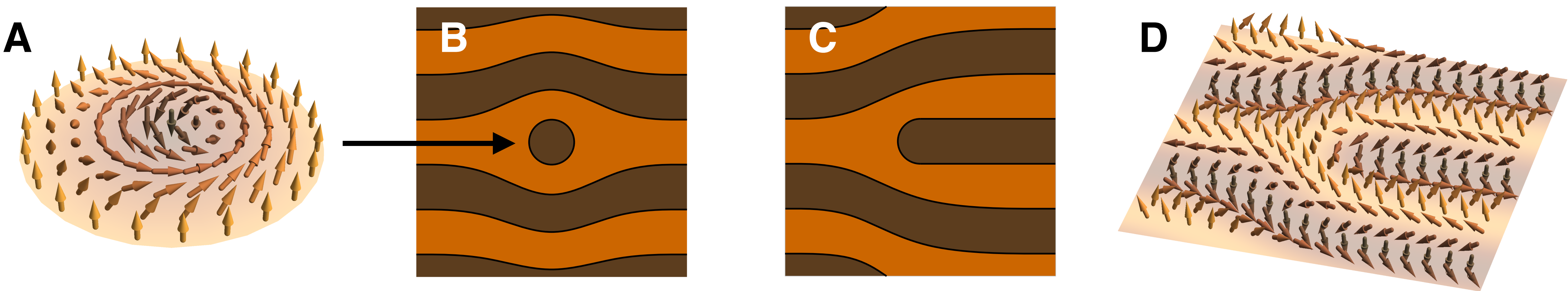

skyrmion number W = -1

skyrmion embedded in a topologically trivial background

skyrmion number W = -1/2

dislocation (with B = λ) = meron

general relation for skyrmion number of dislocation with Burger vector B:

$$|W| = \frac{1}{2}\mathrm{mod}_2\left(\frac{B}{\lambda}\right)$$

$\Rightarrow$

only dislocations with half-integer B contribute to

topological Hall effect & emergent electrodynamics

Topological skyrmion charge of domain walls

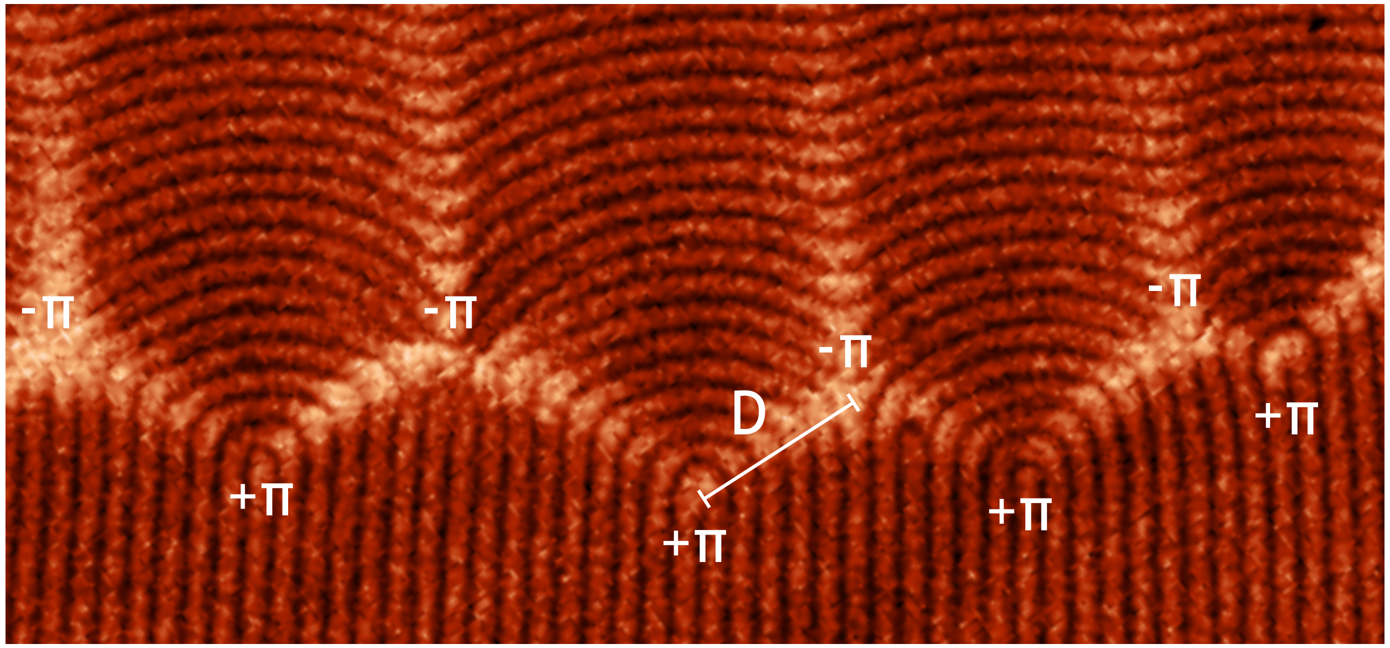

finite skyrmion charge if the distance D:

$$\boxed{\frac{2D}{\lambda} = \frac{B}{\lambda} \quad \text{odd}}$$

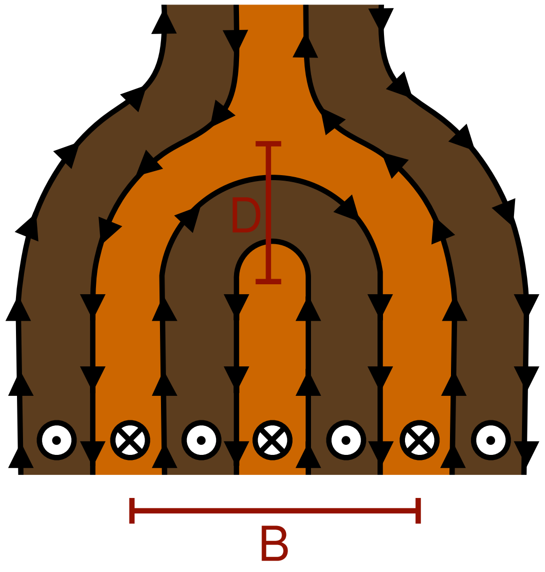

λ : helix wavelength

⇨ topological Hall effect & emergent electrodynamics

Acknowledgments:

theory:

Johannes
Waizner

Laura
Köhler

Achim Rosch
(Cologne)

V. Kravchuk
(Kiev/Dresden)

experimental groups:

B20 compounds

C. Pfleiderer
(TU Munich)

neutron scattering

Peter Böni
(TU Munich)

M. Janoschek
(Los Alamos)

MFM

Dennis Meier
(Trondheim)

magnetic
resonance

Dirk Grundler
(Lausanne)

Spinwave
spectroscopy

Shinichiro Seki
(Riken)

multilayers

C. Panagopolous
(Singapore)

Summary: chiral magnetic crystals

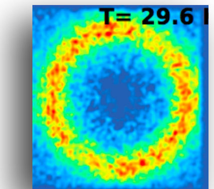

crystallization process: fluctuation-driven 1st order

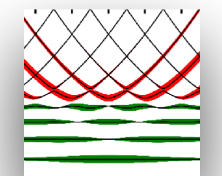

helimagnon band structure

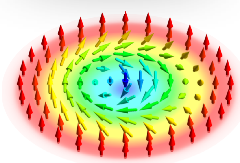

skyrmion: internal modes, skew scattering

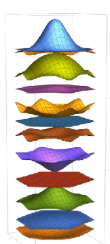

topological magnon band structure of skyrmion crystals

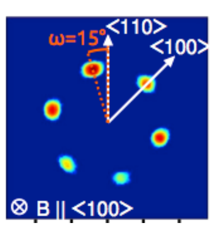

orientation of skyrmion crystals — hairy-ball

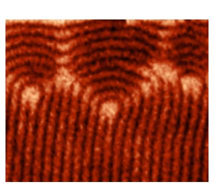

topological domain walls of helimagnets

Outlook: defect-mediated melting process? relation to NFL?